Modeling Connectivity in the Brain: An Application in Huntington's Disease

by

Dhananjay Raghavan Thiruvady, BCompSc(Hons)

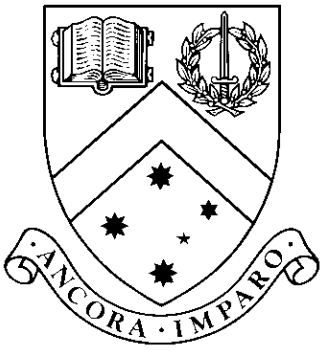

Thesis

Submitted by Dhananjay Raghavan Thiruvady

for fulfillment of the Requirements for the Degree of

Master of Information Technology (Research) (1895)

Supervisors: Dr. Ross Cunnington, Dr. Nellie Georgiou-Karistianis, Dr. Sid Ray

Clayton School of Information Technology
Monash University

August, 2006

Contents

List of Figures

List of Tables

Modeling Connectivity in the Brain: An Application in Huntington's Disease

Dhananjay Raghavan Thiruvady, BCompSc(Hons)
drthi1@student.monash.edu.au
Monash University, 2006

Supervisors: Dr. Ross Cunnington, Dr. Nellie Georgiou-Karistianis, Dr. Sid Ray
R.Cunnington@hfi.unimelb.edu.au,
Nellie.Georgiou-Karistianis@med.monash.edu.au,
Sid.Ray@csse.monash.edu.au

Abstract

This thesis studies functional and effective connectivity between regions of interest in healthy controls and patients with Huntington's disease (HD) using functional magnetic resonance imaging (fMRI). Using the Simon task, critical regions required for task performance were identified in prefrontal and parietal brain areas. Between these regions functional and effective connectivity methods were tested by measuring prefrontal and fronto-parietal interactions in controls and HD patients.

Previously acquired fMRI data for 17 controls and 20 HD patients were used in this thesis. HD patients recruited a larger number of cortical regions than controls, including the anterior cingulate (AC) and lateral prefrontal cortex (PC), to perform the Simon task. These regions are also known to be affected in HD and were therefore selected for functional and effective connectivity analysis. To examine directional influences with effective connectivity, parietal regions (PL) in both hemispheres were also selected. Functional connectivity was assessed by computing correlations between prefrontal regional time courses. Effective connectivity using structural equation modeling (SEM) was used to estimate directional influences of prefrontal

and parietal regions as predicted by the data. Dynamic causal modeling (DCM) for effective connectivity was also tested with the data available.

The functional connectivity results showed significantly reduced connectivity in HD patients compared to controls between the AC and PC regions within hemisphere and between the AC regions across hemispheres. The SEM results also showed this effect in the right hemisphere and between the AC regions. Moreover, reduced fronto-parietal connectivity in the HD group compared to controls was also seen. The DCM results did not show reliable connectivity estimates across all subjects during task performance.

The functional connectivity results demonstrate a high level view of the interactions between the prefrontal regions selected. SEM provides additional insight by providing directionality to the interactions. This thesis shows that functional connectivity and SEM in fMRI are useful methods to assess connectivity in the brain. Although connectivity was not reliable in DCM, this thesis shows that valid connectivity is obtainable when task-activated regions are selected in each subject.

Collectively, the connectivity results show impaired connectivity in HD patients compared to controls which is expected given brain region pathology in HD. This is consistent with previous neurodegenerative connectivity studies and shows that connectivity in fMRI provides valuable information when assessing connectivity impairments in neurodegenerative disease groups. The reduced connectivity seen in HD is possibly attributable to cell loss within the regions selected. Additionally, volumetric studies show deficits in HD and, particularly, reduced volume in white matter tracts will result in the impaired connectivity seen in HD. The increased recruitment of cortical regions by HD patients to perform the Simon task could possibly be to compensate for the impaired regional connectivity seen.

Modeling Connectivity in the Brain: An Application in Huntington's Disease

Declaration

I declare that this thesis is my own work and has not been submitted in any form for another degree or diploma at any university or other institute of tertiary education. Information derived from the published and unpublished work of others has been acknowledged in the text and a list of references is given.

Dhananjay Raghavan Thiruvady
August 4, 2006

Acknowledgments

Undertaking this MIT research project has been a great experience. There were several people involved who guided me through this project. I would first like to thank my supervisors Dr. Ross Cunnington, Dr. Nellie Georgiou-Karistianis, and Dr. Sid Ray who offered me the project to start with. They have each contributed significantly to the multi-disciplinary research presented here. Dr. Anusha Shritharan was particularly helpful with introducing me to the details of neuroimaging and providing help through the course of the project. Dr. Maree Farrow also provided me with significant guidance during the project.

I would like to thank the staff and students at The Howard Florey Institute for discussions on several topics within neuroimaging. They include Dr. Gary Egan, Dr. Maria Gavrilescu, Eugene Duff, Dr. Leigh Johnston, Tamara-Leigh Brawn, and Dr. Hamed Asadi.

I would like to acknowledge scholarships given by National Neuroscience Facility, The University of Melbourne and Clayton School of Information Technology, Monash University to support this work.

I would also like to thank the Clayton School of Information Technology administrative staff, in particular, Shiranthi Ponniah who patiently helped me with administrative issues. I would like to acknowledge the help and support of my PhD/Masters and house mates. Finally, I would like to thank my family and Archana for their support.

Dhananjay Raghavan Thiruvady

Monash University

August 2006

Chapter 1

Introduction

Huntington's disease (HD) is a progressive and fatal neurodegenerative disorder. It is a hereditary disease and its progressive nature leads to dementia and death about 15-20 years from diagnosis (Gaura, Bachoud-Levi, Ribeiro, Nguyen, Frouin, Baudic, Brugieres, Mangin, Boisse, Pal, Cesaro, Samson, Hantraye, Peschanski and Remy, 2004; Georgiou-Karistianis, Smith, Bradshaw, Chua, Lloyd, Churchyard and Chiu, 2003; Gomez-Tortosa, MacDonald, Friend, Taylor, Weiler, Cupples, Srinidhi, Gusella, Bird, Vonsattel and Myers, 2001). HD is rare and its first symptoms are usually seen between 35-44 years of age depending on genetic characteristics and mode of inheritance (Georgiou-Karistianis et al., 2003). The rate of deterioration also appears to be affected by these two factors. In examining brain structure and function in HD, it is important to understand the progressive nature of the disease and what factors may mediate the rate of pathological decline. This will enable medical researchers to determine how to slow down deterioration rate from the disease onset by either replacing damaged tissue in dysfunctional regions and/or to prevent further cell death in patients.

There has been substantial development in medical imaging since the early 1970's. Magnetic resonance (MR) imaging is a recent technique and the images

obtained from this technique provide high spatial resolution. Functional magnetic resonance imaging (fMRI) is a particular method within the class of MR imaging techniques where blood flow in the brain is mapped to images. These images provide a way by which brain region deterioration can be measured as a function of blood oxygenation level dependent (BOLD) response.

Through the use of a cognitive task in fMRI, activation at disparate brain regions can be measured. From activation maps (images of regions with high task related activity) regions used to to perform a task can be identified. A subset of these regions, called regions of interest (ROIs), are selected for further analysis. When measuring differences between two groups of subjects (e.g. a control and patient group) the regions are selected to be able to differentiate the two groups.

In this thesis the two groups to be studied are healthy controls and HD patients. The next stage from activation analysis is to assess functional interactions between regions and to determine which of these interactions are impaired in patients. These regional interactions can be assessed with functional and effective connectivity in fMRI with the influence of brain regions on others measured by effective connectivity. HD patients are expected to show impaired connectivity due to brain region pathology.

The following literature review aims to provide the background necessary to apply computational models to assess connectivity in the brain between HD patients and healthy controls. This chapter is organized as follows: section 1.1 discusses HD, its causes, diagnosis and treatments. A discussion of cortical circuits follows in section 1.2. Medical imaging is reviewed next (section 1.3) followed by connectivity in the brain (section 1.5). Modeling techniques for connectivity in the brain are described in section 1.6 and the hypotheses to be examined in this thesis are listed in section 1.6. Finally, the conclusion (section 1.7) provides an outline of this thesis.

1.1 Huntington's Disease

1.1.1 Overview

George Huntington wrote the paper 'On Chorea' (The Medical and Surgical Reporter, Vol.26 No.15) in 1872 where he describes the symptoms of Huntington's disease (Harper, Houlihan, Jones, MacMillan, Morris, Quarrell, Scourfield, Shaw, Solden and Tyler, 1996). HD, initially known as Huntington's Chorea, is characterized by irregular, abrupt and involuntary movements. Researchers are beginning to understand some of the important characteristics of HD since its gene identification in 1993 (Gusella, Wexler, Conneally, Naylor, Anderson, Tanzi, Watkins, Ottina, Wallace, Sakaguchi, Young, Shoulson, Bonilla and Martin, 1983; Rosenzweig, Breedlove and Leiman, 2002).

HD is classified as a neurological disorder as it is a disorder of the central nervous system. It is neurodegenerative, hereditary, and progressive in nature. As a result HD patients are impaired in their cognitive, emotional and motor functions and develop choreiform movements at onset (Haque, Borghesani and Isacson, 1997; Hennenlotter, Schroeder, Erhard, Haslinger, Stahl, Weindl, von Einsiedel, Lange and Ceballos-Baumann1e, 2004; Jakel and Maragos, 2000; Lawrence, Sahakian and Robbins, 1998; Winograd-Gurvich, Georgiou-Karistianis, Evans, Millist, Bradshaw, Churchyard, Chiu and White, 2003). It is a rare disease, affecting 5-10 individuals per 100,000, but varies in different regions (Georgiou-Karistianis et al., 2003; Vonsattel and Difiglia, 1998). The highest concentration of HD patients is in the Zulia region of Venezuela with 100 individuals out of every 7000 affected (Harper et al., 1996). This disease generally affects patients for the first time in their adulthood, with onset typically at 35-44 years. However, studies have shown that HD onset can occur at the age of 2 or 80 (Harper et al., 1996). Genetic characteristics and mode of inheritance are the main reasons for the variation in

the age of onset, although other modifiers are likely to be implicated. There is no treatment available for preventing or slowing neuronal degeneration in HD patients, however, steps towards providing therapies for the disease have recently been suggested (Gaura et al., 2004; Pavese, Andrews, Brooks, Ho, Rosser, Barker, Robbins, Sahakian, Dunnett and Piccini, 2003). These details are discussed later.

The progression of HD depends on two factors. The first is genetic, where longer tri-nucleotide C-A-G repeat length is associated with more rapid deterioration and earlier age at onset (Pavese et al., 2003; Sathasivam, Amaechi, Mangiarini and Bates, 1997; Thieben, Duggins, Good, Gomes, Mahant, Richards, McCusker and Frackowiak, 2002). The second is mode of inheritance, where paternal inheritance tends to lead to faster deterioration than maternal (Georgiou-Karistianis et al., 2003; Gomez-Tortosa et al., 2001). The next section discusses these two factors in detail.

1.1.2 Hereditary Factors and Clinical Features of HD

The Huntington's Disease Collaborative Research Group developed as a collaboration between six teams in the United States of America and Britain as a result of the Venezuela project (Harper et al., 1996). This group was responsible for the isolation of the HD gene in 1993. HD occurs in individuals who are gene positive and it is transmitted via autosomal dominant inheritance (Harper et al., 1996). This gene is an expanded trinucleotide C-A-G repeat in the IT15 gene near the end of the short arm of chromosome 4, that codes for the protein huntingtin (Cha, 2000; Hoffner and Djian, 2002; Kagan, Hirakura, Azimov and Azimova, 2001; Kahlem, Green and Djian, 1997). This protein is present in all individuals but those with a longer than normal repeat suffer from HD. The number of repeats in normal individuals ranges

between 8-35 repeats but HD patients typically have more than 38 (Georgiou, Bradshaw, Phillips and Chiu, 1995; Rosenzweig et al., 2002; Sathasivam et al., 1997; Stevanin, Fujigasaki, Lebre, Camuzat, Jeannequin, Dode, Takahashi, San, Bellance, Brice and Durr, 2003). The number of C-A-G repeats is inversely correlated with the age of onset and results in faster deterioration from the time of onset. However, this only explains 50% - 69% of the variance suggesting that other modifying factors may also be related to rate of decline (Georgiou-Karistianis et al., 2003). Most patients with early age of onset inherit the HD gene paternally and have earlier onset than their fathers. Paternal inheritance also causes longer C-A-G repeats resulting in earlier age of onset and and faster deterioration in children compared to their fathers (Georgiou-Karistianis et al., 2003). However, this is not the case with maternal inheritance, where children have similar number of C-A-G repeats resulting in similar age of onset and level of deterioration. HD is equally likely to affect men and women and it is passed down by a single dominant gene so that any child of a HD patient has a 50% chance of being affected. The HD gene, being dominant, requires just one copy of the HD allele to be inherited from a parent for an individual to be affected by the disease. It is unlikely that an individual of parents without HD alleles is going to suffer from the disease. The circumstances under which this might happen are rare but possible through a new spontaneous mutation in the individual's DNA (Chen, 2004).

Huntingtin is detected in the fetal tissue in humans and rodents (Harper et al., 1996). This protein product occurs mainly in the brain with low levels in other areas. The brain regions with high levels of huntingtin in their cells are the ones that are first affected. The function of this protein, huntingtin, is not well understood (Block-Galarza, Chase, Sapp, Vaughn, Vallee, DiFiglia and Aronin, 1997; Hoffner

and Djian, 2002; Humbert and Saudou, 2004), but possible functions have been suggested (Harjes and Wanker, 2003; Li and Li, 2004). It was first suggested that huntingtin plays a role in embryonic development (Cattaneo, Rigamonti, Goffredo, Zuccato, Squitieri and Sipione, 2001) and Block-Garlaza et al. (1997) recently showed that huntingtin may have a role in vesicle trafficking. Huntingtin interacts with cellular proteins and Cattaneo et al. (2001) suggest that it may have a key role in cell functioning. This suggests that the deterioration of brain regions may occur due to the interactions between other proteins and huntingtin. Additionally, animal models have been studied to understand the function of huntingtin (Dragatsisa, Dietricha and Zeitlin, 2000; Guidetti, Charles, Chen, Reddy, Kordower, Whetsell, Schwarcz and Tagle, 2001; Snider, Moss, Revilla, Lee, Wheeler, Macdonald and Choi, 2003). C-A-G repeat length does not seem to be important with respect to huntingtin function as it varies in different species (e.g. humans have 9-35 repeats whereas rats have 7 repeats).

Initial symptoms of HD are clumsiness, finger and face twitching, followed by involuntary choreiform jerky movements as the disease progresses (Rosenzweig et al., 2002). During the latter stages of the disease patients suffer from depression and cognitive dysfunctions. This disease can be diagnosed in a person if the following are observed: He/she has a family history of HD; The person suffers from motor, emotional and cognitive dysfunctions; There is gradual deterioration of these functions. Isolation of the HD gene has provided for a method for confirming diagnosis. Genetic testing can determine conclusively whether individuals with a family history are affected, thus carry the affected gene.

1.1.3 Neuropathology of HD

The results of HD are severe after onset. Brain region atrophy occurs over time and patients are eventually affected by dementia (Stevanin et al., 2003; Rosenzweig et al., 2002). The central nervous system is affected at onset and structural damage to cortical and subcortical regions of the brain take place gradually. The region affected most at onset is the basal ganglia (responsible for muscle-based movements), in particular the striatum (caudate and putamen, see Figure 1.1). Due to cell death,

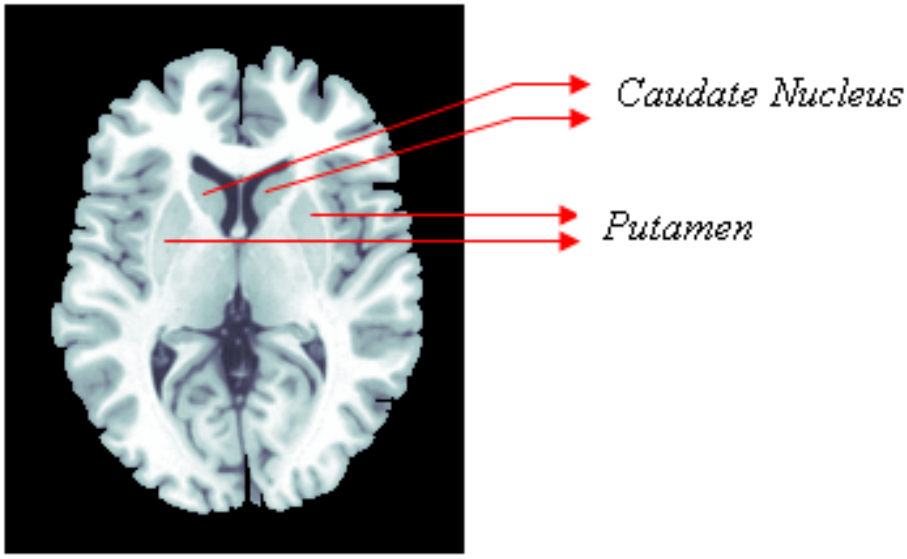

Figure 1.1: The caudate nucleus and putamen on an axial slice of the brain.

the structures in this region are smaller in volume in HD patients (Chen, 2004; Humbert and Saudou, 2004). At more advanced stages of the disease the frontal lobes (Gaura et al., 2004), hypothalamus and hippocampus (Li and Li, 2004) are affected (see Figure 1.2). Neuroimaging studies have also contributed to knowledge about HD by discovering abnormal cerebral blood flow during cognitive and motor tasks and decreased blood flow in the frontal and parietal regions of the brain (Deckel and Cohen, 2000; Thieben et al., 2002).

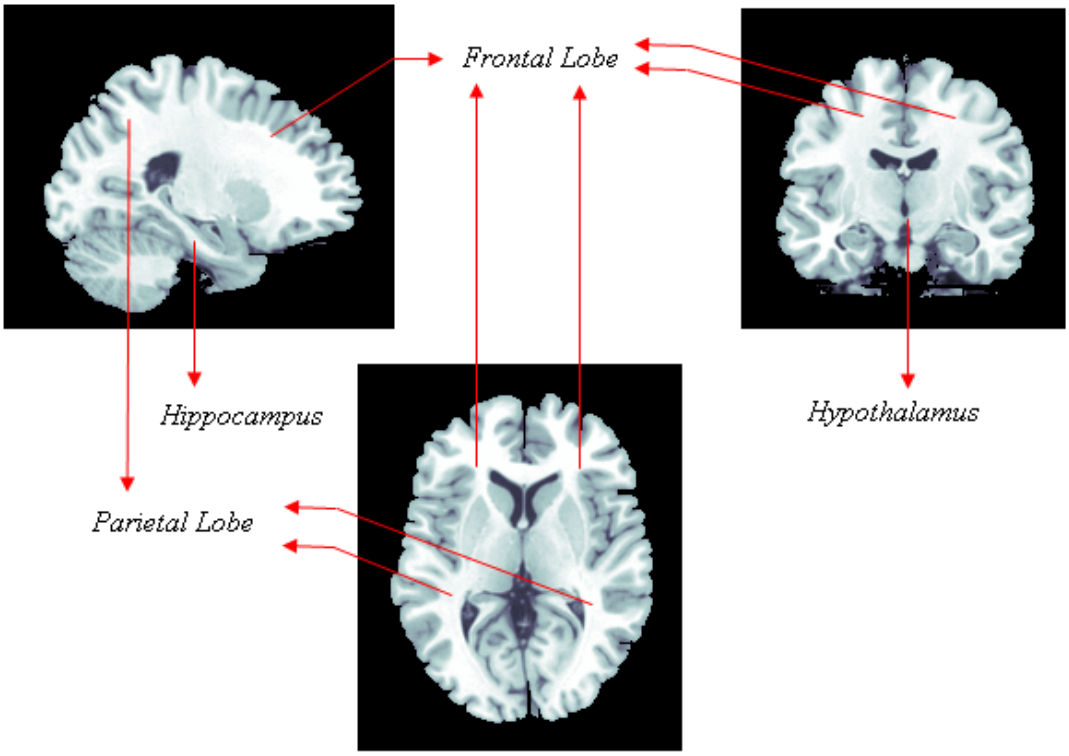

Figure 1.2: The frontal lobe, parietal lobe, hypothalamus, and hippocampus are brain regions affected at the later stages of HD; top left: sagittal view; top right: coronal view; bottom: axial view.

HD eventually leads to dementia and death. The seriousness of the disease has resulted in attempts to propose treatments for patients. Progress made to date in finding solutions is reviewed next.

1.1.4 Solutions

Currently there is no cure for HD but some treatments are available. Suggestions have been made that new pharmaceutical drugs can slow down cell death, and striatal implants can replace damaged brain tissue (Haque et al., 1997; Li and Li, 2004).

Although methods are still relatively new, clinical trials are underway (Georgiou-Karistianis et al., 2003; Pavese et al., 2003). Drugs are mainly administered to suppress choreiform symptoms and at different stages of the disease various drugs could be administered to help patients with HD. Therapies such as replacement, antidopaminergic, GABAergic, chloinergic therapy have been tried with HD patients, unsuccessfully (Haque et al., 1997). Fetal cell implants have also been explored with HD patients, but it is still at an exploratory stage and may provide unexpected results. Additionally, there are ethical issues involved with cell implants. With the isolation of the HD gene, gene therapy seems to be plausible in the future, although it is not used at the clinical level as yet (Harper et al., 1996). Psychological treatment in the form of supportive psychotherapy, memory aids, and behavioural psychotherapy are currently used and are useful to support and help HD patients. It is also suggested that drugs which can improve the role of the huntingtin protein may assist in slowing down the symptoms. Li and Li (2004) and McMurry (2001) suggest that modifying huntingtin's function with genetic modifiers may assist in developing therapies. Additionally, animal models that resemble HD with similar symptoms are being researched to provide insight into potential therapies (Borlongan, Koutouzis, Freeman, Cahill and Sanberg, 1995; Borlongan, Koutouzis and Sandberg, 1997).

1.1.5 Summary

Using fMRI, connectivity models can be used to understand the impairments in interactions between brain regions. Identifying problems in interactions between brain regions in HD is essential to understand brain region pathology. Additionally, detecting HD early in patients, or those in their presymptomatic phases, allows for the possibility to avoid or slow down the disease through therapies.

Modeling the effects of HD over time provides a framework from which future patients can be assessed for deterioration rate of the disease from onset. When drug therapies are made available, they can be administered to patients based on the predicted deterioration rate from the model. It can then be observed how the model changes over time.

1.2 Cortical Circuits

Cortical circuits in the brain can be categorized into three types, functionally. They are the motor, associative and limbic circuits (Alexander, Delong and Strick, 1986). In total, there are five parallel semi-independent frontal-subcortical circuits. The two motor circuits are motor and oculomotor, the two associative circuits are dorsolateral prefrontal and lateral orbitofrontal, and the limbic circuit is the anterior cingulate (Cummings, 1993). Recently, two extensions to this proposed circuitry model were suggested (Middleton and Strick, 2001). Firstly, it has been suggested that each of the five circuits consists of several sub circuits. Secondly, there may be seven circuits instead of five (including also the medial orbitofrontal and inferotemporal/posterior parietal). These additional circuits provide a broad framework to assess connectivity in HD.

Each circuit originates in the frontal lobe and projects sequentially to the striatum, substantia nigra pars reticulata/globus pallidus (internal segment), thalamus and back to the frontal lobe [see Figure 1.3, (Alexander et al., 1986; Beiser, Huat and Houk, 1997; Bergman, Feingold, Nini, Raz, Slovin, Abeles and Vadia, 1998)].

The circuits described above are known as direct circuits (Obeso, Rodriguez and DeLong, 1997; Parent and Cicchetti, 1998). Indirect circuits are those which sequentially project from the striatum to the globus pallidus (external segment), subthalamic nucleus the substantia nigra pars reticulata/globus pallidus (internal

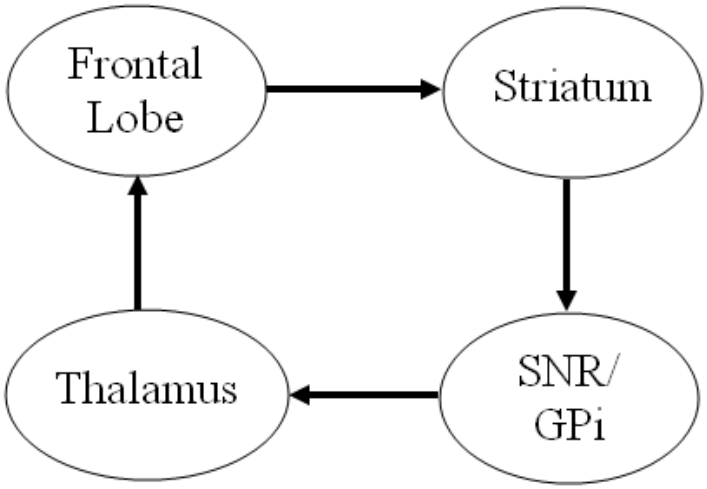

Figure 1.3: Fronto-striatal circuits in the brain; SNR: substantia nigra pars reticulata; GPi: globus pallidus internal segment.

segment), thalamus and back to the frontal lobe (Obeso et al., 1997; Parent and Cicchetti, 1998).

Each region that is part of a circuit consists of subregions with motor, associative or limbic functions. When a subregion of a region projects to a functional subregion of another region, e.g. motor to motor, the circuit is known as closed. Open circuits are those circuits with projections from one subregion to another with different functions, e.g associative subregion connected to limbic subregion (Joel and Weiner, 1997). Each circuit has different subregions that it originates from and it projects sequentially to other brain regions.

1.2.1 Circuitry and Brain Areas Affected in HD

Joel and Weiner (1997) and Lawrence et al. (1998) have reviewed basal ganglia pathology and extended their discussions to consider implications for HD. They also discuss prefrontal circuitry and suggest that prefrontal regions in HD are also affected at early stages. At HD onset, the striatum is generally the first region

affected. The associative circuit is disrupted with loss of neurons in the caudate nucleus causing cognitive dysfunction. This is followed by a loss of projections from the striatum to globus pallidus (external segment) and substantia nigra affecting the direct and indirect circuits.

At later stages of HD the motor circuit is affected with deterioration of the putamen resulting in motor dysfunction. At this stage several brain regions are affected including the cortex and projections from the striatum to the globus pallidus (internal segment). In particular, connections between the caudate and frontal lobes are lost which leads to compromised executive functions (Lawrence et al., 1998; Saint-Cyr, Taylor and Nicholson, 1995). The limbic circuit, involving the anterior cingulate, is also affected which also results in problems of executive functions (Paulsen, Zimbelman, Hinton, Langbehn, Leveroni, Benjamin, Reynolds and Rao, 2004; Reading, Dziorny, Peroutka, Schreiber, Gourley, Yallapragada, Rosenblatt, Margolis, Pekar, Pearlson, Aylward, Brandt, Bassett and Ross, 2004).

Previous volumetric studies in HD have reported grey and white matter loss in cortical and sub-cortical brain areas (Fennema-Notestine, Archibald, Jacobson, Corey-Bloom, Paulsen, Peavy, Gamst, Hamilton, Salmon and Jernigan, 2004; Halliday, McRitchie, Macdonald, Double, Trent and McCusker, 1998; Jernigan, Salmon, Butters and Hesselink, 1991; Rosas, Koroshetz, Chen, Skeuse, Vangel, Cudkowicz, Caplan, Marek, Seidman, Makris, Jenkins and Goldstein, 2003; Vonsattel and Difiglia, 1998). All these studies have established basal ganglia atrophy and reduced volumes of grey matter in cortical areas as expected. Fennema-Notestine et al. (2004) additionally observed significant loss of cerebral white matter with the occipital white matter most affected. Reduction in white matter volumes have also been been reported by Halliday et al. (1998), Jernigan et al. (1991) and Rosas et al. (2003). Halliday et al. (1998) found reduced white matter volumes in the prefrontal areas indicating that connectivity between these areas may be compromised. They

also found that the rate of cortical atrophy correlated with C-A-G repeats. The study by Rosas et al. (2003) examined early to mid stage HD patients and found volumetric reductions in all brain areas in HD patients compared to controls. This study suggests that cortical and subcortical brain areas may be affected in early HD and that prefrontal areas may play an important role in early cognitive and executive function changes.

Previous research in HD has focussed on basal ganglia pathophysiology (Hallett, 1993). However, the prefrontal, fronto-striatal, and fronto-parietal circuitry are also affected [possibly in early HD, see Rosas et al. (2003)] and should be considered when assessing deterioration in HD. Furthermore, the cortico-cortical circuitry could be affected as a result of the deficits in fronto-striatal circuitry.

1.3 Medical Imaging

X-ray computed tomography (X-ray CT) was the first medical imaging technique available in the 1970's. Positron emission tomography (PET) is a technique based on x-ray CT (Pavese et al., 2003; Posner and Raichle, 1997), where positrons and reconstructed computer images (tomographs) are used. The images that are obtained contain detailed information about internal organs and tissues.

Magnetic resonance imaging (MRI) was the next technique to be developed. MRI works by applying radio frequency (RF) pulses to samples which respond by emitting radio signals that indicate the number of atoms in their chemical environment. The nuclei of the atoms, when placed in a uniform magnetic field, align themselves with (parallel) or against (antiparallel) the field. RF coils transmit radio signals to the specific part being imaged which perturb atomic nuclei in the body part. As these nuclei return to their resting state they emit energy which is measured as T_1 (longitudinal, usually 1 s) relaxation when the nuclei realign with the magnetic

field or T_2 (transverse, usually < 100 ms) relaxation of the nuclei when transverse pulse is applied (Hesselink, 2005; Wikipedia, 2005). A variation of T_2 imaging is T_2* imaging [for further details see (Wikipedia, 2005)]. The T_2 and T_2* weighted image have brighter cerebrospinal fluid, i.e., more intense signal, than a T_1 weighted image. These parameters, other imaging parameters, and variable pulse sequences can be used to vary the image contrast. The final result is a map or an image of the MR signal strength. The resolution of these images in medical applications is about 1 mm^3.

The MR imaging system is setup as follows (Hesselink, 2005): A large magnet creates the magnetic field[1]. Shim coils are used maintain homogeneity of the magnetic field and a RF coil transmits the RF signal. A recover coil recovers the returning radio signals and the spatial location of the signals are determined by gradient coils. Finally, a computer is used to construct an image from radio the signals.

MRI images contain more detail than x-ray CT images and hence provide more information about internal organs and tissues. Functional MRI (i.e., fMRI) is a subset of MRI and it measures physiological changes and uses MR imaging to create a map of brain activity from deoxyhemoglobin content in the blood at brain regions (Radiological Society of North America, 2004).

1.3.1 Functional Magnetic Resonance Imaging

FMRI is a new imaging technique that can detect quick changes in activation at brain regions. The fMRI imaging technique allows researchers, radiologists, etc. to determine precisely which parts of the brain are being used for performing tasks (e.g.

[1]The strength of the magnetic field ranges from 0.3 to 3 tesla, however, field strengths as high as 20 tesla have been explored in research.

visual perception, executive functions or motor functions). Statistical methods are used to determine which regions are more active than others.

FMRI measures the intensity of RF signals which indicates functional activity in the brain (Posner and Raichle, 1997; Radiological Society of North America, 2004). The fMRI or BOLD signal is is a measure of the level of deoxyhemoglobin in the blood at every voxel [a volume pixel which is the smallest part of a three dimensional image (Jupitermedia, 2005)] in the brain. Increased blood flow causes an increase in the signal followed by an undershoot according to the hemodynamic response function (HRF, see Figure 1.4). The time period for the signal to peak and undershoot is about seven to eight seconds (Friston, Mechelli, Turner and Price, 2000). Hemoglobin (carries oxygen) in the blood stream becomes deoxygenated hemoglobin

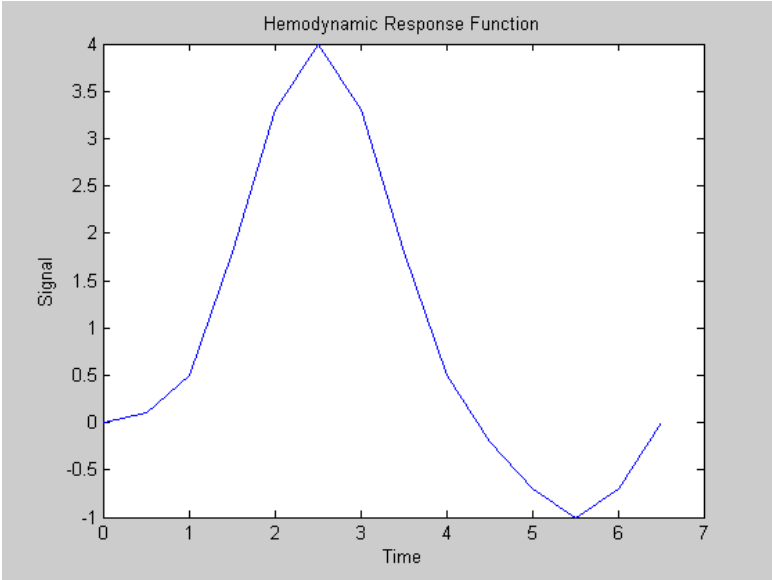

Figure 1.4: The hemodynamic response function.

when the oxygen is absorbed. The ratio of oxygenated hemoglobin to deoxygenated hemoglobin is measured by fMRI detectors. With increased blood flow, this ratio increases as neuronal tissue does not absorb most of the oxygen provided by blood.

Using this ratio, fMRI detectors create a map of blood flow in active regions which reflect neuronal activity (Durston, Thomas, Worden, Yang and Casey, 2002; Friman, Borga, Lundberg and Knutsson, 2002; Friston, Fletcher, Josephs, Holmes, Rugg and Turner, 1998; Gazzaniga, Ivry and Mangun, 1998; Harrison, Penny and Friston, 2003; Horwitz, Friston and Taylor, 2000). FMRI measures are characterized as event-related - response to a single event independently or state-related - response to repeated stimuli (Josephs, Turner and Friston, 2004) .

1.3.2 FMRI: Data Analysis

Marchini and Presanis (2004) have compared methods for detecting activation from fMRI data. They describe the following three steps involved in fMRI analysis.

1. Preprocessing steps: including realignment, smoothing (increase signal-to-noise ratio), noise reduction, etc.

2. For each voxel in the time series Y, the general linear model (GLM) is used:

$$Y = \beta X + \epsilon \tag{1.1}$$

   where X is the design matrix that models the BOLD response and nonlinear trends, β is the parameter to be estimated and ϵ is the error. The model is fitted to each voxel and t and F statistics which reflect the BOLD response are calculated.

3. A statistic image is or statistical parametric map (SPM) is generated from the statistic values. The SPM is analyzed for activations resulting from stimuli. Figure 1.5 is an example of a t statistics SPM. The top-left, top-right and bottom-left views are the sagittal, coronal and axial respectively.

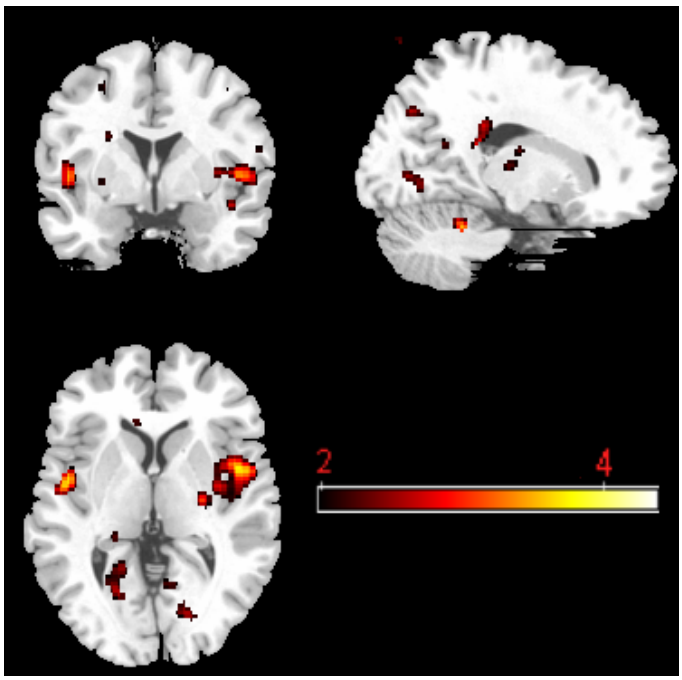

Figure 1.5: A t statistic image.

Preprocessing steps

The initial step in fMRI data analysis is preprocessing which is applied to raw data to reduce variance components of the voxel time courses. This involves several spatial transformations to account for differences in size and shape or movement across scans. It is important to transform the data into the standard anatomical space to be consistent with other studies.

The steps usually involved in preprocessing are realignment, normalization and smoothing. The parameters chosen for each of these steps vary in fMRI studies and are usually based on a researcher's knowledge, experimental design and expected results.

Realignment Head movements in fMRI studies are a problem even though restrictions are placed on subjects. The magnitude of movement can be large but is

usually within 2 mm. Large movements are typically observed in patient groups which affect the signals. To correct for these movements realignment is usually the first step applied to fMRI data.

To realign the images, six parameters of an affine rigid body transformation are estimated by minimizing a cost function between each scan and a reference scan. The reference scan is usually the mean (amongst all scans) or the first scan. An optimum transformation matrix is obtained and used to transform all the scans into the space of the reference scan by re-slicing them.

Even after realignment, movement effects persist in the fMRI signal. This is because of nonlinear effects such as changes in movement between slice acquisition, distortion because of magnetic field inhomogeneities (Anderson and Vastag, 2004), spin history effects (Friston, Williams, Howard, Frackowiak and Turner, 1996), and interpolation artifacts (Grootoonk, Hutton, Ashburner, Howseman, Josephs, Rees, Friston and Turner, 2000). An additional issue to consider is movements that are correlated with the task. This could occur because of the nature of the task (e.g. a motor task) or possibly through uncontrolled movements in a patient group.

Normalization The next preprocessing step is usually normalization. The fMRI images obtained vary in size and shape from subject to subject. When analyzing several subjects it is useful to transform all the images to a common coordinate space thus eliminating size and shape effects. This allows assessing regional effects across subjects.

Normalization involves selecting a template image which is usually a mean image, a T_1 weighted image, or a T_2 weighted image. Some warping parameters that map the template image into a standard anatomical space (e.g. Talairach coordinate space) are then calculated. For example, a transformation matrix from a T_2 weighted image to the T_2 weighted image of SPM2 can be estimated. The mapping is usually

nonlinear (e.g. using discrete cosine basis functions). The transformation matrix is then applied to all the images. Regional effects can now be analyzed in the same spatial location across all subjects.

Spatial Smoothing The spatial scale of the hemodynamic response in fMRI images is 2 mm to 5 mm which is a low frequency compared to the noise components. Therefore spatial smoothing reduces noise in the fMRI signal, or equivalently, increases the signal to noise ratio. Smoothing is generally applied by specifying a Gaussian kernel in three dimensions to all images across subjects. The Gaussian kernel needs to be larger than the voxel size to make inferences about regional effects. However, a very large kernel can lead to blurring activation making analysis of regional effects difficult.

Global Normalization There are likely to be large differences between sessions for each subject. Furthermore, the mean signal difference between subjects within groups is usually large. To analyze the signals within sessions and groups global normalization is applied which convert the signal values to a common range.

Global normalization assumes that task related signal is independent of changes in the global signal between sessions and subjects. The aim is therefore to eliminate inter-session variance which can be implemented using grand mean scaling. Additionally, intra-session variance can be removed using proportional scaling. However, proportional scaling is not often used.

Design Specification

The procedure for fMRI analysis is to design an experiment and to observe regional effects during the performance of a task. An experiment is usually designed as events or blocks. Each event corresponds to a single task (usually a single scan) and a block

design consists of a task or tasks for a long period of time (e.g. spans several scans). Included in the design are baseline blocks and sometimes rest blocks in between tasks or task blocks. The baseline block provides a contrast (i.e., activation at rest) so that regions active exclusively during task performance can be identified. A SPM is calculated for the task contrast and active regions during task performance are identified by applying a threshold to the SPM.

Software, such as statistical parametric mapping software [SPM2, The Wellcome Department of Imaging Neuroscience, London, UK (Friston, Holmes, Poline, Price and Frith, 1996; FIL, 2004)] or FMRIB's Standard Library [FSL, Oxford Centre for Functional Magnetic Resonance Imaging of the Brain, UK (FMRIB, 2004)] can be used to carry out analysis of fMRI data. Both of these software are based on the GLM and Gaussian field theory with SPM2 being the most popular tool for fMRI data analysis.

The task conditions (blocks or events) are modeled by task onset convolved with the HRF. The ensuing design is specified in the design matrix and the parameters of the GLM (see equation 1.1) are estimated to determine the contribution of each of the regressors to the observed signal. A t score for every voxel in the image is calculated according to the level of change from baseline or rest to task. Those voxels with significant t scores (typically $P_{corrected} < 0.05$) represent task related activity.

1.3.3 FMRI: Advantages and Limitations

FMRI has several advantages over other imaging techniques. Hemodynamic responses at brain regions are measured with high spatial resolution. The spatial resolution is finer than PET. Even though the temporal resolution of fMRI is poor, it is much better than PET and it is sufficient for measuring connectivity in the

brain. In PET, subjects undergo a small amount of risk as they are subject to radioactive tracers which are injected into the blood stream. FMRI does not pose any known risk and is also cheaper than PET. The experiments in fMRI can be repeated several times which allows statistical analysis, unlike PET.

Currently, there is limited experience with the fMRI technique but procedures for acquiring images are improving. Task correlated motion is a major issue and accounting for this motion will eliminate activation effects. Correlation between brain regional time courses during a task may not account for effective connectivity (discussed in Section 1.5). Modeling methods are therefore used to assess causal relationships between brain regions. Due to the strong magnetic field, some implants (pacemakers, etc.) might cause problems for patients. Metal objects can also cause distortion in fMRI images. The MR imaging process does not cause pain but may discomfort patients as they need to be still. MRI scanning also has the disadvantage of being more expensive than CT scanning.

1.4 Imaging Prefrontal/Parietal Function in HD

Mentioned earlier, the brain region with most significant neurodegeneration in HD is the striatum, however, imaging studies have also shown other regions that are affected. Structural imaging studies have also demonstrated neuronal degeneration in various extra-striatal regions including cortical and subcortical areas. Imaging studies have been conducted with single photon emission computerized tomography (SPECT) (Deckel and Cohen, 2000) and fMRI (Clark, Lai and Deckel, 2002; Kim, Reading, Brashers-Krug, Calhoun, Ross and Pearlson, 2004) which have demonstrated the effects of this degeneration.

Through fMRI, via the use of cognitive tasks, the cognitive implications of cortical and subcortical neuropathology can be identified. Previous studies have revealed specific changes in prefrontal cortical function during cognitive task performance in symptomatic and pre-symptomatic HD patients (Clark et al., 2002; Kim et al., 2004; Paulsen et al., 2004; Reading et al., 2004). In particular, Paulsen et al. (2004) suggest that the relative hyper-activation in prefrontal regions in presymptomatic HD compared to controls may compensate for striatal degeneration. These studies had some limitations, however, with small population sizes (< 10 HD patients) and mainly presymptomatic subjects.

To assess regional pathology in HD, a cognitive task which activates the affected regions in HD must be chosen. One such task is the Simon task. Imaging studies have been conducted which have shown fronto-striatal and fronto-parietal involvement during Simon task performance (Huettel and McCarthy, 2004; Iacoboni, Woods and Mazziotta, 1998; Liu, Banich, Jacobson and Tanabe, 2004; Peterson, Kane, Alexander, Lacadie, Skudlarski, Leung, May and Gore, 2002). The fMRI studies by Huettel etal al. (2004), Liu et al. (2004), and Peterson et al. (2002) show activation in anterior cingulate, supplementary motor area, inferior temporal, inferior and superior parietal, lateral and medial prefrontal regions, and caudate and putamen. Some of these regions are also affected in HD and the Simon task should therefore show activation differences between HD patients and controls. To perform this task, it is expected that the dorsolateral prefrontal and anterior cingulate circuits will be used by subjets and it is within these circuits that differences between controls and HD patients should be seen.

1.5 Connectivity

1.5.1 Background

Connectivity in the brain can be categorized in terms of *functional connectivity* and *effective connectivity*. Functional connectivity refers to correlations in activation between brain regions (Friston, 1994a; Sun, Miller and DEsposito, 2004), whereas effective connectivity is defined as the influence that one neuronal system exerts over another (Friston, Buechel, Fink, Morris, Rolls and Dolan, 1997; Mclntosh and Gonzalez-Lima, 1994). These definitions indicate that irrespective of the BOLD response at brain regions, functional connectivity can identify interactions between regions. However, connectivity analysis is usually conducted amongst active task-related brain regions. Effective connectivity extends functional connectivity by attempting to provide directionality to the interactions that are observed. For example, modulatory effects can be explored with effective connectivity.

1.5.2 Measuring Connectivity

The definitions of connectivity given above generally refer to connectivity as investigated in fMRI which is the topic in this thesis. However, the concept of connectivity extends to other techniques and some of these techniques are reviewed below.

Connectivity in the brain can be measured in different ways. In nonhuman primates, postmortem studies can determine connectivity with high accuracy. The method used is to inject a tracer into brain regions and observe the transportation of the tracers (Kobbert, Apps, Bechmann, Lanciego, Mey and Thanos, 2001; Ramnani, Behrens, Penny and Matthews, 2004). This method is an efficient way to assess connectivity in the brain, however it is unsuitable for humans.

There are a large number of cells working together in the brain which create electrical activity. This activity (potentials) can be recorded at the surface of the skull. Those potentials which exist without stimuli (spontaneous potentials) are recorded by electroencephalograms (EEG) (Allen and Kline, 2004; Allen, Coan and Nazarian, 2004; Coan and Allen, 2004; Rosenzweig et al., 2002). Unusual brain functioning can be detected by EEG. The potential changes that occur by presenting a stimulus are recorded by event-related potentials (ERPs) (Gazzaniga et al., 1998) (Nitschke, Heller, Etienne and Miller, 2004; Rosenzweig et al., 2002). ERPs are capable of detecting rapid changes in brain activity, however, determining the brain areas which give rise to ERP components is very difficult (i.e., poor spatial resolution). There is also a lot of noise involved with these techniques.

Imaging techniques are an alternative method for connectivity analysis without being invasive. Techniques like MR imaging are able to generate images from which connectivity analysis can be carried out (see section1.3). These techniques are able to precisely determine the location of the brain that is active, however they are slow as they average activity over a number of seconds (typically, TR = 3 seconds). Combining ERPs and fMRI will allow the detection of changes in activity quickly (fraction of a second) and can determine the exact location of the activity. This appears to be an ideal approach with high temporal and spatial resolution. Some recent studies have successfully combined these two methods (Gallinat and Heinz, 2006; Laufs, Lengler, Hamandi, Kleinschmidt and Krakow, 2006).

1.5.3 Functional Connectivity

Functional connectivity, or functional interactions, refer to correlations between simultaneous neuroimaging data obtained from two disparate populations of neurons (Friston, 1994b). The idea behind this measure is that the populations of neurons

co-vary in their activity and should therefore be interacting. High correlation between regions indicates high interactivity between these regions. While functional activation (i.e., BOLD response) identifies a signal of higher magnitude during a time period the functional interactions are independent of this activation. This measure is an indicator of a direct or indirect anatomical link and recently it has been suggested that functional connectivity is indicative of true anatomical regional interactivity (Horwitz, Warner, Fitzer, Tagamets, Husain and Long, 2005).

Connectivity studies (functional or effective) in HD have not been explored thus far. However, functional connectivity studies in progressive diseases have shown reduced connectivity in Alzheimer's, Parkinson's, and Schizophrenic patients (Grady, Furey, Pietrini, Horwitz and Rapoport, 2001; Lekeu, der Linden, Chicherio, Collette, Degueldre, Franck, Moonen and Salmon, 2003; Murphy, Cerf-Ducastel, Calhoun-Haney, Gilbert and Ferdon, 2005; Winterer, Coppola, Egan, Goldberg and Weinberger, 2003). Of particular interest is the study by Grady et al. (2001). They assessed functional connectivity in Alzheimer's disease patients by using a face recognition task. Their hypothesis stated that patients will show increased activity in regions of interest (prefrontal and posterior regions) whereas the correlated activity (i.e., functional connectivity) would be higher in the control group. Their hypothesis was confirmed as the Alzheimer's patients showed increased activity in the left medial temporal regions compared to controls. An analysis of functional connectivity between these regions revealed impaired interactions between the prefrontal cortex and the hippocampus. This method shows that although high regional activation is seen in patients, the regional connectivity does not necessarily have to be high.

In a PET study of patients with schizophrenia, Winterer et al. (2003) observed reduced fronto-temporal functional and effective connectivity. In another PET study, Lekeu et al. (2003) used a free and cued recall task to measure performance in Alzheimer's disease patients. The patients performed poorly on the

tasks and they observed decreased functional connectivity between the frontal and parahippocampal areas. Murphy et al. (2004), using fMRI, determined that older adults and Alzheimer's disease patients suffer from olfactory impairment by observing that the functional connectivity between orbito-frontal cortex and mesial temporal lobe was impaired. These studies demonstrate that reduced connectivity is typically seen in patient groups.

Several methods have been used in the past to examine functional connectivity. For example, selecting regions of interest and obtaining the time courses have been attempted in different ways. These details are discussed in the next chapter. Comparisons between two groups (e.g. controls vs patients) have also been attempted in different ways and these methods will be discussed in Chapter 3.

1.5.4 Effective Connectivity

In contrast to functional connectivity, effective connectivity identifies the direct or indirect interactions between brain regions and aims to eliminate spurious correlations between brain region interactions. Effective connectivity can be described by functional specialization and functional integration. Functional specialization refers to regional effects that are the result of a change in stimulus or task conditions. The correlation in activity between regions, due to the effect of regions on others, is termed as function integration. Therefore effective connectivity is the functional integration of brain regions that have specialized functions.

Effective connectivity is distinguished by forward and backward connectivity (Hertz, Krogh and Palmer, 1991; Penny, Stephan, Mechelli and Friston, 2004). Forward connectivity is also known as the bottom-up model where lower level specialized areas feed processed information to higher level areas. Response to stimuli can be explained by the bottom-up model. However, contextual inputs cannot be explained

by this model. They are explained by the top-down model and are defined as backward connections in which information is sent from higher level areas to lower level areas.

Determining functional or effective connectivity is vital to understand the neuronal pathways in the human brain. Currently, anatomical connectivity in the human brain is not well known, but fMRI provides a means by which connectivity can be measured which is an indicator of anatomical connectivity (Horwitz et al., 2005). Several studies have been conducted to examine brain regional effective connectivity (Gitelman, Parrish, Friston and Mesulam, 2002; Goncalves, Hall, Johnsrude and Haggard, 2001; Lin, McIntosh, Agnew, ZeffiroO and Belliveau, 2001; Mechelli, Price and Friston, 2001); modeling methods to measure effective connectivity have become quite sophisticated.

1.5.5 Regional Interactivity in HD

Measuring effective connectivity between brain regions is useful when assessing brain region atrophy in HD patients. The connections between distal brain regions may not be functioning due to the deterioration or neuronal loss in certain brain regions. Previous studies have found that fronto-striatal connections are affected in HD (Dursun, Burke, Andrews, Mlynik-Szmid and Reveley, 2000; Lawrence et al., 1998; Schmidtke, Manner, Kaufmann and Schmolck, 2002). As a result the prefrontal circuitry is disrupted and there is the possibility of other interactions (e.g. prefrontal with parietal regions) also being affected. Through fMRI, via the use of cognitive tasks, it will be possible to identify impaired regional interactions in HD by measuring functional and effective connectivity. A longitudinal assessment should further show worsening of regional interactions using these measures. Therefore,

assessing connectivity using fMRI will be useful in determining rate of deterioration over time in HD patients at differing stages and differing number of C-A-G repeats.

1.6 Modeling

Effective connectivity in the brain is measured by the application of modeling techniques to fMRI. The modeling techniques aim to determine causal relationships between the signals of brain regions. Causal modeling is used to model variables and their effects on others (Charniak, 1991; Pearl, 1993; Templin and Pieper, 2003). A causal model is a directed acyclic graph (DAG) with a set of nodes and a set of arcs (Anderson and Vastag, 2004; Heckerman, 1995). The nodes model the random variables in the domain and the arcs describe causal relationships between these nodes.

To measure effective connectivity in the brain, linear and nonlinear models have been attempted. The brain involves nonlinear interactions (effects of task or regions on connections) and therefore nonlinear models are better suited. However, for a task which is known not to affect a connection, linear models are appropriate. Approaches to modeling fMRI data include structural equation modeling (SEM) (McIntosh, Grady, Ungerleider, Haxby, Rapoport and Horwitz, 1994; Mclntosh and Gonzalez-Lima, 1994), multivariate autoregressive modeling (MAR) (Harrison et al., 2003) and dynamic causal modeling (DCM) (Friston, Harrison and Penny, 2003; Penny et al., 2004). SEM and DCM are the methods explored in this thesis and are discussed in detail below.

1.6.1 Structural Equation Modeling (SEM)

SEM or path analysis was first used in economics, social sciences, and genetics. In 1994, McIntosh and Gonzalez-Lima (1994) applied SEM to functional neuroimaging

which is regarded as the first application of SEM in brain imaging (Petersson, Reis, Askelof, Castro-Caldas and Ingvar, 2000; Rowe, Friston, Frackowiak and Passingham, 2002). In the same year, McIntosh et al. (1994) conducted a PET study of the cortical visual pathways using SEM.

SEM as applied in functional neuroimaging is a covariance-based method which indicates causal relationships between the time courses of two or more brain regions. This method can be considered as an extension of the GLM analysis to identify effective connectivity between regions. The additional contribution of SEM to functional connectivity (correlations between regional time courses) is to provide directionality to the links or correlations between regions.

Several studies with SEM have been conducted so far in neuroimaging since 1994 (Buchel and Friston, 1997; Coull, Buchel, Friston and Frith, 1999; Goncalves et al., 2001; Mclntosh and Gonzalez-Lima, 1994; McIntosh et al., 1994; McIntosh, 2000; Petersson et al., 2000; Rowe, Friston, Frackowiak and Passingham, 2002; Rowe, Stephan, Friston, Frackowiak, lees and Passingham, 2002). In particular, Rowe et al. (2002) used effective connectivity in Parkinson's disease. They observed increased effective connectivity during an attention to action task between the prefrontal cortex and lateral premotor cortex/supplementary motor area in controls; however, modulation of effective connectivity was not observed in patients between these same areas. They conclude that Parkinson's disease patients, between the supplementary/pre-motor areas and the prefrontal cortex, show a functional disconnection. The underlying details of SEM and its application in the modeling and analysis of HD patients' data are discussed in Chapter 4.

1.6.2 Multivariate Autoregressive Modeling (MAR)

MAR, described by Harrison et al. (2003), is an alternative method for modeling functional integration of brain regions. They are time series models and can extract temporal information from data. An extension of linear MAR, using bilinear terms, provides a method for incorporating nonlinearities in the brain. A linear framework can still be used for inference purposes with this technique. Bayesian methods are used for model order selection and parameter estimation. This method is not explored to model connectivity in this thesis as DCM includes the advantages of MAR.

1.6.3 Dynamic Causal Modeling (DCM)

DCMs were proposed by Friston et al. (2003) to model effective connectivity between brain regions. The brain is regarded as a deterministic nonlinear dynamic system which receives inputs and produces responses. The regional connectivity measured is introduced through external influences and is propagated through the nodes (brain regions) of the network (anatomical model). The connectivity measured is a result of the neuronal activity at a node. The advantage of this technique is the ability to measure the effects of inputs on connections or modulatory effects. These effects enter the DCM as bilinear effects which are nonlinearities that account for changes induced by inputs. This is major change from techniques such as SEM which are linear and consider nonlinearities as noise. However, this requires the experimenter to design a specific experiment to take advantage of the DCM technique.

Since it is a recently proposed technique, only a small number of studies have been explored with DCM (Ethofer, Anders, Erb, Herbert, Wiethoff, Kissler, Grodd and Wildgruber, 2005; Friston et al., 2003; Lee, Friston and Horwitz, 2005; Penny et al., 2004; Mechelli, Price, Noppeney and Friston, 2003; Stephan, Penny, Marshall,

Fink and Friston, 2005). Penny et al. (2004) presented different methods that may be used for DCM model selection which provides an exploratory approach that allows partial determination of the model from the data. Mechelli et al. (2003) conducted the first study with DCM which identified that inputs from the early visual cortex mediate object category effects in the occipital and temporal cortex.

Although DCM is a very powerful technique there are some limitations at this stage. An experiment to be conducted with DCM has to be designed carefully and should include bilinear effects to fully take advantage of the technique. Furthermore, connectivity is a result of the responses at brain regions and therefore significant task-related regional activity is necessary to obtain significant connectivity. DCM is also essentially a confirmatory technique although part confirmatory - part exploratory methods are being explored (Penny et al., 2004).

1.7 Aims

The aim in this thesis is to explore functional and effective connectivity methods in fMRI to distinguish healthy subjects from HD patients. Within functional connectivity two methods are explored (direct and meta-analysis) and it is expected that these methods will reveal similar results. Effective connectivity is modeled with SEM and DCM and both these methods are expected to show similar results. Collectively, these methods are expected to show impaired connectivity in HD patients compared to controls between critical prefrontal and parietal regions required to perform the Simon task.

The conclusions from the methods point of view can be extended to other neurodegerative diseases (i.e., what results would be expected if the same methods were applied to other diseases of this kind). Given the results, connectivity in HD can

be assessed. It is expected that impaired prefrontal and fronto-parietal connectivity will be seen in HD.

1.8 Hypotheses

The hypotheses to be tested in this thesis are:

- Recent functional connectivity and effective connectivity modeling methods in fMRI will show differential patterns of connectivity to distinguish healthy individuals from HD patients.
- HD patients will show reduced prefrontal and fronto-parietal functional and effective connectivity compared to controls during Simon task performance.

1.9 Conclusion

This chapter reviewed HD and the techniques that may be used model connectivity using fMRI. Based on this review three studies of functional and effective connectivity were undertaken to distinguish HD patients from controls.

This thesis is organized as follows. The introduction (Chapter 1) discusses the relevant literature to the studies to be presented. The second chapter is a description of the design of the HD fMRI study which is the basis for the connectivity studies. The first connectivity study is on functional connectivity (Chapter 3). This chapter discusses some of the methods typically used to measure functional connectivity and the analysis for two of these methods is presented. Conclusions regarding prefrontal pathology in HD are drawn based on these methods. Chapter 4 is on effective connectivity using SEM. This chapter focuses on the SEM method, its application to HD and, its application to longitudinal data. The next chapter (Chapter 5) discusses DCM, which is a recently proposed technique for modeling

effective connectivity. The results from this technique are analyzed to determine why significant connectivity estimates are not obtained. The final chapter (Chapter 6) is the conclusion. This chapter brings together the results from functional and effective connectivity. The methods used are compared and the implication of the results to HD are discussed. The thesis concludes with a discussion regarding future directions with regards to using fMRI data to improve our understanding of connectivity in neurodegenerative disorders, such as HD.

Chapter 2

Experimental Design

The studies in this thesis build upon a previously funded National Health and Medical Research Council (NHMRC 2002-2006) study whereby fMRI data previously collected will be used to assess connectivity in HD patients. Prior to carrying out connectivity analysis several aspects of the experiment need to be firstly considered to obtain statistically valid results. These include preprocessing steps for the data (reviewed earlier), specifying an anatomical model, selection of regions of interest and time course extraction. Details of the previous project are first discussed in the topics on participants, cognitive task (i.e., the Simon task), data acquisition, image preprocessing and analysis, activation maps to provide context for the later chapters. Given the activation results and prior knowledge of pathology in HD, an anatomical model is defined. Then the details of region of interest and time course selection are discussed. The steps that lead to activation results can be formalized as an algorithm which is presented in this chapter. Two common methods for comparisons between groups for functional connectivity analysis are considered since these methods require different time course extraction procedures.

2.1 Participants and Cognitive Task

The fMRI data were obtained from 37 subjects, 20 HD patients and 17 controls in the first year of this study. In second year data are available for a subset of 11 HD patients. Demographic and clinical data for these subjects from year one are presented in Table 2.1. The patients' duration of illness ranged from 1-11 years with C-A-G repeat length ranging from 36-51. C-A-G index is a measure of HD severity that is corrected for age (Penney, Vonsattel, MacDonald, Gusella and Myers, 1997). It is computed using $C-A-Gindex = age \times (C-A-G-35.5)$ and in this thesis, the range C-A-G index in HD patients was 29.5 to 666.5. The controls had

Table 2.1: Demographic and clinical data; SD = standard deviation; - = not acquired. (1) n = 17; (2) n = 19; (3) n = 16; (4) n = 18; (5) Duration of illness in years.

	HD Patients		Controls	
	mean	SD	mean	SD
Age	47.9	7.7	49.7	7.3
C-A-G[1]	43.4	3.4	-	-
C-A-G index[1]	363.0	136	-	-
Illness[1,5]	5.4	3.6	-	-
UHDRS	23.1	13.7	-	-
BDI[2]	6.9	6.9	1.5	1.7
IQ[3]	115.5	6.1	119.0	6.1
MMSE[4]	27.1	2.4	29.2	1.3

no history of a neurological or psychiatric disorder. All subjects had normal vision or corrected to normal and were right handed. A neurologist (Dr. Andrew Churchyard[1]) or neuropsychiatrist (Dr. Phyllis Chua[2]) administered the motor subscale of the unified Huntington's disease rating scale (UHDRS: Huntington's Disease Study Group, 1996) to the patients. This was to assess motor symptom severity and the range of the UHDRS motor scores were 8 to 55. Three patients were not on any

[1]Department of Neurology, Monash Medical Centre, Clayton, Victoria, Australia.
[2]Department of Psychological Medicine, Monash University, Clayton, Victoria, Australia.

medication with the others on one or more of the following: antidepressant, antipsychotics or/and mood stabilizer. One patient was on a cholesterol lowering agent. The following tests were administered to all subjects (also see Table 2.1 for the results of these tests):

1. The Beck depression inventory (BDI) (Beck, Ward, Mendelson, Mock and Erbaugh, 1961) was administered to assess depression symptoms which is often observed in HD.

2. The national adult reading test (NART) (Nelson, 1982) was used to assess estimated premorbid IQ.

3. The mini mental state examination (MMSE) (Folstein, Folstein and McHugh, 1975) was used to assess cognitive decline.

The analysis of the clinical data was provided by Dr. Maree Farrow[3]. One-way ANOVAs revealed no significant group differences in estimated IQ ($F(1,31) = 2.85$, $p = 0.10$). However, the HD group had significantly higher BDI scores ($F(1,34) = 9.99$, $p < 0.005$) and significantly lower MMSE scores ($F(1,33) = 10.26$, $p < 0.005$). The Human Research Ethics Committees of Monash University and the Howard Florey Institute approved this study. Written consent was obtained from all participants.

The subjects lay in the scanner with a button box held in each hand. They were presented with two conditions, congruent and incongruent (see Figure 2.1). The congruent condition consisted of the presentation of either a left pointing arrow on the left hand side of the screen or a right pointing arrow on the right hand side of the screen. In the incongruent condition, the arrows were presented on the side of the screen opposite to the direction that they pointed. For example, a left pointing

[3]School of Psychology, Psychiatry and Psychological Medicine, Monash University, Clayton, Victoria, Australia.

arrow was presented on the right hand side of the screen in this condition. In both conditions the subjects were required to press the button in the hand that matched the direction of the arrow head. Hence, if presented with a left pointing arrow they were supposed to press the button in the left hand. The arrows were presented for 2500 ms one at a time. A blank screen for 500 ms followed, giving the subjects 3000 ms to respond.

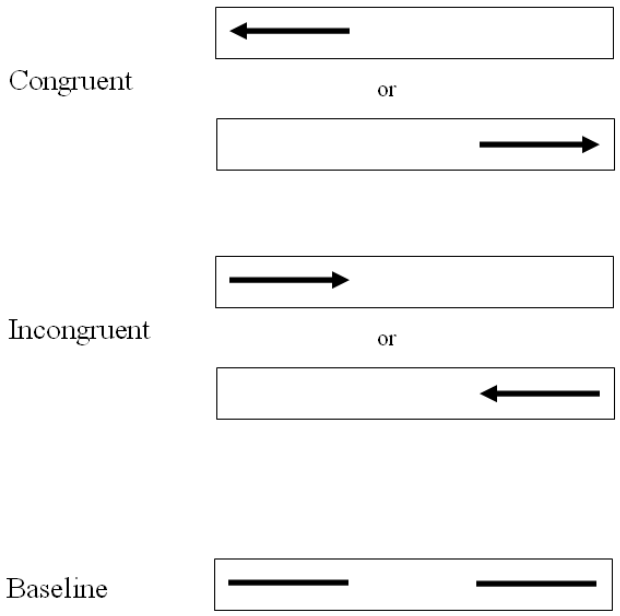

Figure 2.1: The congruent, incongruent and baseline conditions.

The Simon task (congruent and incongruent) was mixed within block followed by a baseline block. The baseline condition consisted of two horizontal lines that were presented on both sides of the screen (see Figure 2.1). Participants were not required to respond to this condition. Scans were acquired for patients and controls across four sessions. In each session, the baseline block was first presented for 12 seconds followed by a task block of six trials (18 s). Each task block consisted of three congruent and three incongruent trials selected randomly and each session consisted

of 16 baseline and 16 task blocks. The total number of trials per subject were 192 congruent and 192 incongruent. See Table 2.2 for reaction times and errors for both groups. The following assessment of behavioural data was provided by Dr. Maree Farrow. Mann-Whitney U Tests were used to assess differences between groups and Wilcoxon Signed Rank Tests were used to assess differences between conditions. To perform the Simon task HD patients were significantly slower than controls (z = -3.22, $p < 0.005$). This was also the case for each condition, congruent (z = -3.11, $p < 0.005$) and incongruent (z = -3.14, $p < 0.005$). To perform the incongruent condition, reaction times were significantly slower than performing the congruent condition for HD patients and controls (z = -5.30, $p < 0.005$). Both groups were equally disadvantaged by the incongruent condition as the difference between groups was not significant (z = -0.81, $p <= 0.42$). For the Simon task HD patients made significantly more errors than controls (z = -2.48, $p < 0.05$). This was also the case with the congruent condition (z = -2.73, $p < 0.01$) but the difference was non-significant for the incongruent condition (z = -1.83, $p <= 0.07$). More errors were made for the incongruent condition compared to congruent for both groups (z = -3.80, $p < 0.0005$). There was no significant difference between incongruent and congruent trials between groups (z = -1.05, $p <= 0.30$).

Table 2.2: Behavioural data. SD = standard deviation; RT = reaction times.

	Patients		Controls	
	mean	SD	mean	SD
RT (ms)				
Simon Task	923	237	738	109
Congruent	893	235	710	104
Incongruent	953	240	766	116
Errors (%)				
Simon Task	2.1	3.7	0.5	0.7
Congruent	1.2	2.7	0.03	0.1
Incongruent	2.9	5.0	0.9	1.3

2.2 Activation in fMRI: An Algorithm

The major use of fMRI thus far has been to assess activation of brain regions. More recently, in addition to activation, connectivity in fMRI has received attention. Typically, connectivity studies use activation maps to define regions of interest to perform connectivity analysis. The process of obtaining connectivity estimates can b described by a set of steps and can therefore be formally written as an algorithm.

There are several ways to obtain information from fMRI data. In this study the procedure to obtain activation maps is presented in Algorithm 1. This is not the only used procedure for fMRI activation analysis but is a commonly used one. Algorithms for functional and effective connectivity are extensions to Algorithm 1 and will be presented in the following chapters.

Algorithm 1: An algorithm for activation studies in fMRI.

Data: Raw data: RD_n, Subjects: S_n, Groups: G_i, Regions: R_p.
Result: Group activation maps; comparison with regions of interest.

```
for s ∈ S_n do
    preprocess data: P(RD(s));
    setup GLM design: SGLM(s);
    assign data to design: D(P, SD);
    estimate: E(D);
end
for g ∈ G_i do
    random effects analysis: REF(G(g));
    obtain regional activation: R(g);
    compare regional activation: C(R(p), R(g));
end
discuss implications: Diss(C);
```

The parameters of algorithm 1 are raw data (RD_n), subjects (S_n), groups (G_i), and regions (R_p). RD_n is the raw fMRI data obtained for n subjects, S_n. The subjects are divided into i groups, G_i, which may be one group if i is equal to one. From prior knowledge, p regions are identified which are expected to be activated, R_p. The first part of the algorithm is to carry out analysis on all the subjects

including preprocessing, setting up the design and estimating the design. The second part involves group analysis and assessment of the group results obtained.

2.3 Data Acquisition

A 3.0 T G.E. Signa whole body scanner at the Brain Research Institute, Austin Hospital, Victoria, was used to record gradient echo echo-planar images. The parameters used were TR=3000ms, TE=60ms, FA=90^0, FOV=24 cm, matrix size 128x128. To cover the entire brain, 25 trans-axial slices with a slice thickness of 5.0 mm with 0.5 mm gap was used. A T_2 weighted image (25 trans-axial slices with 6 mm gap) and T_1 weighted IrP-FSPGR anatomical images were acquired for normalization.

2.4 Image Preprocessing and Analysis

Preprocessing strategies were reviewed in the previous chapter. The preprocessing methods chosen here are standard methods and allow region specific analysis within and between the two groups. In this experiment one consideration is the possibility of reduced cortical volume in HD patients. Image preprocessing was done with SPM2 (Wellcome Department of Imaging Neuroscience, London, UK, (Friston, Holmes, Poline, Price and Frith, 1996)) with the assistance of Dr. Anusha Sritharan[4], Tamara Brawn[5], Dr. Hamed Asadi[6].

The first step was to realign all images to the first image in the same session. This corrects the images for subjects' translation and rotation within session. All the images were then coregistered to the T_2 weighted image of the subject. The T_2

[4]Research Officer, School of Psychology, Psychiatry and Psychological Medicine, Monash University, Clayton, Victoria, Australia.

[5]Research Assistant, Neuro-informatics Platform, National Neuroscience Facility, Melbourne, Victoria, Australia.

[6]PhD candidate, Neuro-informatics Platform, National Neuroscience Facility, Melbourne, Victoria, Australia.

weighted image was then normalized to the Talairach coordinate space. The normalization transformation matrix was found by minimizing the the difference between the T_2 weighted image for the subject and the T_2 weighted template image in SPM2. The template image was based on the template brain of the Montreal Neurologic Institute with discrete cosine basis functions (DCT 7x8x7 functions). A combined normalization matrix was applied to all images for each subject. This procedure results in minimum differences between the subjects' images within and between groups. Issues relating to cortical volume are also minimal. The images obtained were resliced images with voxel size $2\times2\times2$ mm^3. Finally, an 8 mm Gaussian kernel was applied to the images to increase the signal to noise ratio. The translation for head motion for 35 subjects is less than 2 mm (only two subjects' translation was between 1.5 and 2 mm). The rotation for all subjects was less than 2 degrees.

Using SPM2 the design matrix in Figure 2.2 was specified for each subject. Each column in the matrix corresponds to a regressor (see FMRI; Data Analysis in previous chapter). The model was specified in scans where each scan corresponds to 3.00 seconds. The First and third columns are the task and rest regressors. The second and fourth columns are their temporal derivatives and are modeled to account for delayed activations due to the HRF (the basis functions specified were HRF with time derivative). Each condition, congruent and incongruent, is not explicitly specified in the design because there is high correlation between the two conditions and task related activity in either of these conditions is likely to affect the other. Therefore, the two tasks are modeled as a single Simon task which spans six scans. The fifth column (INC - CON) is the regressor for incongruent - congruent and was included to identify differences between the two tasks if necessary. This contrast was modeled to determine which brain regions are activated exclusively for the incongruent condition. However, no results exclusively relating to either of the two conditions

are reported. The next four columns were defined to account for the change between sessions (labeled UDR1 to UDR4). The following six regressors, columns 10 to 16, are the motion correction parameters which are unique to each subject. This regressor will remove any spurious task related activity that appears due to motion. Although, if a subject's motion correlates with the task (first column) then some activity due to the task is modeled out[7]. The last column is a constant regressor. The vertical axis runs over 160 images acquired for each subject. This design

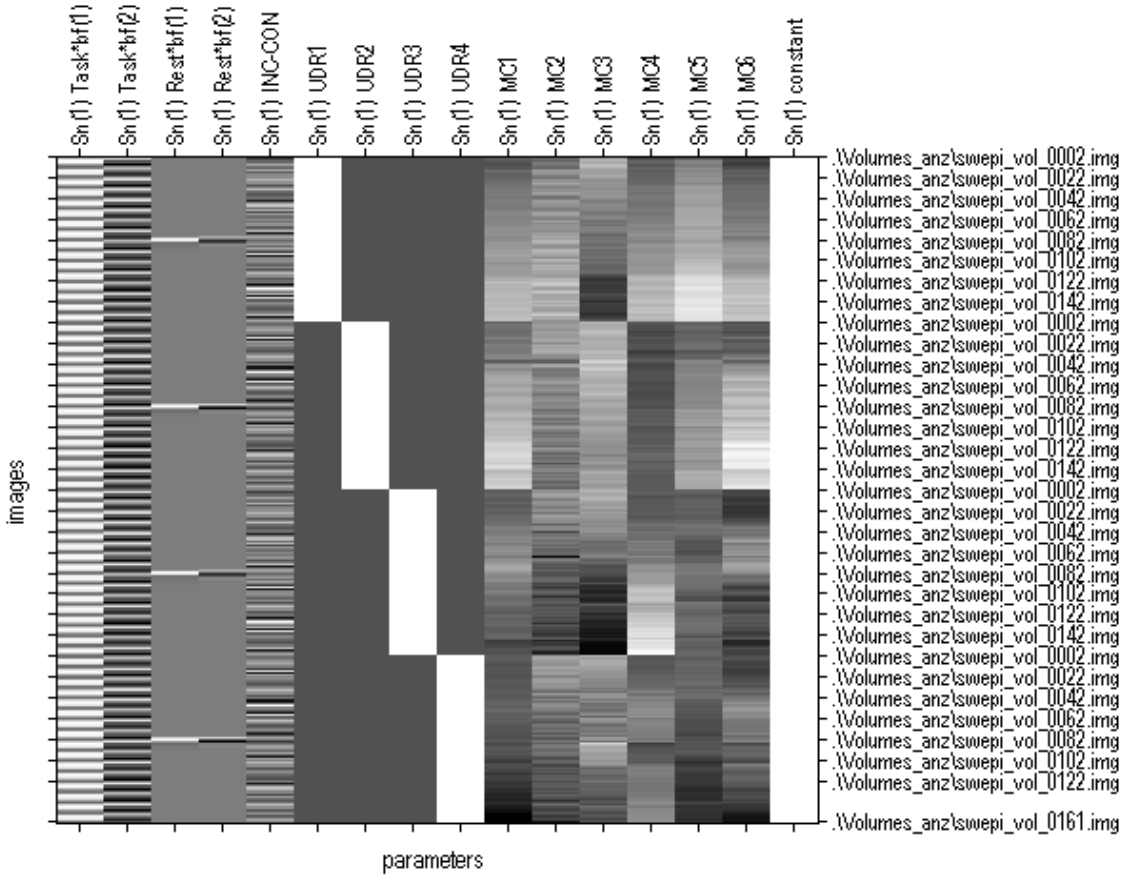

Figure 2.2: The design matrix for each subject.

was configured with some additional parameters. A high pass filter (128 s cutoff)

[7]Examining the design orthogonality (shows whether task is correlated with motion or not) for each subject shows no task related motion for all the subjects.

was applied to eliminate low frequency trends. To correct for serial correlations an AR(1) model was used. Global normalization was applied using Grand mean session specific scaling to eliminate inter-session variance.

2.4.1 Activation Maps

Each task, congruent or incongruent, spans three seconds and the two tasks are repeated randomly in a task block which spans 18 seconds. The resulting effect is high correlation between the two tasks where activity in one task affects the other. Therefore the estimates for the combined Simon task (congruent and incongruent conditions) were used to compute activation maps.

Increased activity during the Simon task for controls and HD patients was seen in both hemispheres in the putamen, precentral gyrus, medial frontal gyrus and inferior parietal lobule. Additionally, the patients activated left/right caudal anterior cingulate gyrus and insula and right dorsal premotor, right inferior frontal gyrus, left superior parietal lobule and left middle frontal gyrus. These results show that patients recruit a larger number of cortical areas to perform the Simon task compared to controls. The analysis of activity and implications to HD are beyond the scope of this project. Rather, the aim of this thesis is to test the interactions between the regions and their implications to HD. Given this hyper-activation in the patient group, the aim is to determine whether the interactions between these regions in the patient group are as tightly coupled as controls. To test the hypotheses, a statistic image of the comparison of patients greater than controls (see Figure 2.3) is computed using SPM2 (also see Table 2.3 for t scores and probabilities). This contrast determines precisely which regions are more activated for the patient group during Simon task performance. Regions for connectivity analysis are restricted to those most activated and include the anterior cingulate (AC), lateral prefrontal

cortex (PC) and parietal lobe (PL) from both hemispheres, regions also known to be compromised in HD (Paulsen et al., 2004; Reading et al., 2004; Saint-Cyr et al., 1995).

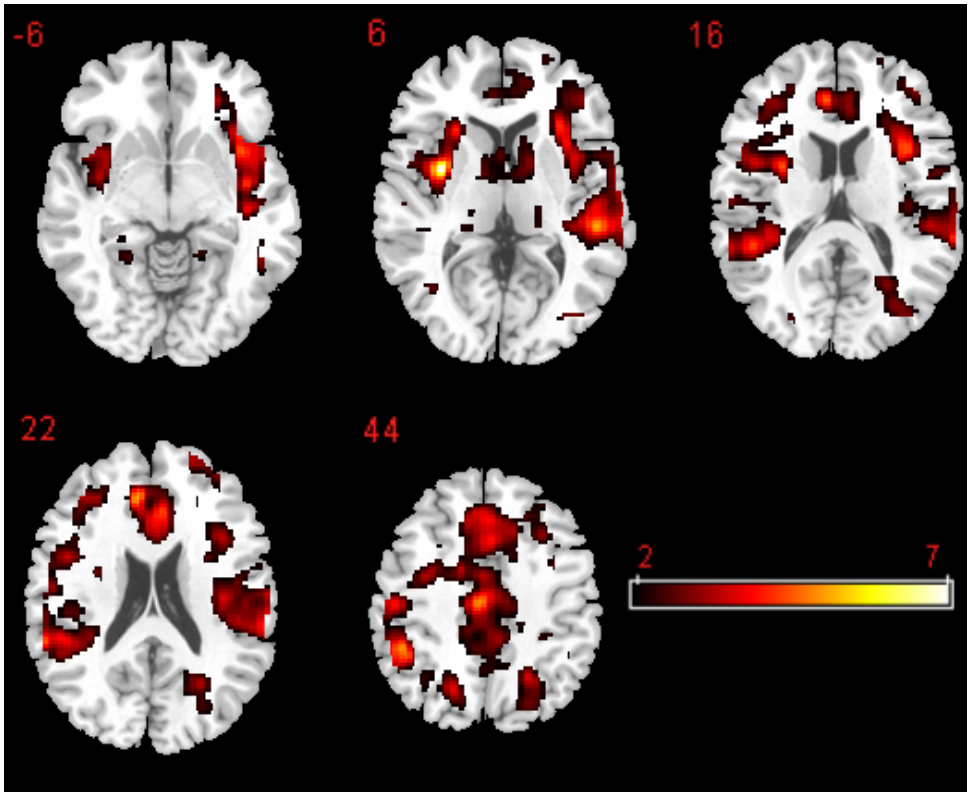

Figure 2.3: The activation map for HD patients greater than controls; axial slices corresponding to z = 16, 6, 16, 22, and 44 are shown.

2.5 The Anatomical Model

The activation map and prior knowledge about HD pathology can be used to define a set of regions that will distinguish HD patients from controls. It is known that several regions in the brain are affected in HD and some of these are activated in the Simon task. It is not feasible to analyze interactions between all affected regions, therefore a small number of regions have been selected based on activation data

Table 2.3: Coordinates and t scores of significantly active clusters (K > 10) for patients greater than controls shown in Figure 2.3. Peak voxels for selected clusters ($T > 3.50$) are reported.

Region	Coordinate	t score	P_{corr}
Left Insula	-36, 0, 6	6.98	0.016
Left Anterior Cingulate	-10, 38, 22	5.67	0.016
Left Inferior Parietal Lobule	-62, -38, 26	5.47	0.016
Left Inferior Parietal Lobule	-46, -48, 44	4.91	0.016
Right Middle Frontal Gyrus	38, 44, 16	4.64	0.016
Left Superior Frontal Gyrus	-18, 6, 66	4.57	0.016
Left Precuneus	-22, -62, 50	4.38	0.016
Left Caudate Head	-4, 14, 2	3.55	0.023

and known pathology in HD. Furthermore, all affected regions need not be chosen since some of these have indirect effects on the correlations measured. The ensuing network of regions is defined in an anatomical model.

The basal ganglia has been the primary area of interest in HD for some time but it is known that the frontal and parietal regions are also affected early in the disease (Rosas et al., 2003). The aim of this thesis is to assess prefrontal and fronto-parietal pathology, including mainly the dorsolateral prefrontal and anterior cingulate circuits [these circuits are likely to be affected indirectly due to basal ganglia pathology, (Joel and Weiner, 1997)]. Secondly, given the resolution of the images acquired ($2\times2\times2$ mm^3) and the smoothing factor (8 mm Gaussian kernel), it will not be possible to differentiate the regions within the basal ganglia. Finally, it is not possible to accurately define bilateral regions within the basal ganglia for the same reasons. Therefore the basal ganglia will not be included in the anatomical model considered in this thesis.

Developing an anatomical model prior to experimenting allows defining a network of regions to test. The anatomical model should show differential patterns of regional interactivity between patients and controls. Specific regions within the

brain areas defined in the anatomical model are selected from the activation map for areas where patients showed significantly greater activation than controls. The prefrontal regions are the primary areas of interest. Figure 2.4 is the anatomical model that follows from these regions. Three regions are specified in this model, however, the anterior cingulate can be further divided into two subregions, one in each hemisphere, resulting in four broad regions to test. The actual location of regions, i.e., coordinates, selected from the activation map are discussed in the next section. This anatomical model will be tested with functional connectivity.

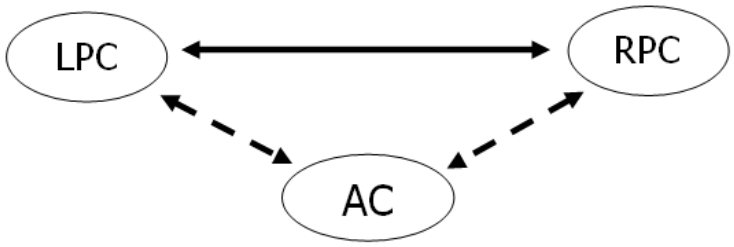

Figure 2.4: The anatomical model; LPC: left lateral prefrontal cortex; RPC: right lateral prefrontal cortex; AC: anterior cingulate; dashed lines: main connections of interest.

The same anatomical model will be tested with effective connectivity which will demonstrate directed influences. In addition to prefrontal connectivity we wish to study fronto-parietal effective connectivity. This done for two reasons from a modeling point of view. Given that the first anatomical model consists of four regions, only six connections in the model can be tested giving six degrees of freedom[8]. Additionally, model fit issues may arise with a network limited to four regions. Thus, known fronto-parietal circuitry deficits in HD and statistical reasons call for a second model in Figure 2.5 that will be examined with effective connectivity modeling. This anatomical model is a direct extension to the first anatomical model and allows testing of combined effects of prefrontal and fronto-parietal circuitry. The additional

[8]Calculated using $n \times (n\text{-}1) \div 2$, where n = number of regions

regions will be selected from the parietal lobe (both hemispheres) as these regions are also affected in HD (Rosas et al., 2003) and were present in the activation maps. Even though additional regions have been included in the second anatomical model below, the emphasis is on the anterior cingulate, the prefrontal cortex and overall connectivity with the anterior cingulate (dashed lines in Figure 2.5).

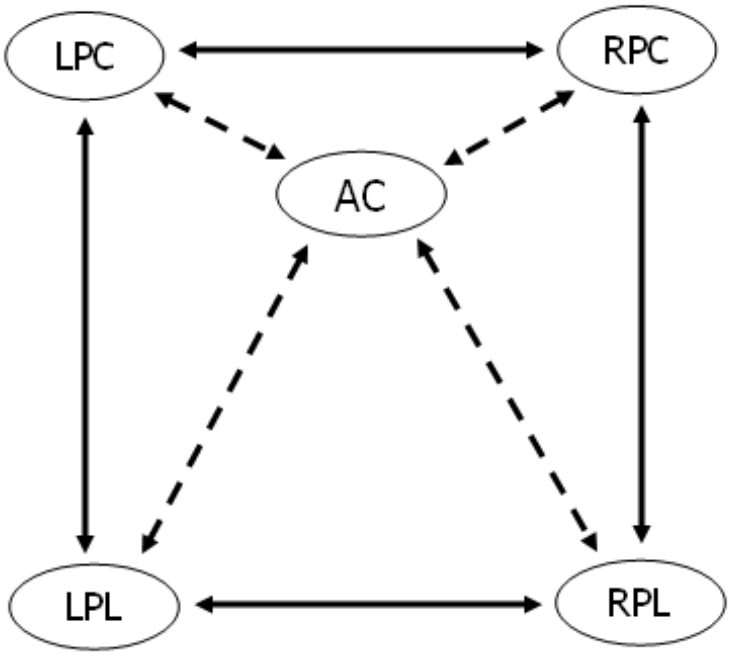

Figure 2.5: The extended anatomical model; LPC: left lateral prefrontal cortex; RPC: right lateral prefrontal cortex; AC: anterior cingulate; LPL: left parietal lobe; RPL: right parietal lobe; dashed lines: main connections of interest.

2.6 Regions of Interest

The activation maps showed hyperactivity in the anterior cingulate, prefrontal cortex and parietal lobes from which anatomical models were defined. The regions of interest (ROIs) were selected by observing the activation maps and defining ROIs around peak activation points.

An issue arises when selecting ROIs close to one another. For example, it is important to ensure that there is no overlap between between regions after considering smoothing effects. In this experiment, the smoothing kernel used is Gaussian with full width half maximum (FWHM) equal to eight. Hence, the centers of the ROIs need to be defined at least 16 mm apart. This will ensure that the signal obtained from the ROIs are distinct and that the functional and effective connectivity results are statistically valid.

ROIs have been defined by previous investigators in different ways, however a common method is to define a sphere of 4-16 mm diameter (Buchel and Friston, 1997; Mechelli, Penny, Price, Gitelman and Friston, 2002; Rowe, Stephan, Friston, Frackowiak, lees and Passingham, 2002). For this project, the ROIs were defined as a 6 mm radius sphere centered on a peak voxel (voxel with the highest z score) obtained from the activation maps. The activation map for patients greater than controls showed activation in the anterior cingulate (AC), prefrontal cortex (PC) and parietal lobe (PL) amongst other regions. From these regions the peak voxels selected were x = -10, y = 38, z = 22 (left AC), x = 38, y = 44, z = 16 (right PC) and x = -46, y = -48, z = 44 (left PL). See Figure 2.6, the intersection of the red crossbars indicates the location of the peak voxel chosen. These ROIs and the corresponding ROIs in the opposite hemisphere were selected to define the final set of ROIs. The AC ROIs are 20 mm apart and their signals should not affect one another. Therefore, the time courses will not be influenced by each other by the explanation provided earlier. The final set of ROIs are presented in Figure 2.7; (a) = AC; (b) = PC; (c) = PL. For modeling connectivity, the time course from each ROI was obtained and extracted so as to examine task and baseline related connectivity separately. These details follow.

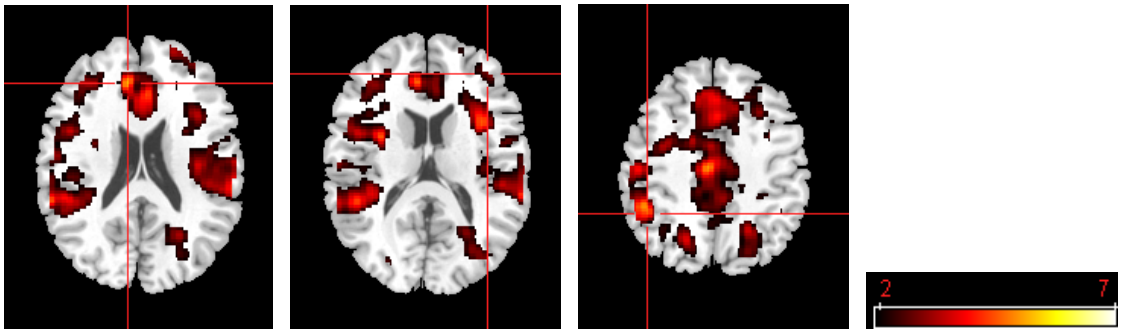

Figure 2.6: The ROIs in axial view. Intersection of the crossbars indicate precise location of the ROI where (a) Left AC, (b) Right PC, and (c) Left PL.

2.7 Time Course Selection

ROI time courses to be used for functional and effective connectivity can be extracted from the images in several ways. Different approaches have been used in the past (Bullmore, Horwitz, Honey, Brammer, Williams and Sharma, 2000; Honey, Fu, Kim, Brammer, Croudace, Suckling, Pich, Williams and Bullmore, 2002; Miller, Sun, Curtis and DEsposito, 2005), however, a common method to extract time courses is as follows (Buchel and Friston, 1997; Mechelli et al., 2002; Rowe, Stephan, Friston, Frackowiak, lees and Passingham, 2002).

A ROI is defined and the first eigenvariate of a principal components analysis for all the voxels in the ROI is used as the time course. This method can be implemented with SPM2 which corrects the time course for the effects of interest and serial correlations using an AR(1) model. The motion parameters were specified as regressors in the design and therefore the signals are corrected for motion related artifacts.

To assess connectivity, task related activity needs to be eliminated from the data points that make up a time course. Different methods have been previously used but two relevant methods are discussed here. One frequently used approach is to

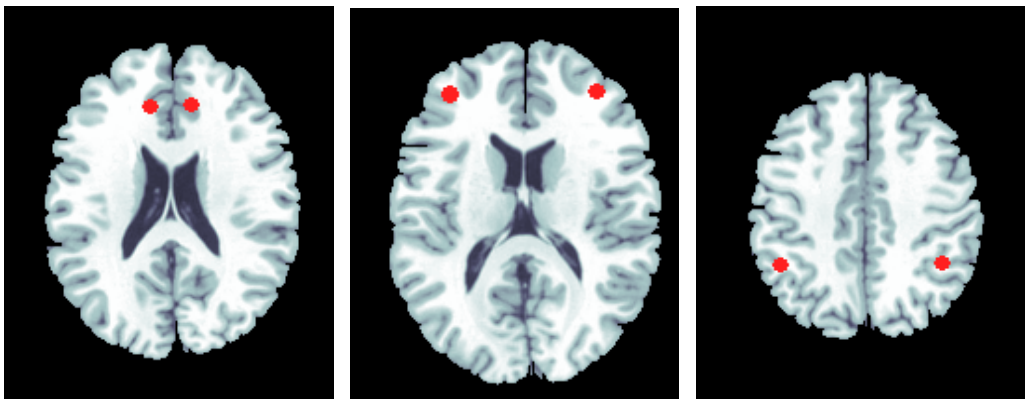

Figure 2.7: ROIs: (a) Left/right AC, (b) Left/right PC, and (c) Left/right PL.

extract a time course during a particular condition as it appears in the experiment design (Gavrilescu, Stuart, Waites, Jackson, Svalbe and Egan, 2004; Kemmotsu, Villalobos, Gaffrey, Courchesne and Muller, 2005; Miller et al., 2005). Other methods, to account for the rise in the HRF (see previous chapter), choose a delay period before extracting scans (Homae, Yahata and Sakaia, 2003; Just, Cherkassky, Keller and Minshew, 2004; Honey et al., 2002; Kondo, Osaka and Osakac, 2004). This is the approach selected for this project and is similar to Homae et al. (2003). While they move their time course forward by one scan (TR = 5 s) and eliminate the first scan, we have chosen to eliminate the first two (TR = 3 s). The data points are extracted from the task block (four points per task block) and concatenated across the four sessions for each subject. The time courses are then mean centered (Bullmore et al., 2000; Kondo et al., 2004) and will be free of task related changes. This is also done to obtain baseline time courses. Eliminating the first two scans during baseline allows for the HRF to undershoot and settle (i.e. activation effects from task performance are not carried over to baseline).

Functional connectivity studies have suggested that interactions between regional fMRI signals can be obtained from correlations between low frequency components

(less than 0.1 Hz) (Hampson, Peterson, Skudlarski, Gatenby and Gore, 2002; Kemmotsu et al., 2005; Lowe, Mock and Sorenson, 1998; Lowe, Dzemidzic, Lurito, Mathews and Phillips, 2000; Xiong, Parsons, Gao and Fox, 1999). This amounts to assessing connectivity just above the frequency as that of the task. Other studies have however suggested that important correlations can be be obtained from the high frequency components of the signals (Honey et al., 2002; Rowe, Stephan, Friston, Frackowiak, lees and Passingham, 2002; Whalley, Simonotto, Marshall, Owens, Goddard, Johnstone and Lawrie, 2005). In this thesis, the aim is to assess connectivity and in particular the fluctuations within the task and baseline blocks. Therefore high frequency components will be assessed and the method of time course selection outlined earlier allows for this.

For functional connectivity analysis, the time courses obtained above are compared between groups using two methods. Previous studies have concatenated each subject's time course (the direct method) within group. The second method is a meta-analytic approach using Q statistics (Hedges and Olkin, 1985) where a connectivity estimate is obtained for each individual within a group.

The direct method is a common method used and results are statistically significant given the large number of data points within a group. This method has some disadvantages, however. For example, across subject variability is likely to affect the group results and the correlation estimates may really be due to differences in the magnitude of regional activation across subjects. The meta-analytic approach accounts for these issues; however, a larger number of subjects is necessary to obtain significant differences between groups.

For effective connectivity using structural equation modeling (SEM), the first method of concatenating time courses across subjects within group is used. This results in statistically valid regression coefficients, but baseline connectivity is not examined as the number of baseline data points available are less than 2500. One of

the assumptions of the SEM method is that every variable in the model is Gaussian distributed. Hence before any modeling of the regional time courses is attempted they are assessed for normality. Under certain conditions non-normal data can be be modeled with SEM. For example, with a large sample size (> 2500) and either maximum likelihood or generalized least squares estimation methods, significantly non-normal distributions can be modeled (Hu and Bentler, 1992; Tabachnick and Fidell, 2001). The DCM method for effective connectivity analysis is conducted on each individual within group similar to functional connectivity with Q statistics.

In the current study, 640 images per subject (four sessions) were acquired. The resulting ROI time courses consist of 640 data points per subject. From this time course, the task related data at each ROI were selected by concatenating the task time points after eliminating the the first two scans (256 points per subject). These time courses were mean centered[9]. The baseline time course was obtained in a similar way (128 data points per subject). For the direct method all the time courses were concatenated across subjects within group (Table 2.4). The number of task data points are very large for controls and HD patients (> 4350) whereas the baseline condition had fewer data points (< 2500).

Table 2.4: Data points for task and baseline; (1) = Year one; (2) = Year two

	Controls	Patients (1)	Patients (2)
Task	4352	5120	2560
Baseline	2160	2414	-

[9]Note: the time courses were also detrended.

2.8 Conclusion

This chapter detailed the experimental design for this thesis. Some of the topics discussed were participants, data acquisition and image preprocessing which are a part of a previous HD fMRI functional activation study. This thesis aims to extend the data collected in the previous study by determining functional and effective connectivity based on the activation results. An algorithm to obtain activation maps from fMRI data is presented. Given the experimental design, the motivation for the experimental procedure used in this project is developed. In particular, the selection of ROIs and time course extraction were carefully considered as the final results will be affected by the methods chosen. Methods of functional and effective connectivity analysis are tested in the following chapters to see how the HD patient group differs from controls.

Chapter 3

Functional Connectivity

Functional connectivity studies have previously been conducted in fMRI to examine brain regional interactivity. In neuroimaging literature, functional connectivity refers to correlations in activations between brain regions (Friston, 1994a). This connectivity method provides quantifiable estimates of interactions between disparate brain regions which can be compared statistically between two or more populations. The definition of functional connectivity can be interpreted in different ways therefore methods to assess this type of connectivity vary.

Functional connectivity is not the same as functional activation and is usually considered as a second level analysis after activation results are known. Correlations that represent functional connectivity estimates are computed in different ways, but two commonly used methods obtain a correlation coefficient across subjects within a group or for each subject within a group. The correlations are usually computed during the performance of a task after eliminating functional activation effects (i.e., by allowing for the HRF delay) and the resulting correlations serve as functional connectivity estimates. Therefore it is possible to have high task-related activation at several regions but low functional connectivity between some or all of these regions. The estimates are not a direct measure of anatomical connectivity but

are representative of connections between regions, i.e., a high connectivity estimate between two regions does not necessarily imply a direct anatomical connection. It is possible that high connectivity is a result of the influence of a third region or that intermediate regions link these two regions. Therefore, functional connectivity describe direct or indirect influences of brain regions on others.

There are two main methods used in the fMRI literature to carry our functional connectivity analysis. Some studies use an exploratory approach by specifying a seed voxel (a voxel that is representative of a brain region) and correlate this voxel's time course with all other voxels in the brain (Bokde, Tagamets, Friedman and Horwitz, 2001; Cordes, Haughton, Arfanakis, Wendt, Turski, Moritz, Quigley and Meyerand, 2001; Homae et al., 2003; Rissman, Gazzaley and D'Esposito, 2004). In the second confirmatory method, an anatomical model is pre-specified and a correlation matrix is obtained for all the the regions included in the model (Gavrilescu et al., 2004; Grady et al., 2001; Rowe, Friston, Frackowiak and Passingham, 2002; Whalley et al., 2005). There are several issues to consider when specifying regions within an anatomical model, some of these were pointed out in the previous chapter.

An important consideration in functional connectivity analysis is in determining which correlations are significant. Statistically, very low correlations may be significant (e.g. using a one sample t test) as there are typically a large number of data points obtained across sessions for each subject. This may be true even after new threshold are computed after correcting for multiple comparisons (e.g. Bonferroni correction or False Discovery Rate). However, these correlations could arise due to noise components or smoothing effects and it is therefore important to consider using a threshold that will result in inferences made from biologically significant correlations. Several studies use statistically significant thresholds (Mizuhara, Wang, Kobayashi and Yamaguchi, 2005; Peltier, LaConte, Niyazov, Liu, Sahgal, Yue and Hu, 2005; Rissman et al., 2004) and corrected thresholds (Lowe et al., 1998; Welchew,

Ashwin, Berkouk, Salvador, Suckling, Baron-Cohen and Bullmore, 2005); however, others have applied further threshold levels (Bokde et al., 2001; Koshino, Carpenter, Minshew, Cherkassky, Keller and Just, 2005; Xiong et al., 1999). For example, Bokde et al. (2001) and Koshino et al. (2005) only report correlations above 0.4 which they consider biologically significant.

Time course selection was discussed in the previous chapter and the application of those methods will affect the functional connectivity estimates. Gavrilescu et al. (2004) have studied the effects of preprocessing strategies on functional connectivity estimates, in particular the effects of task-correlated motion. This is not an issue in this thesis as subjects movements did not correlate with the task. Connectivity will also be affected by global normalization. Some investigators use proportional scaling [the overall mean is used to scale each scan (Bokde et al., 2001)], however, this can result in changes that are opposite to the change in the global signal. To correct for this the time course can be mean normalized (Boksmana, Thebergea, Williamson, Drost, Malla, Densmore, Takhar, Pavlosky, Menon and Neufeld, 2005; Bullmore et al., 2000; Foucher, Vidailhet, Chanraud, Gounot, Grucker, Pins, Damsa and Danion, 2005; Kondo et al., 2004).

In this study, functional connectivity estimates that are representative of HD patients and controls are computed. The aim is to determine differences between the two groups by testing the relevant hypotheses given the anatomical model (i.e., a confirmatory approach). It is expected that significant differences within group (comparison of baseline versus task) and between group (patients and controls) will be seen. Interactions between prefrontal regions are expected to increase with the onset of each task block in both groups and task-related prefrontal functional connectivity is expected to be impaired in HD patients. Two statistical methods are considered that are commonly employed to compare functional connectivity estimates between two groups. These are the direct group comparison and the

meta-analytic method. The pros and cons of these two methods were provided in the previous chapter and the validity of each of these methods is tested here. An algorithm which specifies the steps to obtain functional connectivity from fMRI is also presented.

The results will be discussed in two parts. The first part relates to the methods used to obtain functional connectivity estimates by presenting the strengths and weaknesses of these methods. In particular, two methods for comparing groups is discussed. The second part will discuss implications to HD from the combined results obtained.

3.1 Methods

The confirmatory approach employed in this connectivity study is as follows. An anatomical model (ROIs and connections) was specified given prior knowledge of connectivity and the activation results (see Figure 3.1 for the functional connectivity model to be tested in this study). The time courses are then extracted from the ROIs and a correlation matrix for these time courses is computed (two different methods are used to obtain the correlation matrix). This is followed by testing the correlations for statistical significance. All correlations are reported, however, only those which are considered biologically significant ($r > 0.2$) are used to make inferences. Furthermore, high negative correlations were not considered (one-tailed test) because the aim is to determine differences between large positive correlations between the two groups[1]. The significant connectivity estimates are analyzed during task (comparison with baseline) and compared between groups using two different group comparison methods.

[1]High negative correlations between two regions show that are functionally disconnected, but given the regions chosen, it is expected that they will be connected.

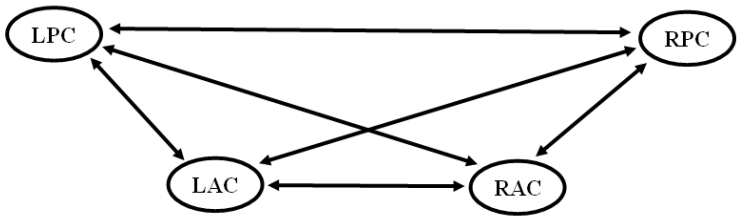

Figure 3.1: The functional connectivity model.

The methods used for identifying ROIs and selecting time courses were discussed in the previous chapter. To recapitulate, the ROIs are defined as 6 mm radius spheres centered on a peak voxel chosen from the activation maps. The time courses of the task condition at ROIs are extracted in two different ways. The first is to concatenate the task time points over all subjects within a group (see Table 3.1 for data points and corresponding thresholds). The second is to concatenate the task time points for each subject. The second method is a meta-analytic approach where Q statistics are used to compare the two groups. The baseline time courses are obtained in the same way.

Table 3.1: Data points and thresholds for task and baseline; s: per subject; thresholds for significance provided in parentheses ().

	Controls	Patients
Task^s	256	256
Baseline^s	119	119
Task	4352 (0.040)	5120 (0.037)
Baseline	2160 (0.057)	2414 (0.054)

3.1.1 Comparison Between Groups

Two methods were tested when comparing estimates between HD patients and controls. The first was the direct method where a single regional correlation coefficient

was obtained for each group. This is where all task-related data points across all subject are concatenated to form a single time course. In the second method, a regional correlation coefficient is calculated for each subject and averaged followed by within and between group analysis using Q statistics.

The Direct Method

Correlations between the time series of the ROIs were calculated for the task and baseline conditions. This method leads to a very large number of data points contributing to the correlations. Therefore the threshold for statistical significance was very low (see Table 3.1) and was not used. Alternatively, biologically significant correlations were identified as those coefficients which are equal to or greater than 0.2. To compare correlations between conditions and between groups the following test was used. Each correlation coefficient (r) was transformed using Fisher's z transformation:

$$r_z = \frac{1}{2} \times ln\left(\frac{1+r}{1-r}\right) \tag{3.1}$$

This normalizes the distribution of the correlation coefficient (r) and stabilized the variance of its distribution. To compare between baseline and task states a statistic r_{tb} for the difference between transformed correlation for task (r_t) and baseline (r_b) was calculated (Zar, 1997) according to:

$$r_{tb} = \frac{r_t - r_b}{\sigma_{t-b}} \tag{3.2}$$

where

$$\sigma_{t-b} = \sqrt{\frac{1}{n_t - 3} + \frac{1}{n_b - 3}} \tag{3.3}$$

Here, σ_{t-b} was the standard deviation and n_t and n_b were the number of task and baseline points respectively. The resultant statistic, r_{tb} was normally distributed.

In the same way the differences between controls and patients were measured (i.e., z_t was replaced by z_c and z_b was replaced by z_p).

Meta-Analysis

The meta-analytic method employed was an alternative to the direct method described above and it was a fixed effects meta analysis. This method was tested with the same data as the direct method to examine which method was more effective when inferring differences between two groups. Correlation coefficients were calculated for each subject[2] and they were compared within and between groups using Q statistics (Hedges and Olkin, 1985). See Table 3.1 for the number of data points.

For a homogeneity analysis (i.e., to test whether the correlation coefficients represent the same population) the following method using Q statistics was employed (Hedges and Olkin, 1985). A transformed correlation coefficient was computed for each subject according to equation 3.1. This stabilized the correlation coefficients. A corresponding inverse variance weight w was also computed which is an indication of the precision of the correlation coefficients. For Fisher's z transformation the inverse variance weight was set to:

$$w = n - 3. \tag{3.4}$$

where n was the sample size (i.e., number of subjects). Given these statistics, the Q statistic was as follows.

$$Q = \sum_{i=1}^{n}(w \times r_{iz}^2) - \frac{[\sum_{i=1}^{n}(w \times r_{iz})]^2}{n \times w}$$

$$df = n - 1 \tag{3.5}$$

[2]Correlations equal to or greater than 0.2 are considered significant.

where r_{iz} were the z transformed correlation coefficients. The resulting Q statistic was χ^2 distributed and this statistic can be used to determine whether the all the correlations tested come from the same population using a corrected significance level (e.g. $p = 0.05$). Within group connectivity variances are also plotted to compliment Q statistics results.

To test differences between two groups (heterogenous distributions), i.e., controls and HD patients, a method analogous to the ANOVA is used. A Q_t (total) statistic was calculated combining both groups (i.e., using correlation coefficients for all subjects within a group) using the method described above. The Q statistic for each group was also calculated obtaining Q_c and Q_p for controls and patients respectively. A within group Q_w statistic was calculated next:

$$Q_w = Q_c + Q_p$$

$$DF_w = n - j \tag{3.6}$$

where DF_w was the degrees of freedom, n was the number of subjects in one group and j was the number of groups. The Q statistic to measure differences between group was:

$$Q_b = Q_t - Q_w$$

$$DF_b = j - 1 \tag{3.7}$$

3.1.2 Functional Connectivity in fMRI: An Algorithm

The procedure described above, to estimate and compare functional connectivity, can be formalized as an algorithm (see Algorithm 2). The methods for comparison

result in two different procedures for computing correlations that are representative of regional connectivity for a group.

The parameters of Algorithm 2 are preprocessed data (P_n), subjects (S_n), groups (G_i), and regions (R_p, R_a). P_n is the preprocessed obtained for n subjects, S_n, from the activation studies algorithm (see Chapter 2). The subjects are divided into i groups, G_i, which may be one group if i is equal to one. From prior knowledge, p regions are identified which are expected to be activated, R_p, and R_a are the regions identified from the activation maps. The first two steps of the algorithm identify the final set of regions for connectivity analysis (R_f) and the ensuing anatomical model or models (AM_j with j possible models). The first part of the algorithm is to identify regional connectivity using the direct method. The second part is the procedure for meta-analysis, with a homogeneity analysis included. The last part of the algorithm compares groups using either the direct or meta-analytic methods.

3.2 Results

The results obtained from both methods are expected to be similar with minor differences. The interpretation of these results will follow in the discussion where both methods will be compared. Similarities and differences between methods will also be discussed.

3.2.1 Results: Direct Method

Significant connectivity observed in both groups is presented in Figure 3.2 (also see Table 3.2 and Table 3.3 for numerical values). Highest correlations in both groups are between the LAC and RAC (red line). These correlations ranged from 0.67 to 0.74, respectively. The connectivity between LPC and RPC was not significant, ranging

Algorithm 2: An algorithm for functional connectivity in fMRI using a confirmatory approach; comparison methods chosen are the direct method and meta-analysis.

Data: Preprocessed data: P_n, Subjects: S_n, Groups: G_i, Regions: R_p, R_a.
Result: Functional connectivity estimates across subjects; comparison between groups.

$R_f = R_a \cap R_p$;
$AM_j(R_f)$;
if *direct method or single group* **then**
    for $g \in G_i$ **do**
        for $r \in R_f$ **do**
            for $s \in S_n$ **do**
                extract time course: $T(P(s), r)$;
                concatenate time course: $CCAT(t(r), g, T)$;
            end
        end
        determine connectivity: $corr(g, t)$;
        statistical analysis: $Stat(g, corr)$;
    end
end
else
    for $g \in G_i$ **do**
        for $r \in R_f$ **do**
            for $s \in S_n$ **do**
                extract time course: $T(P(s), r)$;
                $corr(s, r) = corr(s, r) + T(P(s), r)$;
            end
            $corr(s, r) = corr(s, r) \div n(g)$;
        end
        homogeneity analysis: $H(g, T)$;
        statistical analysis: $StatQ(g, corr)$;
    end
end
if $i > 1$ **then**
    for $g \in G_i$ **do**
        compare groups: $C(corr, g, g + 1)$;
    end
end

from -0.13 to -0.03, respectively. The connection from LPC to RAC is statistically significant, however, since it is below the 0.2 threshold it is not considered (range: 0.09 to 0.18). All remaining connectivity is significant between the AC and PC regions ($r > 0.20$).

Table 3.2: Correlation matrix for controls - task and baseline states.

	Baseline				Task			
	RAC	LAC	RPC	LPC	RAC	LAC	RPC	LPC
RAC	1				1			
LAC	0.71 (*)	1			0.73 (*)	1		
RPC	0.50 (*)	0.22 (*)	1		0.52 (*)	0.32 (*)	1	
LPC	-0.01	0.20 (*)	-0.13	1	0.09	0.25 (*)	-0.03	1

Table 3.3: Correlation matrix for patients - task state and baseline states.

	Baseline				Task			
	RAC	LAC	RPC	LPC	RAC	LAC	RPC	LPC
RAC	1				1			
LAC	0.70 (*)	1			0.66 (*)	1		
RPC	0.38 (*)	0.30 (*)	1		0.37 (*)	0.31 (*)	1	
LPC	0.17 (*)	0.28 (*)	-0.06	1	0.16 (*)	0.20 (*)	-0.06	1

The connectivity changes from baseline to task are presented in Figure 3.3 (also see Table 3.4 for numerical values). The solid line represents an increase in connectivity in controls. The dashed line shows reduced functional connectivity from baseline to task in HD patients. These results show that controls recruit an inter-hemispheric connection to perform the task between LAC and RPC ($z = 4.32$, $p < 0.001$), whereas patients show reduced connectivity from baseline to task between and LAC and LPC ($z > 2.40$, $p < 0.05$). The changes while significant do not represent a major change from baseline to task.

A comparison of task related connectivity between the two groups is presented in Figure 3.4 (also see Table 3.5 for numerical values). The solid lines show increased

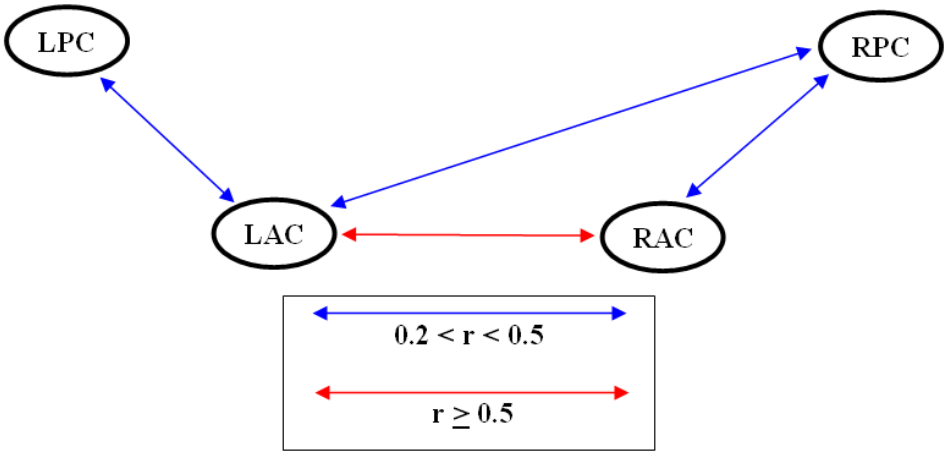

Figure 3.2: Significant functional connectivity.

Table 3.4: Matrix for task versus baseline states (r_{tb}); - : correlation not considered.

	Controls				Patients			
	RAC	LAC	RPC	LPC	RAC	LAC	RPC	LPC
RAC								
LAC	1.44				-2.4			
RPC	1.13	4.32 (*)			-0.3	0.08		
LPC	-	1.88	-		-	-3.17	-	

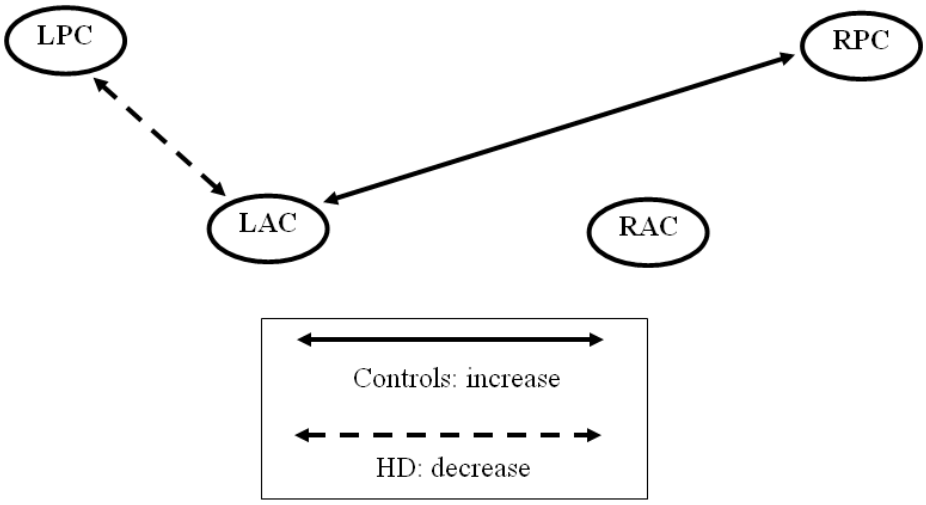

Figure 3.3: Connectivity changes from baseline to task. Solid lines: controls show increased connectivity; Dashed lines: patients show reduced connectivity.

connectivity in the control group or equivalently impaired connectivity in the patient group. Significantly reduced connectivity is seen in HD patients between the AC regions ($z = 6.38$, $P < 0.001$) and the AC and PC within hemispheres ($z > 2.14$, $P < 0.05$).

Table 3.5: Matrix for difference in task performance between controls and patients (r_{cp}) using the direct method; - : not considered.

	RAC	LAC	RPC	LPC
RAC				
LAC	6.38			
RPC	8.92	0.82		
LPC	-3.28	2.15	-	

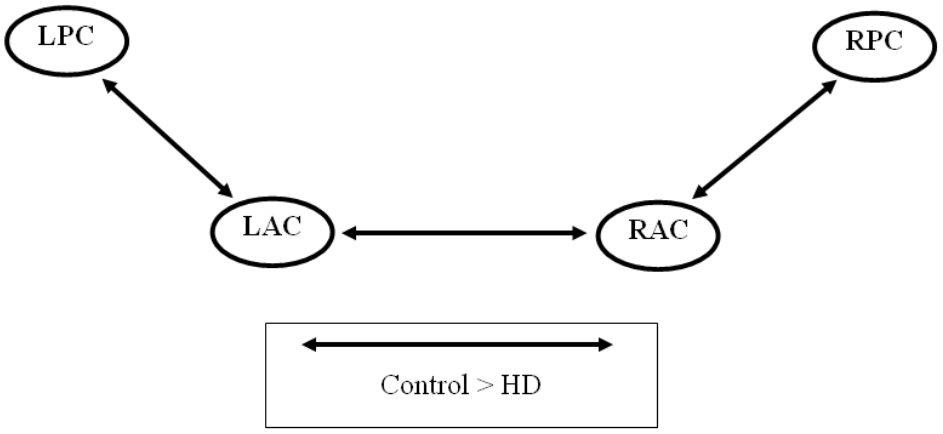

Figure 3.4: Difference in connectivity between HD patients and controls using the direct method.

3.2.2 Results: Meta-Analysis

In the control group, significant functional connectivity is seen between all ROIs except for the connections between RAC-LPC and RPC-LPC (Table 3.6). The same pattern of connectivity is also seen in the patient group (Table 3.7). Largest estimates of connectivity were between the AC ROIs (LAC-RAC). These results are similar to the direct method with Figure 3.3 representing the functional connectivity observed.

Table 3.6: Meta-Analysis: Correlation matrix for controls - baseline and task; significant correlations are marked with (*).

	Baseline				Task			
	RAC	LAC	RPC	LPC	RAC	LAC	RPC	LPC
RAC	1				1			
LAC	0.70 (*)	1			0.73 (*)	1		
RPC	0.45 (*)	0.20 (*)	1		0.52 (*)	0.34 (*)	1	
LPC	0.05	0.23 (*)	-0.05	1	0.15	0.28 (*)	0.05	1

Table 3.7: Meta-Analysis: Correlation matrix for patients - baseline and task; significant correlations are marked with (*).

	Baseline				Task			
	RAC	LAC	RPC	LPC	RAC	LAC	RPC	LPC
RAC	1				1			
LAC	0.67 (*)	1			0.67 (*)	1		
RPC	0.32 (*)	0.26 (*)	1		0.41 (*)	0.33 (*)	1	
LPC	0.10	0.22 (*)	0	1	0.16	0.21 (*)	0	1

Differences in functional connectivity estimates from baseline to task in both groups are non-significant. In controls, task-related connectivity is always higher than baseline for all significant connections, and in one case the difference is very large (LAC-RPC, difference = 0.14). In the patient group, all significant connections are higher in the task state except for the connection from LAC to LPC (difference = 0.01).

The comparison between controls and HD patients during task performance showed no significant differences in the functional connectivity estimates; however, these connectivity estimates were larger for controls compared to HD patients over all connections that were significant.

Homogeneity Analysis

To test for homogeneity in the control group Q statistics are used which are χ^2 distributed (DF = 16, see Appendix A for the matrices). The results show almost all of the functional connectivity estimates are consistent across subjects. Only one connection, LAC-RPC, is not homogeneous ($p < 0.05$), i.e., the correlation coefficients across all subjects for this connection is unlikely to have come from the same population. The Q statistics for HD patients show that most of the correlation

coefficients are variable across subjects except for four connection in the task state (RAC to LAC, RAC to LPC, RPC to LAC, LAC to LPC).

The graphs in Figure 3.5 and Figure 3.6 show the mean connectivity and variability, respectively, for all connections assessed in this study. The variance across all connections is highest for patients in baseline except for LAC-LPC where controls show higher variability during the baseline state compared to HD patients. The variability across all connections is lowest for controls during task performance except for the same connection (LAC-LPC) where patients during task performance exhibit lower variability. Connectivity within hemisphere is less variable in controls compared to patients between RAC-RPC but higher between LAC-LPC. For the connection between RAC-LAC controls exhibit lower variability than patients. Overall, the variability within group is higher for both baseline and task states for HD patients compared to controls.

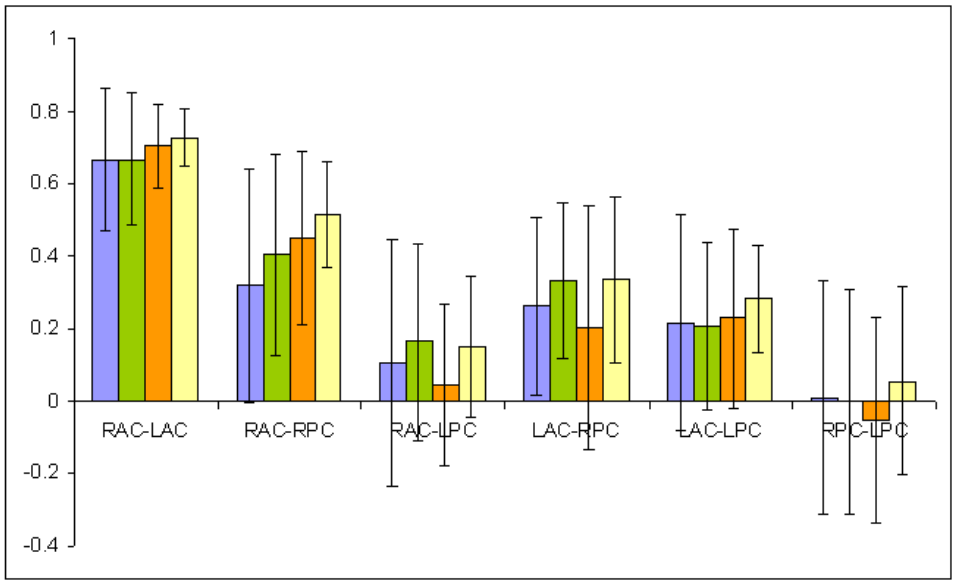

Figure 3.5: Mean connectivity within group for task and baseline; Purple bars: patients in baseline state; Green bars: patients during task performance; Orange bars: Controls in baseline state; Yellow bars: Controls during task performance.

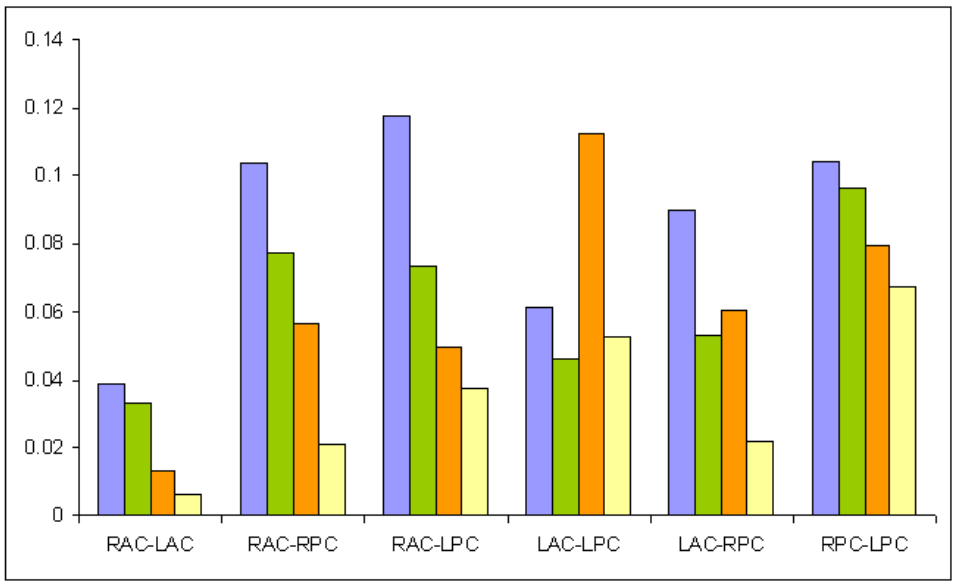

Figure 3.6: Variability of connectivity within group for task and baseline; Purple bars: patients in baseline state; Green bars: patients during task performance; Orange bars: Controls in baseline state; Yellow bars: Controls during task performance.

Correlating Functional Connectivity with Clinical and Behavioural Data

Correlations were performed on the six functional connectivity estimates obtained for each group with clinical and behavioural data (see Appendix B). None of the correlations were significant and are therefore not discussed. It is expected that with larger group sizes, significant effects may be seen.

3.3 Discussion

Using the Simon task in fMRI, functional connectivity between prefrontal ROIs was tested for controls and HD patients. The ROIs were identified from the functional activation maps and limited to those that appeared in the prefrontal regions that are known to be affected in HD (Lawrence et al., 1998). The interactions between these ROIs can be determined using functional connectivity by performing correlations

between the ROIs across subjects or individually for each subject. This distinction creates two different approaches to functional connectivity analysis, the direct and the meta-analytic methods, which are commonly used. In particular, these methods differ when comparing between two or more groups of subjects.

Results from the direct method showed significant connectivity representing inter- and intra-hemispheric connectivity between all ROIs except for the inter-hemispheric connections between the PC regions and RAC to LPC. This represents a high level of AC-PC connectivity. A significant increase in inter-hemispheric coupling was observed from baseline to task in controls (RPC-LAC), whereas patients showed a decrease in AC-PC connectivity in the left hemisphere for the same comparison. Comparing functional connectivity between the two groups during task performance revealed significantly increased inter-hemispheric connectivity between the AC ROIs and intra-hemispheric AC-PC connectivity in the control group, compared to HD patients.

The pattern of significant functional connectivity results with meta-analysis was similar to the direct method. Significant connectivity was seen between all prefrontal regions except between the two connections between the PC ROIs and RAC to LPC. Results obtained using Q statistics showed no significant differences between baseline and task for each group or between task-related connectivity for HD patients and controls. On close examination of the results it can be seen that only controls showed a large increase in inter-hemispheric connectivity from baseline to task between LAC and RPC. All significant connectivity was stronger in the control group compared to patients. The homogeneity analysis revealed that while functional connectivity estimates for controls are homogeneous across subjects this is not so with HD patients, particularly during the baseline state. The variability was mainly higher in patients except for the connection between LAC-LPC.

3.3.1 Comparison of Methods

The disadvantage of the direct method is that the correlation coefficients obtained could be could be influenced by changes between subjects rather than the temporal correlation between their time courses during task performance. The homogeneity analysis with Q statistics showed that this was not the case with controls except for one connection. Additionally, the plot of variance shows that correlations for controls are homogeneous. However, the same statistics for HD patients showed that differences between the subjects could contribute to the correlations observed. This is expected as the rate of deterioration across subjects would vary given their C-A-G repeat length and age at onset. These results indicate that care should be taken in interpreting results when concatenating time courses especially for patient populations.

While individual changes do not affect meta-analysis it can be seen that obtaining significant statistics requires large differences in correlation coefficients or the population sizes have to be very large. The results obtained from both methods are not dissimilar and inferences about HD can be made combining them. Note that only those connectivity estimates that are biologically significant were considered.

3.3.2 Functional Connectivity: Implications for HD

Regional interactions measured with functional connectivity show that to perform the Simon task, controls require increased coupling between ROIs (between LPC and RAC). During the performance of a cognitive task, previous studies have shown increased connectivity between prefrontal cortical regions (Egner, Jamieson and Gruzelier, 2005; Grady et al., 2001; Lowe et al., 2000; Valet, Sprenger, Boecker, Willoch, Rummeny, Conrad, Erhard and Tolle, 2004). The same is not true with HD patients who conversely show a loss of synchrony during task performance at

an intra-hemispheric level between the left AC and left prefrontal region. This is despite increased activation seen at these regions during task performance which shows that patients fail to dynamically increase coupling during task performance.

In HD, degeneration of brain regions affects cortical circuits which results in loss of cognitive, motor and executive functions (Lawrence et al., 1998). The loss of synchrony seen suggests prefrontal regional interactions are compromised in HD. This is consistent with previous knowledge regarding the neuropathology of HD, and strongly supports the notion of deficits in prefrontal circuitry (Dursun et al., 2000; Schmidtke et al., 2002).

During task performance, HD patients show significantly reduced connectivity between the AC regions and the AC and PC regions within hemisphere compared to controls. This impaired connectivity is consistent with prior research with neurodegenerative diseases such as Alzheimer's or Parkinson's diseases (Grady et al., 2001; Lekeu et al., 2003; Murphy et al., 2005; Rowe, Friston, Frackowiak and Passingham, 2002; Winterer et al., 2003). Furthermore, the homogeneity meta-analysis and variability analysis within group showed that interactions between all prefrontal regions are more variable in HD patients compared to controls. This is expected and patients who are more severe are likely to exhibit reduced connectivity compared to those who are the initial stages of the disease. However, this was not clear from the correlations carried out with connectivity and clinical data.

Overall the functional connectivity results illustrate that functional interactions between critical ROIs, necessary for cognitive performance, may be compromised in HD. This may be due to neuronal cell death since inputs and outputs between certain regions are compromised (Lawrence et al., 1998). Furthermore, previous studies have shown white matter volumetric loss in cortical and subcortical areas (Halliday et al., 1998; Rosas et al., 2003) which may account for the impaired connectivity seen. The increased prefrontal activity seen in HD patients compared to controls

could arise to compensate for the impaired interactivity between these regions (i.e., several regions' activities may be mutually restricted given that they are well interconnected).

Chapter 4

Effective Connectivity: Structural Equation Modeling

In Chapter 1, effective connectivity and studies conducted with SEM were reviewed. Effective connectivity is an extension of functional connectivity and is defined as the influence of one neuronal system on another. In fMRI this method is implemented by estimating directed connection strengths from the covariance of brain regional BOLD responses. The estimated connection strengths serve as a quantitative measure of brain region interactions and can be used to distinguish two or more groups of subjects. To determine regional interactivity modeling methods that have been used are structural equation modeling (SEM), multivariate autoregressive modeling (MAR), and dynamic causal modeling (DCM).

In this study SEM is used to identify prefrontal and fronto-parietal interactions in controls and HD patients during the performance of the Simon task. The primary aim is to make inferences about SEM. This involves assessing a part confirmatory - part exploratory approach with fMRI data, comparison with functional connectivity, and usefulness of an exploratory approach in analyzing longitudinal data. The hypothesis states that a combined confirmatory and exploratory approach to

determining interactions will provide useful information to distinguish two groups of subjects. Furthermore, it is hypothesized that the same approach will be useful in assessing connectivity changes over time. A secondary aim of this study is to make inferences about the pathology of regional connectivity in HD.

The data used in this thesis is acquired from a longitudinal study. While only first year data was discussed and examined in the previous study on functional connectivity, this study makes use of a limited amount of second year data to make inferences about SEM and HD. The analysis of second year data is restricted to HD patients (as regional deterioration and associated connectivity changes are expected in HD) and the data available is limited as only 11 second year patients have been scanned thus far. The data from the same 11 patients in first year will be used to compare the two groups (patients in year one with patients in year two). This is to identify differences between the same HD patients in their performance of the Simon task in the first and second year of this study.

This chapter is outlined as follows. The details of the SEM technique are first provided. Then the application of SEM to fMRI is discussed with a focus on modeling connectivity in this experiment. The procedure to do this is presented as an algorithm in the methods section. The anatomical model, and its extension as defined in Chapter 2, are tested with SEM and the ensuing results are presented. This chapter concludes with a discussion of the SEM technique and its application to the HD fMRI data.

4.1 SEM Nomenclature

Brain regions in a structural equation model are represented as independent and dependent variables. Each variable is either measured (observed) or latent (no measurements available). Latent variables are common in the social sciences, whereas in

neuroimaging we only deal with measured variables. The relationship between dependent and independent variables is defined by estimating a weight of contribution of the each independent variable to the dependent variable. In other words, the variance at one region as accounted for by weighted variances of other regions that are expected to influence it (either specified through an anatomical model, or revealed from the data, or both). Variables that are independent in one relationship maybe dependent in a second relationship. Any variable that is dependent throughout a model is known as an endogenous variable whereas a variable that is independent with respect to all relationships is called exogenous.

The result of modeling with SEM is a DAG with estimated directional path coefficients. These estimates which describe regional interactions are a quantitative measure of effective connectivity in fMRI. The estimates can be unstandardized or standardized. The unstandardized estimates describe the change in the dependent variable (in units) for a unit change in the independent variable with all other variables held constant. Alternatively, the estimates can be reported as standardized, which is the change in standard deviations (in units) of the dependent variable for a unit standard deviation change in the independent variable.

The directional path coefficients obtained from an SEM analysis are usually tested for significance to determine if a good model fit is achieved. To assess model fit the chi-square (χ^2) index is usually examined followed by other goodness of fit indices (GFIs). The GFIs are usually complimentary and are reported to confirm the findings from the χ^2 fit of the model. Each path coefficient divided by its standard error determines whether a path coefficient is significant or not.

There are usually two approaches when applying techniques to fMRI data. The first is a confirmatory approach where a theoretical model (defined from prior knowledge) is tested with the data and is accepted if a good fit is obtained[1]. In the second

[1]Some studies do not require good fit but still assess connectivity.

method, the combined confirmatory and exploratory method, an anatomical model is defined from prior knowledge but the relationships between brain regions are determined from the data. A theoretical model is first developed and tested with the data. If a good model fit is not achieved, modification indices are used to define directional connections between regions so that a good model fit may be obtained (Bullmore et al., 2000). Modification indices are a measure that specify a change in the χ^2 fit of the overall model if a particular path in the model is set as a free parameter. For each possible parameter in the model (path coefficient and error terms) the first and second-order partial derivatives are used to compute modification indices. Care must be taken to make sure that new paths included in a model are biologically feasible. The paths included in a model using modification indices provides a useful method to identify biologically feasible models.

After a satisfactory model is obtained, the next step is to compare models between two groups. Mentioned earlier, the aim in neuroimaging is usually to compare two groups of subjects. The nested (stacked) model approach has been used in previous studies (Mclntosh and Gonzalez-Lima, 1994) and is a commonly used method in fMRI (e.g. (Bullmore et al., 2000)). The models defined for both groups (may have different anatomical connections) are constrained to be equal. A combined χ^2 value and a combined degrees of freedom are obtained. Then the models are allowed to vary and a new χ^2 value and degrees of freedom are obtained. The difference between the two χ^2 values follows a χ^2 distribution with degrees of freedom equal to the difference in degrees of freedom obtained for both models. The resultant probability value is compared with a significance level (typically $p = 0.05$). If the p value is less than 0.05 then the null hypothesis is rejected (the null hypothesis states that both models are equal) and we can infer that the models for the two groups are significantly different.

Each connection between groups can also be compared similarly. All the connections in the model are constrained to be the same except the connection to be tested which is allowed to vary. The difference between the χ^2 values and degrees of freedom can be compared as described above. This method provides a feasible way to test differences in longitudinal data from different years of a study.

The relationships between brain regions in SEM are linear in nature. That is, the model assumes linear influences of brain regions on others and the unexplained variance at a region is accounted for by residuals. Furthermore, SEM requires that temporal information is removed from the data, i.e it is an instantaneous model. While this is a limitation of SEM, the temporal resolution of fMRI is not very high (e.g. two or three seconds) and temporal changes below this resolution will not be captured in the data. Therefore the SEM technique does not lead to a significant loss of information with current fMRI data.

4.2 Mathematical Notation

Using the covariance structure of the data the connection strengths are estimated. SEM tests the discrepancy between the covariance matrix predicted by the the theoretical model [M(a)][2] and the observed interregional covariance matrix (C). The following mathematical notation is similar to that of McIntosh and Gonzalez-Lima (1994) and Bullmore et al. (2000) [for an extensive treatment see (Bollen, 1989)]. This relationship is mathematically described by the following linear equation:

$$y = \alpha + \beta_{y.x} x + e \tag{4.1}$$

[2] a_j are the non-zero path coefficients.

This equation is an example of a relationship between a single independent variable (x) and dependent variable (y). Here, y and x are brain regions, $\beta_{y.x}$ is the influence of x on y and is a path coefficient, α is the y intercept and e accounts for the variance of y not accounted for by x. Additional brain regions can be included within equation 4.1 as independent variables. For example, if it is known that region z influences region y then equation 4.1 would change to:

$$y = \alpha + \beta_{y.x}x + \beta_{y.z}z + e \tag{4.2}$$

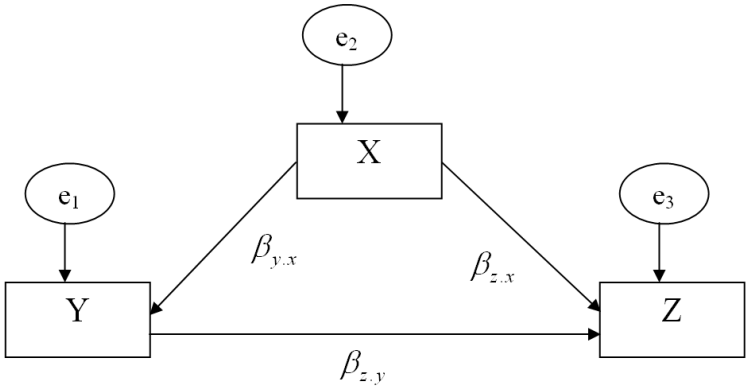

Figure 4.1: An SEM between three brain regions

An example of an SEM between three regions is illustrated in Figure 4.1. The connections (βs) could have been specified through prior anatomical knowledge or determined from the data. There is one exogenous variable (x) and two endogenous variables (y and z) in this model. The equations that describe the SEM above are:

$$x = e_2 \tag{4.3}$$

$$y = \beta_{y.x}x + e_1 \tag{4.4}$$

$$z = \beta_{z.x}x + \beta_{z.y}y + e_3 \tag{4.5}$$

The equations above can be represented in matrix form as:

$$\begin{pmatrix} x \\ y \\ z \end{pmatrix} = \begin{pmatrix} 0 & 0 & 0 \\ \beta_{y.x} & 0 & 0 \\ \beta_{z.x} & \beta_{z.y} & 0 \end{pmatrix} \times \begin{pmatrix} x \\ y \\ z \end{pmatrix} + \begin{pmatrix} e_2 \\ e_1 \\ e_3 \end{pmatrix} \tag{4.6}$$

or simply as:

$$R = \beta R + E \tag{4.7}$$

Given n regions, the components of R ($n \times 1$ vector) represent regional variances, β is the $n \times n$ matrix of path coefficients, and E is $n \times 1$ residual vector. Equation 4.7 can be written as

$$R = (I - \beta)^{-1}E \tag{4.8}$$

The McArdle-McDonald equation gives the predicted correlation matrix:

$$M(a) = (I - \beta)^{-1}EE^T[(I - \beta)^{-1}]^T \tag{4.9}$$

The estimation of the βs is done iteratively by minimizing the maximum likelihood (ML) function according to:

$$ML = log|M(a)| + tr(CM^{-1}(a)) - log|C| - n \tag{4.10}$$

where n is the number of connections (free parameters), $|.|$ denotes the determinant of a matrix, and tr is the trace operator[3].

The observed and predicted covariance matrices are compared at each iteration. The ML function is minimized and re-calculated at each step by setting the path

[3]M(a) is the estimated covariance matrix and C is the observed covariance matrix.

coefficients as free parameters. The ML function is asymptotically χ^2 distributed and for q free parameters is χ^2 distributed with $\frac{n\times(n+1)}{2}$ degrees of freedom. ML is represented by a probability value which tests the null hypothesis that the observed covariance matrix is the same as the predicted covariance matrix ($p > 0.05$ implies that a model fits the data well).

4.3 Methods

The activation maps for a random effects group analysis for patients greater than controls were used to identify the ROIs. They were defined as 6 mm radius spheres centered around peak activation voxels. From these ROI time courses those data points that correspond to the task state were extracted and concatenated across all subjects within group. The resultant time courses were analyzed using SEM (AMOS 4.0, www.smallwaters.com). For further details on ROI and time course selection see Chapter 2.

To test the anatomical model the ROIs were used as a starting point (confirmatory part). Connections were identified as those ones that best describe the data (exploratory part). The method used was the same one suggested Bullmore et al. (2000), who started with a model where path coefficients were set to zero. Then they used modification indices to build up a model by setting the path coefficient for the largest change in the χ^2 value free at each step. Models built this way tend not to contain any bidirectional links, this was compensated for by indirect influences.

The first connection incorporated in the model was between the AC ROIs (this connection was chosen as it had the highest functional connectivity estimate, see previous chapter). To determine the direction of this connection (LAC→RAC or RAC→LAC) each connection was included individually in the model and tested to see which one described the data best (i.e., incorporating that connection which led

to a lower χ^2 value). This connection was set as the starting point for the model. Modification indices were then used to build the model[4].

The effective connectivity estimates are all reported, however only those that were equal to or greater than 0.2 were considered biologically significant and are discussed. This is also consistent with the previous study. This makes sure that very small path coefficients, although significant (due to the large amount of data available), were not considered to make inferences about HD. After building a model it is assessed for goodness of fit and the results are reported with a χ^2 value followed by a probability level. The probability level indicates whether or not the data fits the theoretical model with a high probability (i.e., a low χ^2 value) implying a good model fit. Accompanying goodness-of-fit statistics are reported in the Appendix C. The following descriptions of the GFI statistics were obtained from (Arbuckle, 2003; Tabachnick and Fidell, 2001).

The root mean square residual (RMR) are the average differences between observed and estimated variances and covariances. Models with good fit tend to have small RMR statistics. The goodness-of-fit index (GFI) is the weighted proportion of the observed variance accounted for by the estimated variance. A statistic close to the value 1.00 indicates good model fit with 1.00 being a prefect fit. The root mean square error of approximation (RMSEA) estimates the fit of a model compared to a saturated model (a model that is said to have perfect fit). Good fitting models have values less than 0.06 where poor fitting models tend to have values greater than 0.11. Akaike information criterion (AIC) and Bayesian information criterion (BIC) consider model parsimony. The model with the smallest AIC statistic is the most parsimonious model. BIC tends to penalize complex models and has a greater tendency to pick parsimonious models.

[4]Note that each new connection incorporated into the model was examined for biological feasibility.

To compare between the models between HD patients and controls the nested or stacked models approach was used (Mclntosh and Gonzalez-Lima, 1994). A ${\chi_c}^2$ statistic for controls was first obtained after developing the model. In the same way a second ${\chi_p}^2$ statistic was calculated for HD patients. The difference between the χ^2 values and degrees of freedom for both groups was calculated as:

$$\chi^2_{diff} = \chi^2_c - \chi^2_p \tag{4.11}$$

$$DF_{diff} = DF_c - DF_p \tag{4.12}$$

where DF_c and DF_p were the degrees of freedom for the control and HD patient models respectively. In a similar way the models for the first and second year data (HD patients) were built and compared (e.g. ${\chi_c}^2$ becomes ${\chi_{p1}}^2$ and ${\chi_p}^2$ becomes ${\chi_{p2}}^2$). The numerical results of the comparisons are presented in Appendix D. The data available to compare patients in the first and second year of task performance was limited to 11 patients. For all these comparisons models were considered similar if the anatomical connections obtained were the same but the relative strengths of these connections may vary[5]. The models are considered different if the connections themselves differ.

4.3.1 Effective Connectivity Using SEM: An Algorithm

A similar algorithm to functional connectivity is used to obtain connectivity using SEM (see Algorithm 3). The time course selection is based on the direct method and comparisons between group are based on the nested models approach.

[5]Note that models may be statistically different.

Algorithm 3: An algorithm for effective connectivity using SEM; the same approach can be used to determine differences in models over time.

Data: Preprocessed data: P_n, Subjects: S_n, Groups: G_i, Regions: R_p, R_a.
Result: Effective connectivity estimates across subjects; comparison between groups.

```
1  R_f = R_a ∩ R_p;
2  AM_j(R_f);
3  for g ∈ G_i do
4      for r ∈ R_f do
5          for s ∈ S_n do
6              extract time course: T(P(s), r);
7              concatenate time course: CCAT(t(r), g, T);
8          end
9      end
10 end
11 for g ∈ G_i do
12     for r ∈ R_f do
13         if confirmatory approach then
14             determine connectivity: CON(g, t, AM);
15             statistical analysis: Stat(g, CON);
16         end
17         else
18             determine connectivity: CON(g, t);
19             statistical analysis: Stat(g, CON);
20         end
21     end
22 end
23 if i > 1 then
24     for g ∈ G_i do
25         compare groups: C(corr, g, g + 1);
26     end
27 end
```

The parameters of algorithm 3 are preprocessed data (P_n), subjects (S_n), groups (G_i), and regions (R_p, R_a). P_n is the preprocessed obtained for n subjects, S_n, from the activation studies algorithm (see Chapter 2). The subjects are divided into i groups, G_i, which may be one group if i is equal to one. From prior knowledge, p regions are identified which are expected to be activated, R_p, and R_a are the regions identified from the activation maps. The first two steps of the algorithm identify

Table 4.1: Assessment of normality for controls; c.r. = critical ratio; Min: minimum and Max: maximum; Kur: kurtosis.

	Controls						Patients					
	Min	Max	Skew	c.r.	Kur.	c.r.	Min	Max	Skew	c.r.	Kur.	c.r.
RAC	-11.4	6.7	-0.77	-22.4	11.10	162.1	-4.5	5.02	-0.61	-16.4	2.96	39.9
LAC	-9.5	7.9	-0.49	-14.2	8.57	125.2	-4.0	3.56	-0.68	-18.4	2.21	29.8
RPC	-9.3	8.0	-0.15	-4.5	8.08	117.1	-5.8	6.67	0.31	8.3	6.18	83.2
LPC	-9.3	12.4	0.06	1.7	9.83	143.6	-7.2	5.83	-0.29	-7.7	4.54	61.2
RPL	-9.1	9.8	0.52	15.3	12.90	188.5	-3.4	3.70	-0.31	-8.2	1.83	24.7
LPL	-7.0	12.0	0.32	9.2	10.06	146.9	-4.3	4.09	-0.44	-11.8	2.48	33.4

the final set of regions for connectivity analysis (R_f) and the ensuing anatomical model or models (AM_j with j possible models). The first part of the algorithm is used to determine the regional time courses to be used for effective connectivity. The second part of the algorithm determines connectivity and performs statistical analysis within each group. The third part of the algorithm compares groups using stacked models approach. Note that when comparing models over time, each model for a time period can be considered as a group and the analysis can proceed as described in the algorithm.

4.4 Results

4.4.1 Data Normality

See Table 4.1 for normality of regional time courses in controls and HD patients. Columns five, seven, 11, and 13 are critical ratios which are equal to the statistic in the previous column divided by its standard error (e.g. in controls for RAC the critical ratio for the skewness is -0.77). Given the skewness and kurtosis critical ratios it appears that none of the regional time courses are Gaussian distributed for this data (consequences are discussed in the discussion section).

Table 4.2: Covariance matrix for controls and HD patients.

	Controls						Patients					
	RAC	LAC	RPC	LPC	RPL	LPL	RAC	LAC	RPC	LPC	RPL	LPL
RAC	0.72						0.91					
LAC	0.53	0.71					0.59	0.85				
RPC	0.36	0.23	0.68				0.37	0.30	1.096			
LPC	0.08	0.20	-0.03	0.95			0.20	0.25	-0.08	1.70		
RPL	0.22	0.17	0.26	0.23	0.58		0.22	0.24	0.33	0.27	0.96	
LPL	0.25	0.29	0.10	0.23	0.19	0.56	0.23	0.22	0.08	0.31	0.28	1.00

4.4.2 Task Connectivity - Year One

Connection weights in an SEM are estimated by minimizing the maximum likelihood discrepancy function between the observed interregional covariance matrix and the expected covariance matrix. The observed covariance matrices are presented in Table 4.2.

The SEM obtained for 17 controls is presented in Figure 4.2. The model fit is very good ($\chi_c{}^2 = 0.003$, $p = 0.955$) [6]. The first connection incorporated was the link between the AC ROIs (RAC→LAC = 0.79). This is also the connection with the highest connectivity estimate. High within hemisphere AC-PC connectivity is seen in this model (LAC→LPC = 0.44, RPC→RAC = 0.55); whereas all inter-hemispheric connectivity is negative between these regions ($r < 0.00$). The AC-PL connectivity reveals only one significant intra-hemispheric connection (LAC→LPL = 0.26) with the link from RPL to RAC unique to this model ($r = 0.16$). Between the PL ROIs low significantly connectivity is also seen (RPL→LPL = 0.22). The PC-PL connectivity shows two significant connections; one intra-hemispheric link from RPC to RPL ($r = 0.43$) and one inter-hemispheric link from LPC to RPL ($r = 0.23$). There are no bidirectional connections in this model.

[6] See Appendix C for accompanying GFI statistics.

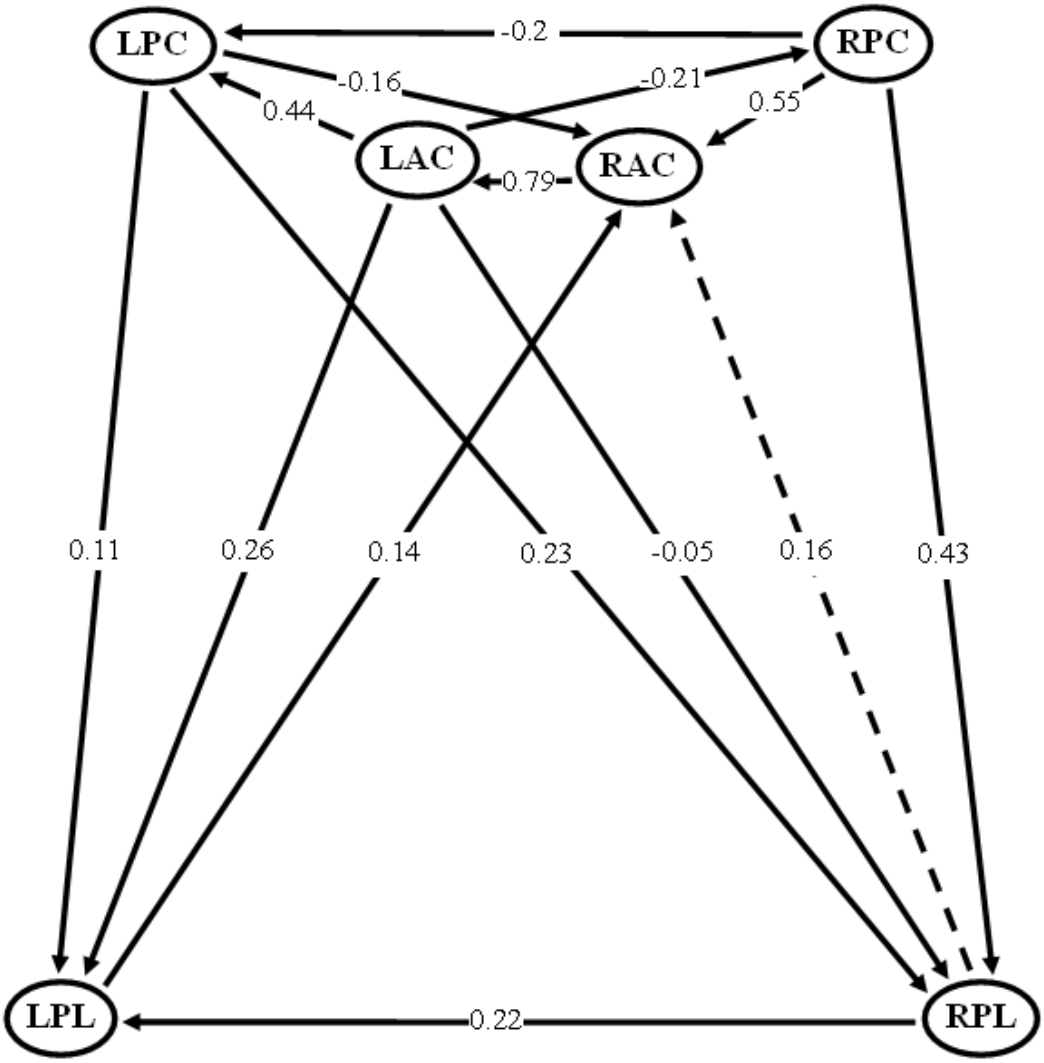

Figure 4.2: Model derived for control group; solid lines: connectivity common with HD patients; dashed lines: connectivity unique to controls.

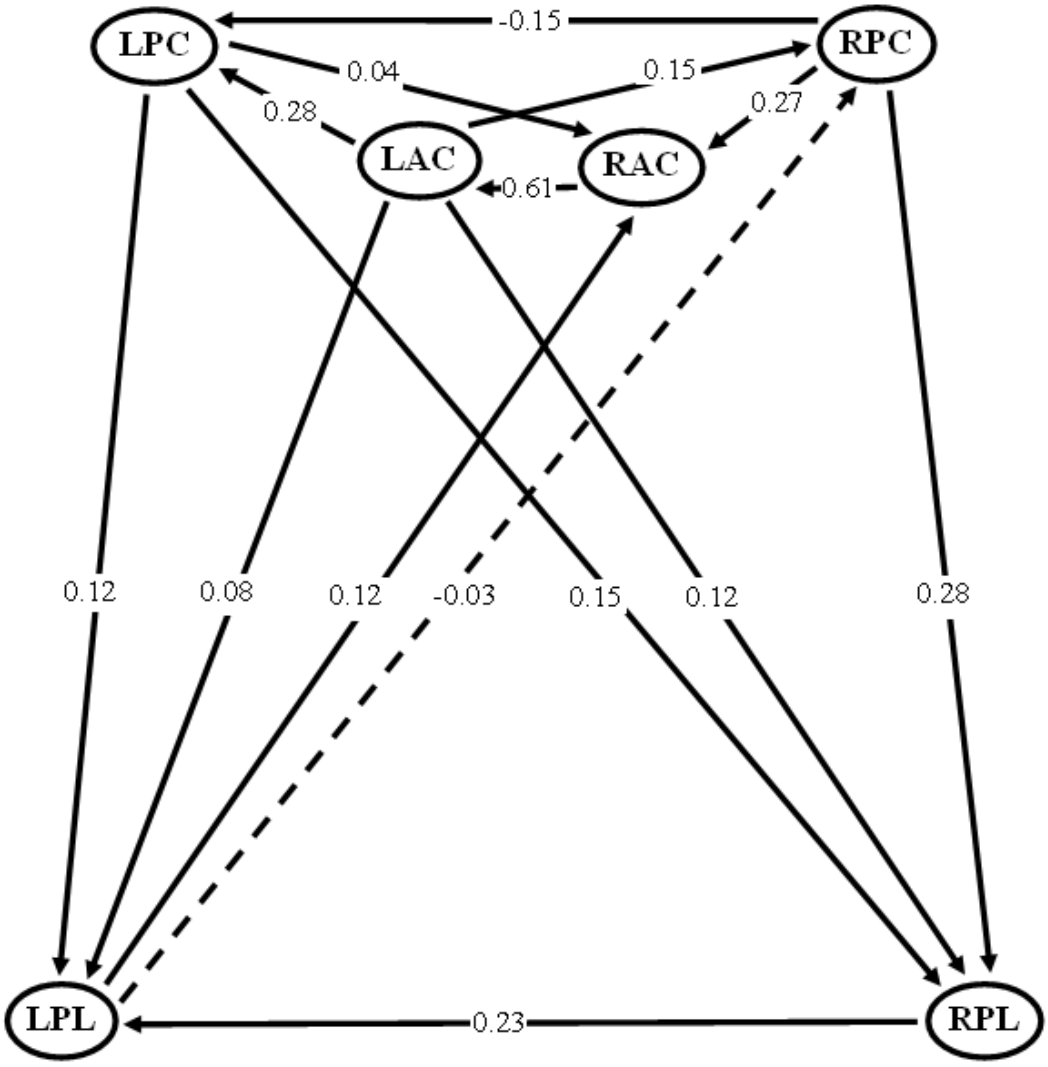

Figure 4.3: Model derived for patient group; solid lines: connectivity common with HD patients; dashed lines: connectivity unique to HD patients.

For 20 HD patients the SEM is presented in Figure 4.3. The model fit is also very good ($\chi_c{}^2 = 0.72$, $p = 0.396$). Again, the first connection incorporated was the link between the AC ROIs (RAC→LAC = 0.61) which resulted in the highest connectivity estimate. High within hemisphere AC-PC connectivity can also be seen in this model (LAC→LPC = 0.28, RPC→RAC = 0.27) and the inter-hemispheric connectivity is either negative or non-significant between these regions ($r < 0.15$). There is no significant connectivity between the AC-PL regions ($r < 0.15$) with the link from RPL to RAC missing in this SEM compared to the control group SEM. Between the PL ROIs significantly connectivity is seen similar to the controls model (RPL→LPL = 0.23). There is only one significant intra-hemispheric connection between the PC-PL regions from RPC to RPL ($r = 0.28$). One connection in this model is not present in the controls model (LPL→RPC = -0.03). There are no bidirectional connections in this model.

Stronger connectivity seen in controls is presented in Figure 4.4 (see Appendix D for measurements). Connectivity estimates for controls are always stronger for common significant connections except for two links (RPL→LPL and LAC→LPL). HD patients showed no increased connectivity compared to controls. The link LPL→RPC is not present in the controls model and it is non-significant.

To compare results with functional connectivity the following models are built exclusively between the AC and PC ROIs without consideration of model fit. Figure 4.5 shows the models derived using modification indices between the AC and PC regions. Again, the first connection included was the link from RAC to LAC ($r > 0.64$). The biologically significant connections parallel the results see earlier (Figure 4.2 and 4.3) with significant connectivity seen within hemisphere from LAC to LPC ($r > 0.28$) and RPC to RAC ($r > 0.34$). The differences between controls and patients are similar to the results seen earlier (see Figure 4.5 (c)). There is one connection that is stronger in patients; however, the connection was non-significant.

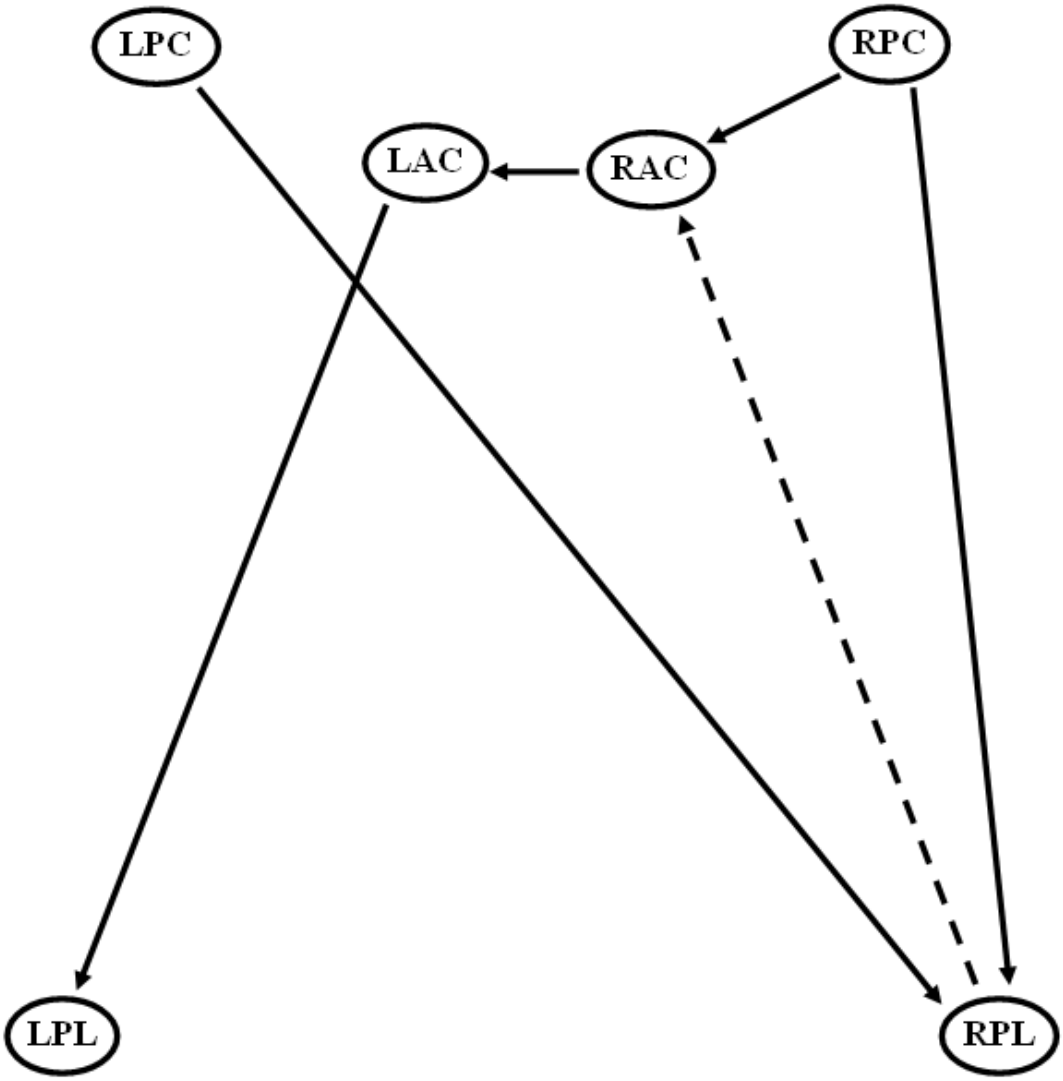

Figure 4.4: Difference in connectivity: solid lines: controls show stronger connectivity; dashed lines: connectivity unique to controls.

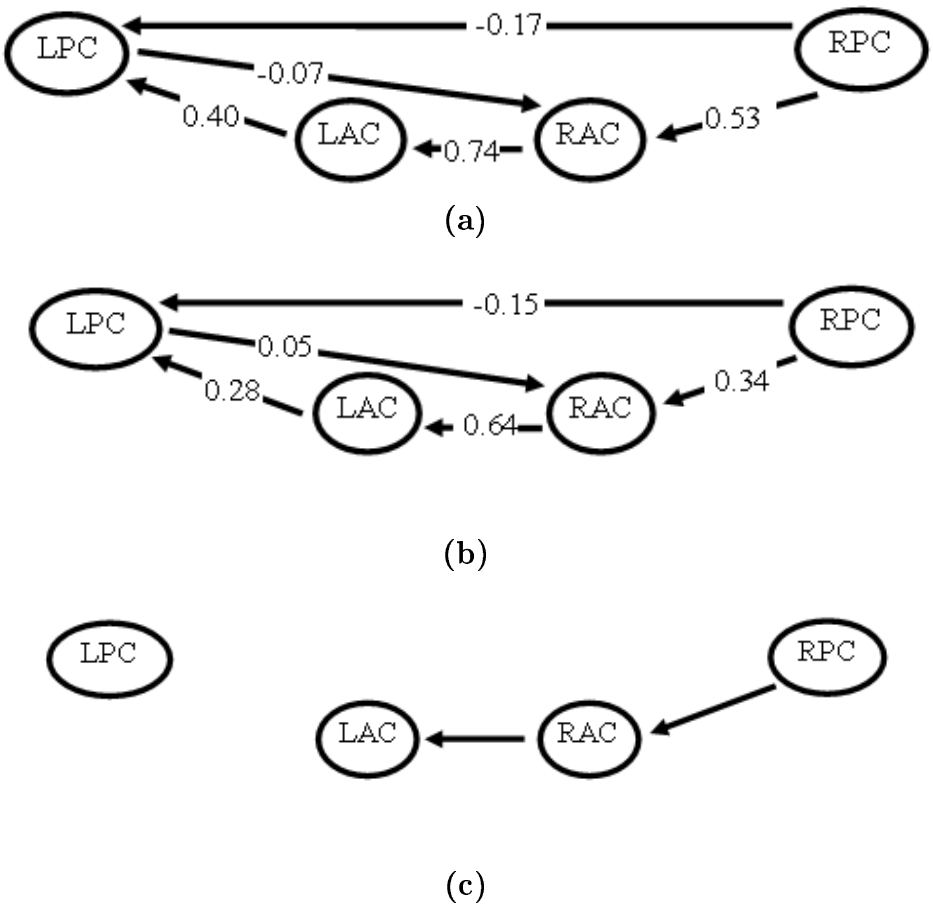

Figure 4.5: (a) AC-PC model for controls; (b) AC-PC model for patients; (c) Differences between controls and HD patients; solid lines: controls show increased connectivity.

4.4.3 Task Connectivity for 11 HD Patients - Year One and Two

Table 4.3: Covariance matrix for 11 HD patients. Y1 = year 1; Y2 = year 2

	Patients Y1						Patients Y2					
	RAC	LAC	RPC	LPC	RPL	LPL	RAC	LAC	RPC	LPC	RPL	LPL
RAC	0.98						1.50					
LAC	0.64	0.94					0.64	0.98				
RPC	0.44	0.35	1.18				0.99	0.47	1.84			
LPC	0.38	0.36	-0.01	1.72			0.19	0.35	0.20	2.06		
RPL	0.38	0.38	0.44	0.44	1.24		0.05	0.16	0.11	0.72	2.29	
LPL	0.32	0.31	0.11	0.34	0.34	1.09	0.25	0.15	0.03	0.27	0.74	2.14

The covariance matrices for the 11 patients in year one and year two are presented in Table 4.3. The links and their directions which are identified using modification indices for 11 patients in first year shows that the same model is representative of the connectivity observed for the larger sample of 20 patients (see Figure 4.6). The model fit to the data is good ($\chi_{p1}{}^2 = 0.66$, $p = 0.418$).

Figure 4.7 shows the model developed for the data for same 11 patients in year two. This model also fits the data well ($\chi_{p2}{}^2 = 0.19$, $p = 0.658$). Strongest connectivity, again, is seen between the AC regions ($r = 0.60$ and $r = 0.51$) with significant within-hemispheric connectivity also seen between the prefrontal regions. The interactions with the parietal regions are mainly non-significant except for LPC→RPL and RPL→LPL in both models and RAC→RPL in patients year one. One connection in each model is different in the other (see both Figure 4.6 and Figure 4.7) and these connection are marked with dashed lines in the figures.

The significant differences between the two models are presented in Figure 4.8. The solid lines show stronger connectivity in patients year one whereas dashed line show stronger connectivity in year two. These results show that there are significant increases in connectivity during task performance in the first year (RAC→LAC and

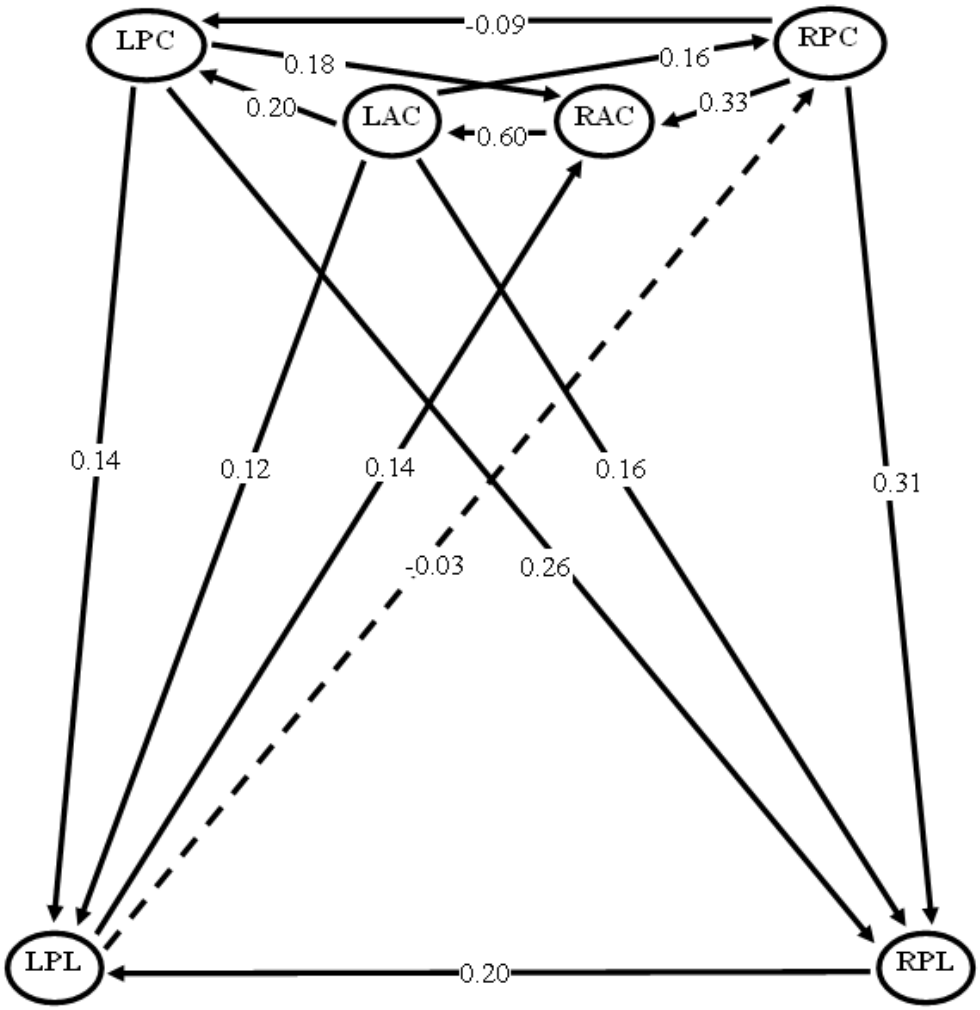

Figure 4.6: SEM for 11 patients - year one; dashed lines: connectivity is unique to HD patients year one model.

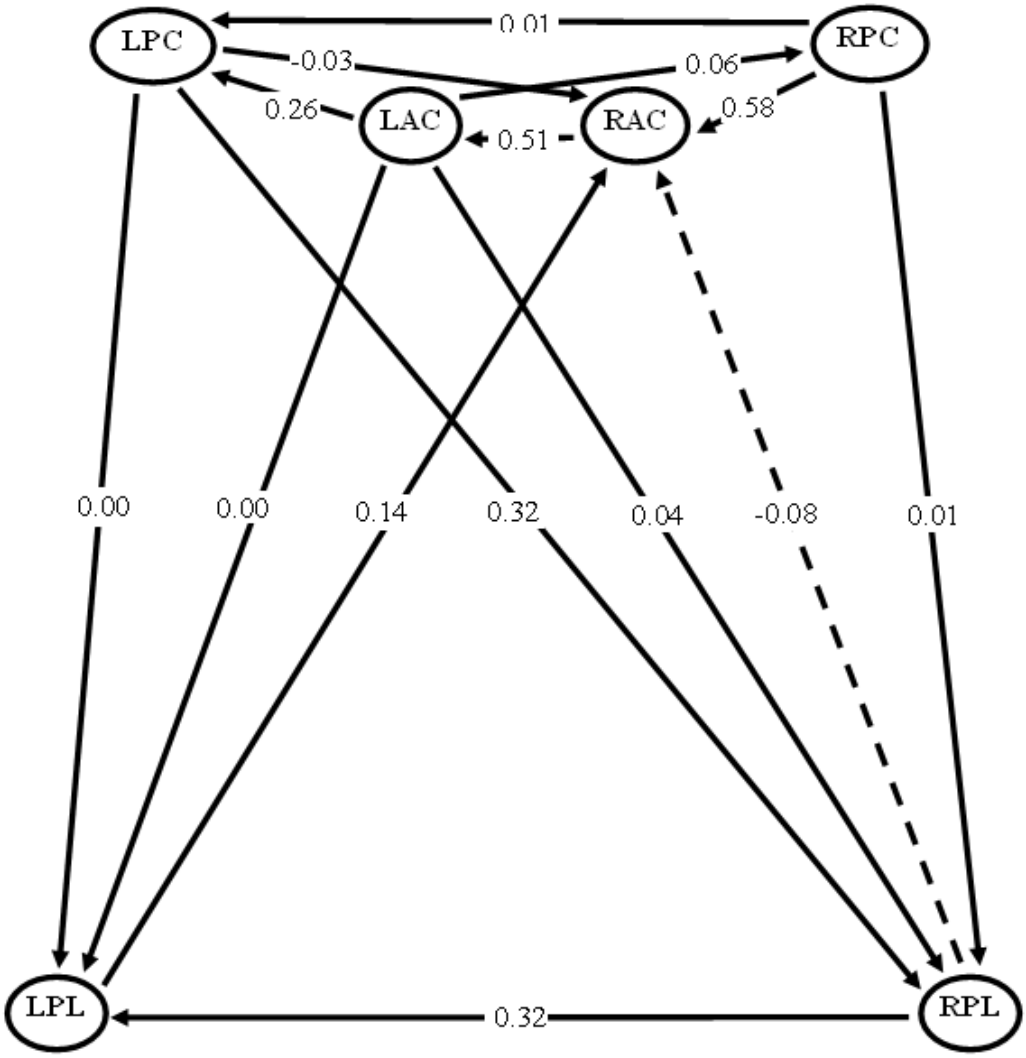

Figure 4.7: SEM for 11 patients - year two; dashed lines: connectivity is unique to HD patients year two model.

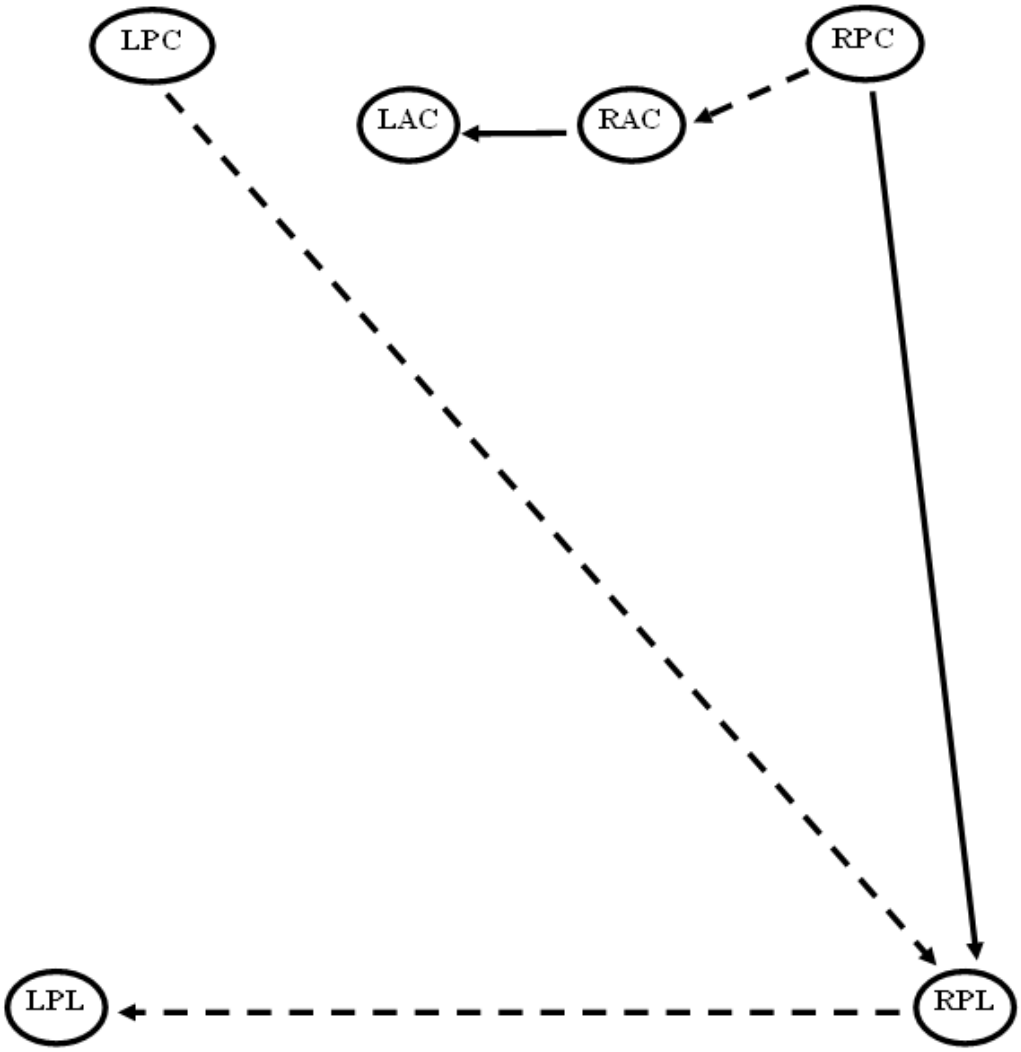

Figure 4.8: Significant differences in connectivity; Solid lines: connectivity in year one is greater; dashed lines: connectivity in year two is greater.

RAC→RPL) and in the second year (LPC→RPL, RPL→LPL and RPC→RAC). The prefrontal connectivity (AC-PC connectivity) parallels the prefrontal connectivity for both groups seen in Figures 4.6 and 4.7 and are therefore not reported. The prefrontal and frontoparietal interactions are variable and are not biased towards greater connectivity the first or second year of this study.

4.5 Discussion

This study uses SEM to determine influences of AC, PC, and PL regions on each other during Simon task performance. Effective connectivity estimates are obtained for the control and patient groups and compared to identify differences in causal influences of brain regions on other. Significant AC-PC connectivity was observed between AC ROIs (RAC→LAC being the largest effective connectivity estimate) and the AC and PC ROIs within hemisphere for both groups. Significant connectivity with the PL ROIs were observed in the control group (LAC→LPL, LPC→RPL, RPC→RPL and RPL→LPL), however, most of this connectivity is non-significant in the patient group except for two links (RPC→RPL and RPL→LPL). This result is apparent in the comparison between the two groups where controls show significantly increased connectivity across several connections whereas patients show no significantly increased connectivity compared to controls. The models developed for the longitudinal study with HD patients show a similar set of connections used to perform the Simon task. These results are seen with both groups of HD patients in year one and year two of the study. However, the differences from year one to year two are variable with some interactions greater in year one (RAC→LAC and RPC→RPL) and others greater in year two (LPC→RPL, RPL→LPL, RPC→RAC and LAC→LPC).

4.5.1 Structural Equation Modeling

The SEM modeling method in this study has provided interesting results. In particular, using modification indices to build a model for a data set has been useful to identify regional connectivity. This is the case on two counts. First, the final set of connections obtained are biologically feasible. Second, a nearly identical network with good model fit is obtained for two different groups performing the same task. This is a valuable indicator of the true network used during task performance. In HD patients, connection strengths were expected to be significantly lower than controls. This is seen in the results obtained from the comparisons between HD patients and controls.

The final SEMs for each group are similar. The resultant models generated using modification indices consist of similar connections and directions except for one connection in each model for controls and patients. This implies that in Simon task performance, controls and HD patients recruit a similar network of connections, which is predicted by the data. The models do not contain any direct loops, however, indirect loops exist. This accounts for bidirectional influences which probably exist between these regions (e.g. bidirectional links will exist between the AC ROIs). The subset of HD patients from year one recruit the same connections to perform the Simon task as the larger sample (20 HD patients). In year two, a similar network is also obtained. This further illustrates that when regions, known to be recruited for task performance, are selected, the data can be used to predict connectivity between these regions. Given that the network of interactions are similar in all models during Simon task performance these results provide evidence true network to preform the Simon task. Overall, these results demonstrate that a combined confirmatory/exploratory approach to identify regional connectivity is a valid method to identify connectivity in fMRI.

There are some concerns with the SEM technique which have been assessed previously with regards to psychological studies (Breckler, 1990; Tomarken and Waller, 2003). These issues were considered before the methods were selected and the methods chosen were aimed at solving potential problems. The following are possible concerns with explanations related to the datasets used in this study.

Linear and Instantaneous

These are two inherent limitations of the SEM technique. While interactions in the brain are nonlinear, the functional form of these interactions are not well known. Therefore, a linear approximation of these interactions at this stage is most commonly examined (either functional connectivity, i.e., linear correlation or effective connectivity, SEM). Interactions measured in SEM are instantaneous, thus temporal information is eliminated with this method. The temporal resolution in this study is 3.00 seconds and temporal information is not going to provide any new insights as this resolution is very low. Friston et al. (2003) have proposed dynamic causal modeling which fits a bilinear model to the data where modulatory effects can be measured. This is a step towards modeling nonlinearities but experiment designs have to be chosen carefully to elicit desired nonlinear effects. DCM is also a time series model, however, lower temporal resolutions are necessary to exploit this method.

Number of Connections

After obtaining time courses, the data points in an SEM analysis refer to the number of variances and covariances in the observed covariance matrix. This number is $c = \frac{n \times (n+1)}{2}$ where n is the number of measured variables or regions. The number of connections that can be tested in a SEM analysis is equal to c, however, it is recommended that no more than $c - 1$ connections be tested (Tabachnick and

Fidell, 2001). The reasons for this are discussed in the next section. This is a limitation of SEM; however, given that six regions were selected in this study, a large number of connections can be tested (20). This was also one of the motivations for using the PL regions in the extended anatomical model.

Model Identification

The problem of identification refers to whether or not a unique solution for the parameters in the model is possible. To obtain a unique solution the number of parameters to be estimated needs to be less than the number of data points available. If the number of data points is equal to the number of parameters to be estimated, the system is said to be just-identified. This is however not interesting where the estimated covariance matrix is equal to the observed covariance matrix (chi^2=0, df=0) and testing goodness of model fit is not possible. When more data points than parameters to be estimated are available the system is said to be over-identified and the SEM analysis can proceed.

In this SEM study all the models are over-identified with degrees of freedom greater than zero and model identification is therefore not an issue. The goodness of fit indices were assessed and some related issues are discussed next.

Model Fit

One of the major concerns regarding SEM is how well the models fit the data. For ML estimation the discrepancy function is χ^2 distributed under appropriate assumptions (the two assumptions are that observations are independent and the exogenous variables must be multivariate normal distributed). While the second assumption is violated with the data here, under certain conditions the ML estimation method is acceptable (these details are discussed later). Therefore, the χ^2 statistic was reported in the results section as a measure of model fit. Previous researchers

also advise that multiple goodness-of-fit be examined to determine good model fit (Breckler, 1990) the reader was directed to Appendix C to examine these additional statistics. Considering all of these GFIs, the model fits for each model indicate that they fit the data well except for the AC-PC network. The AIC and BIC values indicate that the models developed are complex, however, given that the brain is complex system this is expected.

Equivalent Models

A major problem with the SEM method is the non-uniqueness of the solution or equivalent models (MacCallum, Wegener, Uchino and Fabriger, 1993). The means that given the covariance structure of the data it is possible that equivalent models can fit the data. Equivalent models are those which explain the covariance structure of the data equally well (i.e., same χ^2 value). It is also possible that non-equivalent well fitting models exist. All of these models are plausible explanations of the data. To solve this problem, traditionally, a theoretical model is specified which is tested with the data. If this model fits then it is a good explanation of the data. Conversely, this study suggests that the best explanation of the data will result in a biologically feasible model.

For all models, examining different starting locations (making sure that these connections were not present in the SEMs seen earlier) and using modification indices did not result in well fitting models and equivalent or non-equivalent well fitting models were not found. If the sample sizes were small, alternative well-fitting models may not be found (due to data being non-normal), but this is not the case in this study. This shows that the causal influences measured are the best explanation regional connectivity from the data for all the groups.

Violation of Data Normality

The data used for this study is skewed and not normallly distributed (see Table 4.1 and Table 4.1). This issue is accounted for by the large sample sizes used in this study (all models have sample sizes > 2500) and the maximum likelihood estimation method. Hu et al. (1992) showed that these methods work well when normality assumptions are violated.

The effects of deviation from normality are twofold. Firstly, non-normal distributions will result in a bigger than expected rate of rejection of true models. This effect is not seen in this study as good model fits are obtained for all models obtained using modification indices (except for AC-PC connectivity). Since only four regions are included in the AC-PC model it is unlikely that good model fit will be obtained even with normally distributed data (i.e., this model is too simple an explanation of the data).

The second effect of non-normal data is that the critical ratio for the path coefficients are inflated. Generally, to overcome this problem a higher threshold must be selected to identify significant path coefficients. In this study biologically significant path coefficients were chosen as those that are equal to or greater than 0.2. This threshold is never too low given the number of data points used (e.g. even after using a corrected threshold in the patients' model, only the path from LPL$\rightarrow$RPC is considered non-significant).

Causal Inferences

One of the advantages of SEM for effective connectivity over functional connectivity is the ability to infer causal effects. However, if one causal structure (one model) is accepted then it should be noted that other well fitting models should be acceptable (Breckler, 1990). This implies that causal influences should really be determined

outside of the data with a theoretical model and test whether this model fits the data (i.e., the confirmatory approach).

The approach used for this study is different, where the causal effects are determined from the data. The models obtained were biologically feasible and equivalent well fitting models were not found for any of these groups. This implies that the complex nature of the interactions can be approximated with SEM using a part exploratory approach. In conclusion, SEMs derived from the data provide useful information about causal interactions between brain regions used in performance of a task. Furthermore, a combined confirmatory/exploratory approach using SEMs can provide useful information to make inferences in longitudinal studies.

4.5.2 Implications for HD

The effective connectivity results in this study are equivalent to those obtained in the previous study on functional connectivity. Additionally, SEM demonstrates the following. In addition to reduced prefrontal connectivity, reduced fronto-parietal connectivity is also seen. It is known that the parietal regions are affected in HD (Bush, Luu and Posner, 2000; Fennema-Notestine et al., 2004; Halliday et al., 1998), and these results show that fronto-parietal interactions during the performance of the Simon task are significantly reduced in HD patients. Moreover, a recent study showed that projections from an output component of the striatum, the substantia nigra pars reticulata, to the posterior parietal cortex exist (Clower, Dum and Strick, 2005). Since effective connectivity measures influence of regions directly or indirectly on other regions, the results seen can be explained by impaired fronto-parietal connectivity in HD patients.

To perform the Simon task the first region recruited appears to be the prefrontal cortex in the right hemisphere (Peterson et al., 2002; Huettel and McCarthy, 2004).

This region influences the AC and PL ROIs within hemisphere and these effects propagate to the left hemisphere via the AC and PL regions. All these interactions are weaker in HD patients compared to controls. These results further demonstrate that the interactions between ROIs recruited for cognitive performance are possibly compromised in HD. Since effective connectivity has not been explored in previous studies with the Simon task, further investigation of prefrontal and frontoparietal interactions will be useful.

A possible issue with the interpretation of the results using this modeling method is the threshold level used. Higher thresholds (e.g: 0.4) will render the fronto-parietal interactions as non-significant (except for RPC→RPL in the control group). The significant prefrontal connectivity remains statistically valid.

Differences in connectivity between the first year and second year in HD patients show no consistent results. With the acquisition of more fMRI data some of these differences are likely to become consistent (i.e., the sample size for second year data was too small). It is worth noting that the model for second year patients is the same model developed for controls during task performance. This raises the possibility that the network recruited by patients is the same as controls with increased familiarity of the Simon task. Also, the brain areas and connections recruited may change over time in HD patients with deterioration of regions. Therefore, the inconsistent differences seen from year one to year two are plausible.

Chapter 5

Effective Connectivity: Dynamic Causal Modeling

DCM was proposed by Friston et al. (2003) to model effective connectivity between brain regions. Compared to previous methods such as SEM or MAR, DCM treats the brain as a deterministic nonlinear system. When measuring regional interactions in fMRI DCM is more comprehensive than previous methods, because, in addition to intrinsic connectivity (this is the same connectivity measured with SEM), modulatory effects can be measured. It is based on the assumption that external inputs drive the connectivity observed, i.e., the effects of inputs propagate through the brain regions in an anatomical model. DCM is a confirmatory method where theoretical models need to be identified before testing with data continues.

DCMs can also be used to test hypotheses about which brain regions are coupled together (i.e., as an exploratory or part exploratory approach). Penny et al. (2004) conducted a study on comparing dynamic causal models. This study considers hypothetical DCMs of connectivity in the brain. The DCMs are compared to identify which model performs best on a given data set. This is a part confirmatory - part

exploratory approach in which several plausible theoretical models and the one that fits the data the best (assessed using Bayes factor) is selected.

The aim of this study is to determine whether DCM can be used to make inferences about two populations of subjects when performing the Simon task. A confirmatory approach is used by defining a theoretical model based on group activation data and the SEM models developed in the previous chapter. To examine task-related connectivity only the Simon task is included within the anatomical model. If it is possible to obtain valid connectivity estimates a secondary aim is to compare HD patients with controls to determine differences in regional interactions between the two groups.

The study above, although a usual procedure, is flawed when applying DCMs to each subject. Activity patterns for the Simon task have been previously suggested (Liu et al., 2004; Peterson et al., 2002), however, the locations of these regions are not precisely the same for each individual. This requires that the anatomical model relies on group activation maps and prior knowledge to define specific location of the regions. However, DCMs are applied at the individual level and group activation is not necessarily the same in each individual. Low activity will result in low intrinsic connectivity because connectivity in DCM is a result of task-related responses at a region. Due to this reason an additional study is conducted in this chapter to determine intrinsic connectivity from activated regions in a subset of five controls during Simon task performance. It is expected that low levels of activity ($p_{uncorrected} < 0.01$) should give rise to higher connectivity estimates. Moreover, higher levels of activity will possibly result in higher overall connectivity. No data for HD patients is included in this study and no inferences about HD are made. No conclusions are made about the Simon task either. This study aims to show that known activation patterns for a task at the individual level can result in useful connectivity estimates obtained with DCM.

5.1 DCM Nomenclature

In a DCM, brain regions are called nodes and links are called arcs. The connection strengths that are estimated are placed on the arcs which are an indicator of the strength of the directed links. This terminology is not different from the terminology of the other causal modeling methods, e.g. SEM.

In DCMs, neuronal activity and hemodynamic response of a node are modeled by the bilinear model and the hemodynamic model respectively. The bilinear model for activity is composed of three sets of parameters. They are those that mediate the intrinsic connectivity between regions, those that modulate the change in connectivity through input (bilinear), and those that mediate the influence of the extrinsic inputs to the system. The difference here from previous methods is the bilinear parameter which essentially accounts for the effects of inputs on connections or nonlinear interactions.

Friston et al. (2003) suggest the following effective connectivity model:

$$\dot{z} = F(z, u, \theta) \tag{5.1}$$

where z are the activities at brain regions, u are the inputs, and θ are the parameters of the model. Following Friston et al. (2003), the bilinear model is summarized by the following differential equation:

$$\dot{z} = (A + \sum B^j u_j)z + Cu \tag{5.2}$$

$$A = \frac{\delta F}{\delta z} \tag{5.3}$$

$$B^j = \frac{\delta^2 F}{\delta u_j \delta z} \tag{5.4}$$

$$C = \frac{\delta F}{\delta u} \tag{5.5}$$

The neuronal activity of a node, z, is a linear combination of the three sets of parameters. A is a first order connectivity independent of input, B is the change in coupling induced by the j^{th} input and C models the extrinsic influence of inputs.

An example of a DCM with four regions is presented in Figure 5.1. In this DCM, the brain regions are Z_1, Z_2, Z_3, and Z_4 with connectivity strengths a_{21}, a_{24}, a_{32}, a_{34} between regions. Note that the activity at each region is a function of its own activity (at a previous time point), hence each node has an addition parameter to account for this (e.g. a_{11}). The inputs are u_1 and u_2, which are stimuli and contextual inputs, respectively. The contextual input modulates the connection from Z_4 to Z_2 with the estimate b^2_{24}.

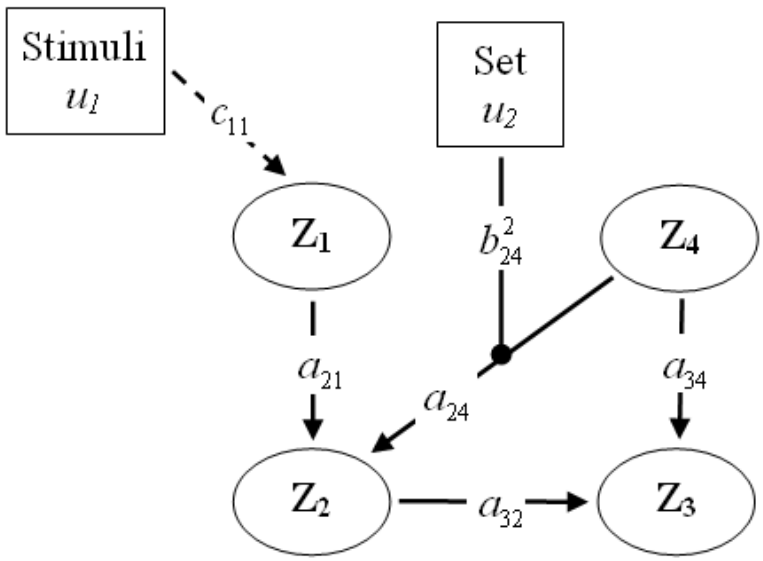

Figure 5.1: A DCM example.

The diagram in Figure 5.1 can be described using the following matrix notation:

$$\begin{pmatrix} \dot{z}_1 \\ \dot{z}_2 \\ \dot{z}_3 \\ \dot{z}_4 \end{pmatrix} = \left\{ \begin{pmatrix} a_{11} & 0 & 0 & 0 \\ a_{21} & a_{22} & 0 & a_{24} \\ 0 & a_{32} & a_{33} & 0 \\ 0 & 0 & 0 & a_{44} \end{pmatrix} + u_2 \left[\begin{pmatrix} 0 & 0 & 0 & 0 \\ 0 & 0 & 0 & b_{24}^2 \\ 0 & 0 & 0 & 0 \\ 0 & 0 & 0 & 0 \end{pmatrix} \right] \right\} \begin{pmatrix} z_1 \\ z_2 \\ z_3 \\ z_4 \end{pmatrix} + \begin{pmatrix} c_1 & 0 \\ 0 & 0 \\ 0 & 0 \\ 0 & 0 \end{pmatrix} \begin{pmatrix} u_1 \\ u_2 \end{pmatrix} \tag{5.6}$$

5.1.1 The Balloon Model

The response at a brain region is the result of activity at that region and the BOLD response at coupled regions. This response is modeled by the hemodynamic model (Friston, 2002; Friston et al., 2000). This model is an extension of the balloon model (Friston et al., 2000). The balloon model is an input-state-output model with blood volume (v) and deoxyhemoglobin content (q) as the state variables. To the model, blood flow f_{in} is input. The output, y, is a function of the blood volume and the blood deoxyhemoglobin content, v and q, respectively. Increase in blood flow results in an increase in the size of the 'balloon' which in turn results in expelling deoxyhemoglobin at a greater rate. This is the increased BOLD signal response measured by fMRI detectors.

An extension of the balloon model is the hemodynamic model. This model combines the balloon model and a linear dynamic model. The extension is to model changes in regional cerebral blood flow (rCBF) due to neuronal activity. The input to the model is neuronal activity (z) and the state variables are activity (z), vasodilatory signal (s), flow (f), blood volume (v) and deoxyhemoglobin content (q). The hemodynamic response of a region is a function of v and q:

$$y = \lambda(v, q) \tag{5.7}$$

For further details of the hemodynamic model refer to Friston et al. (2000).

5.2 Methods

In research contexts, applying DCMs to fMRI data will result in estimating a set of connectivity and a set of hemodynamic parameters. The connectivity estimates can be used to compare prefrontal effective connectivity between controls and HD patients.

DCM is implemented in the SPM2 package. Given the model developed in the previous study with SEM, a new model was adapted to include the external influences (see Figure 5.2). That is, in addition to the regions chosen, the connections derived from the SEM model were used to identify an anatomical model that was tested with DCM. Additionally, external influences were incorporated as DCM assumes that the task drives the connectivity measured. Note that bilinear interactions were not tested in this model as the Simon task was not designed for this. This anatomical model was tested with each individual. Region definition and

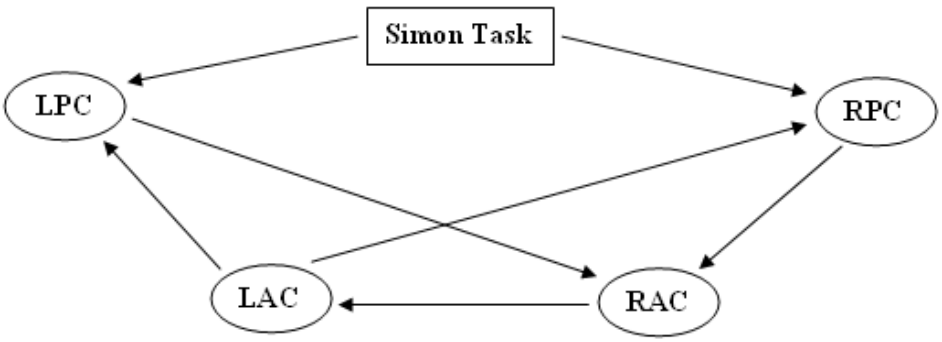

Figure 5.2: The anatomical model to be tested with DCM.

time course selection were done by the same method that is described in Chapter 2. Since DCM uses a Bayesian framework, the probability value associated with each connectivity estimate was not compared to a probability threshold, whereas the experimenter makes a decision about the significance of the estimate given the probability level.

The group results were obtained by averaging over the estimates of all individuals in the group. A t score is computed for each estimate to determine whether an estimate is significantly different from zero. Biologically significant correlations were not limited to those estimates greater than 0.2 in the case of DCM, however, the probability associated with a connection will determine its significance[1]. To compare between significant connections of both groups a two sample t test was used.

5.2.1 DCM Applied to Individuals

The method described above was a confirmatory method where the anatomical model was specified based on prior knowledge (and the SEM models) which was tested with the data available. The model was derived using group activation maps which may not represent the activation in each individual.

To examine connectivity at the individual level, five controls are chosen at random. The activation maps for each control was examined and regions were selected that fall within the broad regions in the anatomical model. Connectivity was carried out on forward and backward connections between all regions and the Simon task was included as an external influence. It was expected that the task has inputs to the prefrontal regions. A region was selected as a 6 mm radius sphere centered on a peak voxel ($t > 2.33$, $p_{uncorrected} < 0.01$). Connectivity estimates greater than 0.04 and less than -0.04 were reported in the results as an indicator of connectivity between regions.

[1]Note that higher significant estimates indicate high connectivity.

5.2.2 Effective Connectivity Using DCM: An Algorithm

The algorithm to assess connectivity in fMRI using DCM is presented in Algorithm 4. This algorithm is similar to the SEM algorithm with the major difference being that connectivity estimates are computed for in each individual in DCM opposed to connectivity computed at the group level in SEM.

Algorithm 4: An algorithm for effective connectivity using DCM.

Data: Preprocessed data: P_n, Subjects: S_n, Groups: G_i, Regions: R_p, R_a.
Result: Effective connectivity estimates across subjects; comparison between groups.

```
1  R_f = R_a ∩ R_p;
2  AM_j(R_f);
3  for g ∈ G_i do
4      for r ∈ R_f do
5          for s ∈ S_n do
6              extract time course: T(P(s), r);
7          end
8      end
9  end
10 for g ∈ G_i do
11     for r ∈ R_f do
12         for s ∈ S_n do
13             determine connectivity: CON(s, g, t, AM);
14             statistical analysis: Stat(s, g, CON);
15         end
16     end
17     if i > 1 then
18         compare groups: C(CON, g, g + 1);
19     end
20 end
```

The parameters of algorithm 4 are preprocessed data (P_n), subjects (S_n), groups (G_i), and regions (R_p, R_a). P_n is the preprocessed obtained for n subjects, S_n, from the activation studies algorithm in Chapter 2. The subjects are divided into i groups, G_i, which may be one group if i is equal to one. From prior knowledge, p regions are identified which are expected to be activated, R_p, and R_a are the regions

identified from the activation maps. The first two steps of the algorithm identify the final set of regions for connectivity analysis (R_f) and the ensuing anatomical model/models (AM_j with j possible models). The first part of the algorithm is used to determine the regional time courses to be used for effective connectivity. This is followed by the second part where effective connectivity estimates are obtained. If the approach is part exploratory then Bayes factor is used to select one of the j models that best describes the data. If there are more than two groups in the study, their connectivity estimates can be compared statistically .

5.3 Results

See Figure 5.3 for the average connectivity estimates for controls and patients (also see Appendix E for the breakdown of estimates for both groups). These results represent a low degree of connectivity between the prefrontal ROIs. While the links RAC→LAC and RPC→RAC are significant at $p = 0.05$ for HD patients, the actual strength of connectivity between these connections is zero. No probabilities for the connection strengths are presented as they are all extremely low ($p < 0.05$). None of the connections, across all individuals, are statistically significant. Group comparisons for these results were not attempted.

Further models were tested with the AC-PC network to identify significant connectivity, however, such significant connectivity was not obtained.

5.3.1 DCM at the Individual Level

Five controls are chosen who showed activation in at least one prefrontal and one parietal region. See Table 5.1 for the location of the regions and their t scores (also see Appendix F for activation maps). No regions are activated in the anterior

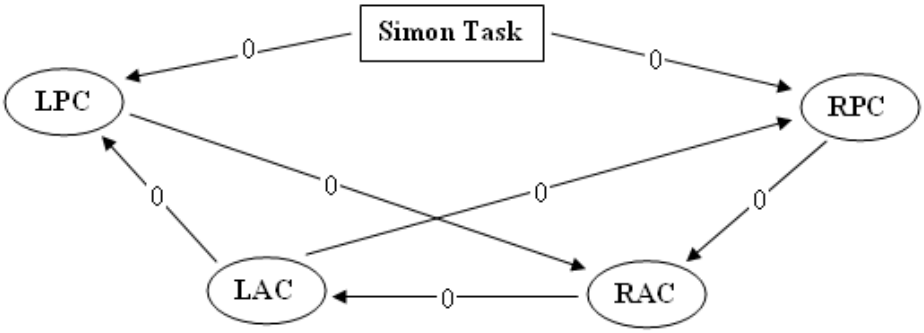

Figure 5.3: Average model for controls; this model also represents the connectivity estimated by DCM for HD patients.

Table 5.1: Regions activated during task performance in five controls; t scores follow peak voxel location and are presented in parenthesis (); - : activity was not seen in this region; Cont.: controls;

Cont.	RPC	LPC	RPL	LPL
C1	46, 26, -10 (3.66)	-42, 22, 36 (3.09)	-	-54, -22, 20 (3.97)
C2	50, 18, 40 (3.02)	-48, 42, -2 (3.45)	38, -48, 52 (3.81)	-54, -50, 44 (4.00)
C3	44, 38, 6 (2.94)	-44, 40, 24 (2.69)	42, -34, 62 (3.30)	-54, -8, 16 (2.78)
C4	58, 6, 14 (3.59)	-42, 26, 38 (2.85)	42, -22, 56 (3.72)	-50, -18, 18 (3.64)
C5	34, 30, 38 (3.62)	-38, 18, 22 (4.18)	42, -34, -34 (2.92)	-56, -52, 26 (2.95)

cingulate, which is expected since the activation maps for HD patients > controls showed activity in the anterior cingulate.

The DCMs for each of the controls are estimated with all connections present between all regions. See Figures 5.4 - 5.8. The activation map for C1 does not show any activity in the right parietal lobe, but the left prefrontal, left parietal, and right prefrontal are defined (Figure 5.4). In all the other models the left/right prefrontal and left/right parietal regions are activated and included.

C1 shows high within hemispheric connectivity between LPC and LPL ($r \geq 0.10$). Connectivity between hemispheres is high, especially directed from the right

prefrontal region to the other two regions in the model ($r > 0.10$). Feedback connectivity to this region is also present ($r \geq 0.05$). There was no influence of the Simon task on the prefrontal regions for this control.

High connectivity is seen in C2 directed from the prefrontal regions to the parietal regions (LPC→LPL, LPC→RPL, RPC→LPL, and RPC→RPL). This is true for inter- and intra-hemispheric connectivity ($r > 0.10$). There is high connectivity from LPC to RPC ($r = 0.10$) and low connectivity between the parietal regions. Again, The Simon task showed no influence on the prefrontal regions.

In the C3 model, high connectivity directed from the prefrontal regions to the parietal regions is also seen (LPC→LPL, LPC→RPL, RPC→LPL, and RPC→RPL) with $r \geq 0.08$. There is low connectivity between the prefrontal regions and between the parietal regions ($r \leq = 0.04$). The estimate of the influence of the Simon task was greater than zero, but still very low ($r = 0.01$).

The model for C4 shows high intra-hemispheric connectivity in the left hemisphere ($r > 0.20$), but lower connectivity in the right hemisphere ($r < 0.10$). High inter-hemispheric connectivity is seen between LPC and RPL ($r \geq 0.25$), but lower connectivity between RPC and LPL ($r < 0.10$). There is high connectivity from LPC to RPC and very high connectivity between the parietal regions (LPL↔RPL, $r > 0.20$). The Simon task, again, shows no influence on the prefrontal regions.

The model for C5 shows low intra-hemispheric connectivity in the left hemisphere ($r \leq 0.04$) but high connectivity from RPC to RPL ($r = 0.26$). There is high inter-connectivity directed from the prefrontal regions to the parietal regions ($r \leq 0.10$). Connectivity from RPC to LPC is high ($r = 0.11$) and low connectivity is seen between the parietal regions ($r \leq 0.04$). The Simon shows no influence on the prefrontal regions.

See Table 5.2 for the mean connectivity estimates across the five controls. Forward connectivity estimates are large from the right prefrontal region to the parietal

Table 5.2: Mean connectivity estimates across controls; t scores are provided in parenthesis (); - : t score was not computable; ST: The Simon task influence on regions.

	From				
To	RPC	RPL	LPC	LPL	ST
RPC	0.00 (-)	0.02 (47.5)	0.06 (65.4)	0.04 (47.9)	0.01 (149.0)
RPL	0.09 (8.6)	0.00 (-)	0.02 (13.7)	0.07 (18.28)	0.00 (-)
LPC	0.05 (35.7)	0.06 (10.5)	0.00 (-)	0.07 (16.25)	0.00 (-)
LPL	0.16 (9.4)	0.06 (12.2)	0.17 (18.5)	0.00 (-)	0.00 (-)

regions (RPC→RPL, RPC→LPL, $r > 0.08$), however, backward connectivity is low between these regions ($r < 0.05$). The connectivity between the prefrontal regions is low (LPC→RPC = 0.06, RPC→LPC = 0.05), but present. Interaction between right parietal region and both regions in the left hemisphere is also low (RPC→LPC and RPL→LPL, $r = 0.06$). The connectivity from the left prefrontal region to left parietal lobe is high (LPC→LPL, $r = 0.17$). All other connectivity is very low. The probabilities associated with the connectivity estimates are variable (range: 0.00 to 1.00).

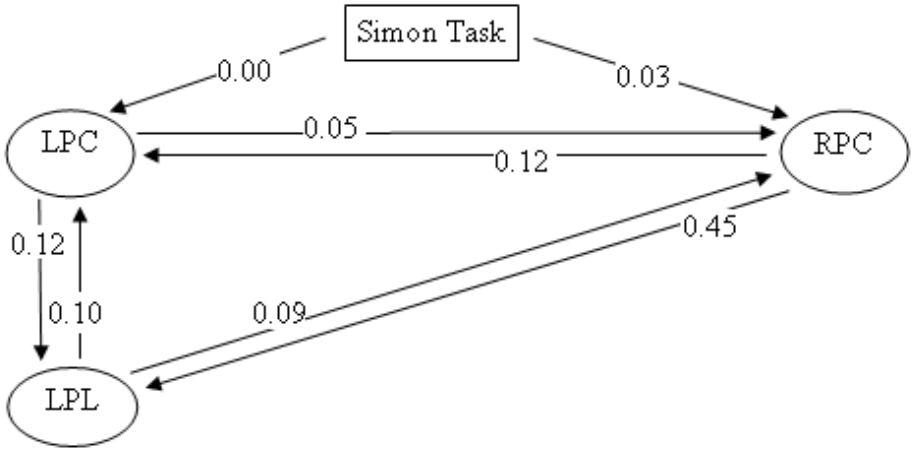

Figure 5.4: Connectivity in control one (C1).

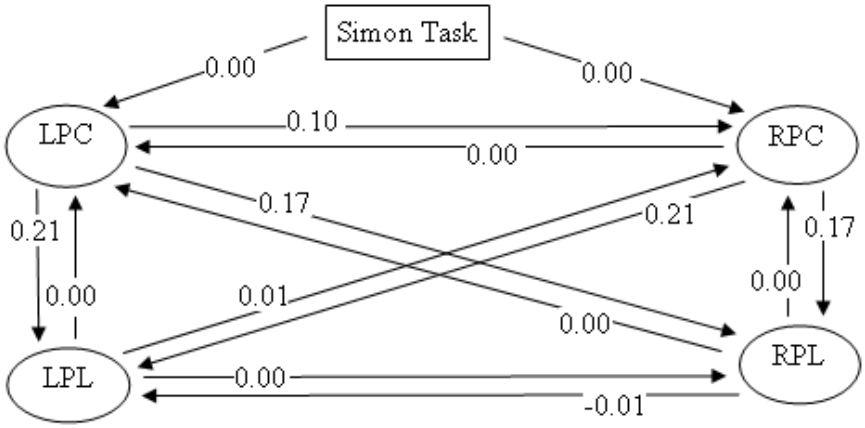

Figure 5.5: Connectivity in control two (C2).

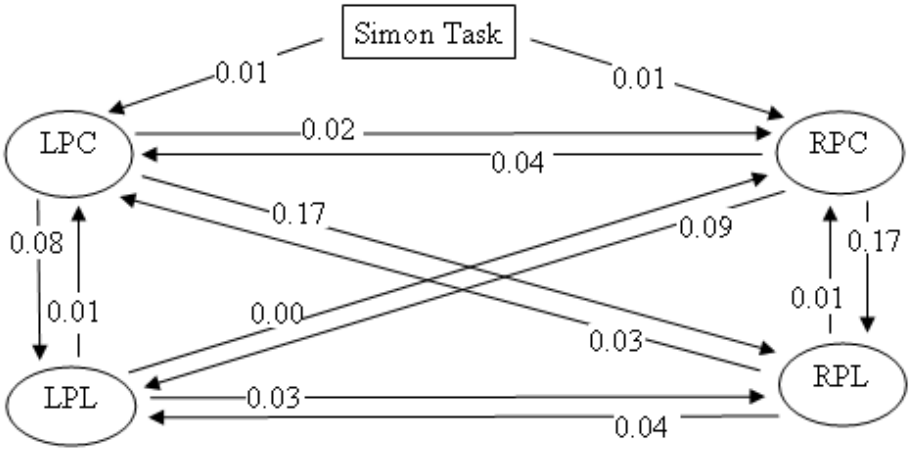

Figure 5.6: Connectivity in control three (C3).

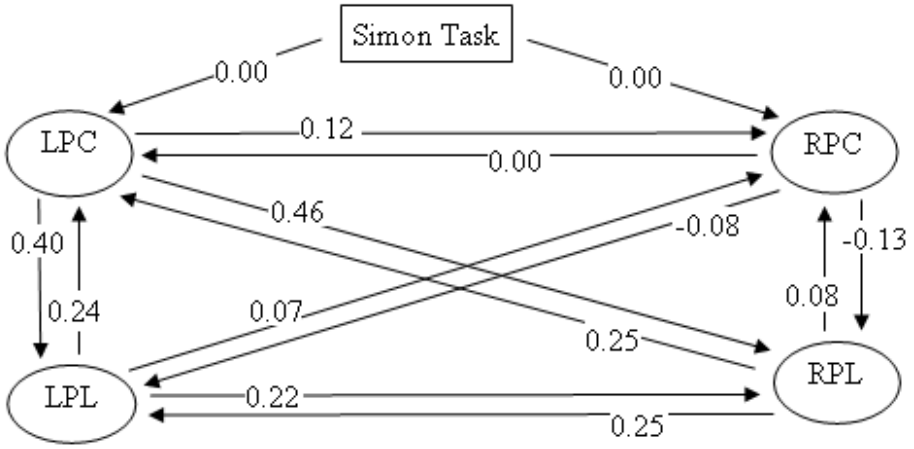

Figure 5.7: Connectivity in control four (C4).

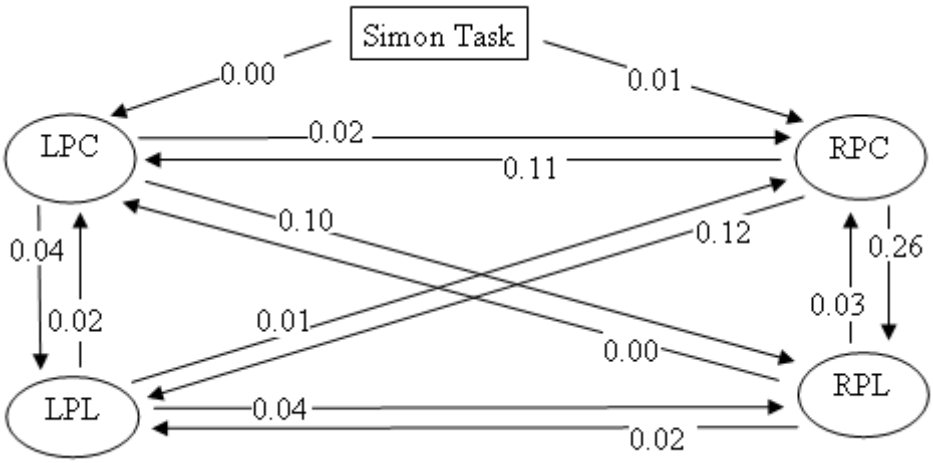

Figure 5.8: Connectivity in control five (C5).

5.4 Discussion

The results from the DCM analysis do not provide evidence of significant interactions between the prefrontal regions for each individual. The actual degree of connectivity is low, and furthermore, the probability levels associated with each connection is less than 0.05. Examining connectivity at the individual level shows that activated regions result in potentially high connectivity.

Low effective connectivity may be seen due to several reasons (e.g. no direct or indirect influence between regions). In this study, low connectivity is probably seen because of the lack of task-related activity at each region selected. On close observation each individual does not show high task-related activation in the regions chosen. It is not absolutely necessary that high activity is needed for high connectivity, but in DCM the intrinsic connectivity is defined as the influence of regions on others by inducing a response $A = \frac{\delta \dot{z}}{\delta z}$ and high connectivity can be expected only if high activation is seen first. This method of selecting regions (i.e., based on group activation maps) used here will not result in high connectivity estimates. In order to obtain reliable connectivity estimates in DCM, task activation at the regions selected must be seen first. Since regional connectivity was very low, no group comparisons were made. For the same reason, the results obtained are not used to make inferences about HD.

The results of DCM with a subset of controls showed increased task connectivity between prefrontal and parietal regions within and between hemispheres. However, these results are not used to make inferences about the Simon task, rather than to point out that connectivity using DCM is obtainable if clear activation patterns are known for a task. Therefore, in order to use DCM in fMRI, the first step is to ensure that the task used elucidates similar activation patterns in every individual in the

study. This allows testing the anatomical model with each subject. Connectivity differences between groups can then be assessed.

Irrespective region selection, DCM estimates connectivity at low frequency components of a region's time course[2], whereas in the previous SEM study, connectivity was examined with high frequency components of the regional time courses. Therefore, the results obtained by these two methods may not be similar unless low frequency components are examined with SEM. In order to compare SEM and DCM, regions with high task activation in each individual must be selected, and the same time courses must be used to estimate connectivity. In this case the connectivity estimates obtained from SEM can be expected to be similar to the intrinsic connectivity estimates obtained from DCM.

To exploit the DCM technique an experiment needs to be designed that includes bilinear interactions. This allows extracting more information than previous methods such as SEM from the BOLD signal, i.e., intrinsic connectivity, bilinear connectivity, and external influences. The influence of the Simon task on the connections tested is not clearly known, although, the functional connectivity results revealed a significant increase in one inter-hemispheric connection from baseline to task in controls (LAC-RPC). This suggests that the Simon task influences this connection by increasing its functional connectivity estimate during task performance. However, it was not possible to test this increase in task-related connectivity with DCM, since connectivity estimates were not reliable for the regions chosen.

[2]Due to definition of connectivity in DCM (i.e., connectivity is a result of responses at coupled regions), high frequency components of the signal are not assessed.

Chapter 6

Conclusions and Future Work

The aim of this thesis was to apply fMRI connectivity methods to distinguish two populations of subjects, healthy controls and HD patients, during the performance of a cognitive task (the Simon task). Given commonly used preprocessing strategies and model specification methods, group analysis of functional and effective connectivity was conducted. Functional connectivity, or correlations between regional time courses, are assessed between prefrontal regions for the two groups. To compare between groups, two methods, the direct and the meta-analytic methods are explored. Effective connectivity quantifies regional interactions that are directed, i.e. to measure the influence of brain regions on others. The most common method for modeling effective connectivity has been SEM which is one of two methods explored in this thesis. This method is used to distinguish controls and HD patients in their recruitment of directed regional connectivity to perform the Simon task. SEM is also tested to determine if modeling HD fMRI data over time is feasible. Additionally, DCM is tested with the data available to determine the usefulness of this technique in measuring effective connectivity.

Given the functional and effective connectivity results, inferences about HD are made in this thesis. These inferences are specific to the interactions between prefrontal and parietal regions, which are crucial for cognitive performance and are known to be compromised in HD. In particular there is much evidence to suggest that the Simon task implicates such regions (Huettel and McCarthy, 2004; Liu et al., 2004; Peterson et al., 2002). The regions are selected with assistance from previous research such as animal studies, volumetric studies, fMRI activation studies, etc. Connectivity measures using fMRI have not yet been examined with the Simon task or HD and interactions between these regions during task performance remains unclear. These connectivity measures, being good indicators of regional interactions or anatomical connectivity (Horwitz et al., 2005), provide a useful way to examine deficits in HD patients compared to controls during performance of the Simon task.

6.1 Connectivity Measures

For functional connectivity analysis a confirmatory approach was used by defining a theoretical model that was expected to show differences between HD patients and controls. For effective connectivity using SEM a combined confirmatory and exploratory approach was used, where a theoretical model of critical regions (regions that will show differences between controls and HD patients) was defined, but the connections between these regions was obtained from the data. A confirmatory approach was used with DCM. Functional connectivity estimates were computed using correlations between regional time courses and effective connectivity estimates were obtained using SEM and DCM.

The functional connectivity study showed reduced connectivity during Simon task performance in HD patients compared to controls (LAC-LPC, RAC-LAC, and

RAC-RPC). Variability in connectivity within the HD group was also high whereas in controls it was low as expected. This shows that true anatomical connectivity can be obtained though fMRI functional connectivity.

As pointed out earlier, the meta-analytic method for functional connectivity does not provide statistically significant results, but it allows assessment of variability of connectivity within a group (i.e. a homogeneity analysis with Q statistics) given that correlation coefficients are computed for each subject.

The effective connectivity (SEM) results show differences between healthy subjects and HD patients which are similar to the functional connectivity results. In SEM, the network of brain regions and the directionality of interactions are consistent across groups (except one connection in each model for controls and HD patients) and over time (except one connection in each model for first year HD patients and second year HD patients). Overall, significantly reduced connectivity is seen in HD. The part exploratory approach reveals that prefrontal regions in the right hemisphere initiate task-related connectivity and it is between these regions that HD patients show impaired connectivity. While previous research does not suggest directionality during Simon task performance, these results reveal, through the data, that there is directionality in the coupling between prefrontal regions to perform this task. This is inferred because the connectivity directions are consistent across groups. This demonstrates that a part exploratory approach to determine directional connectivity between brain regions results in feasible interactions.

Given a large number of subjects, or large amount of data (i.e. > 10 subjects) in a group, an exploratory approach with SEM can approximate a model for connectivity between activated regions during the performance of a task. Once the models have been estimated, comparisons between SEM models can be used infer differences between two or more populations.

Collectively, the results demonstrate that functional and effective connectivity between brain regions are a good indicator of regional interactions in fMRI. This is consistent with Horwitz et al. (2005). In addition to correlations, SEM provides directional information without changing the major result (i.e. interactions are impaired in the patient group). The two connectivity techniques (i.e. functional and effective connectivity) used in conjunction with one another can provide useful information about fMRI brain connectivity that can be used to analyze or compare groups of subjects. The partial exploratory method used with SEM shows that the data can indicate the network of interactions required to perform the Simon task. This can be potentially extended to other tasks to identify interactions between regions known to be activated by the task. This confirms the hypothesis that connectivity method in fMRI can approximate regional interactions for a task. The DCM connectivity estimates are not conclusive, i.e. all connection strengths are all close to zero, however, connectivity measured with activated regions demonstrates how this technique can be applied in a similar way when activation patterns for a task are known at the individual level.

6.2 Connectivity Implications to HD

The functional connectivity results revealed a loss of synchrony between prefrontal regions on two counts. Firstly, to perform the Simon task reduced connectivity was seen in HD patients instead of increased connectivity that was seen in controls. Secondly, during task performance HD patients showed impaired connectivity within a hemisphere and between the AC regions. The variability in connectivity across HD patients was higher except for the connection between LAC and LPC.The homogeneity analysis also showed that the correlations obtained for the control group were mainly homogenous (except LAC-RPC during baseline), whereas correlations

in the patient group were all heterogenous during baseline and some were homogenous during task (RAC-RPC and LPC-RPC). Similar connectivity results were seen in SEM where reduced effective connectivity was seen between RPC→RAC and RAC→LAC. These results further revealed that impaired fronto-parietal regional interactions were seen in HD patients.

Overall, these results suggest that the interactions between prefrontal regions are compromised in HD. The loss of interactivity is most likely due to brain region pathology which results in cognitive, motor and executive dysfunction (Lawrence et al., 1998). It is known that the associative component of the striatum is affected in HD causing disruption to fronto-striatal circuitry (Joel and Weiner, 1997). Furthermore striatal-parietal connectivity has recently been shown to be affected in HD (Clower et al., 2005). This could in turn lead to the impaired interaction between prefrontal and parietal regions observed herein. Behaviorally, inter-hemispheric abnormalities, or lateralization deficits, have also been previously identified in HD (Ho, Nestor, Williams, Bradshaw, Sahakian, Robbins and Barker, 2004).

Previous studies have demonstrated white matter volumetric loss in cortical and subcortical areas in HD (Fennema-Notestine et al., 2004; Halliday et al., 1998; Jernigan et al., 1991; Rosas et al., 2003). Such white matter loss in prefrontal and parietal regions in HD would be expected to affect the physical connections between regions. This physical disconnection will be reflected in reduced functional and effective connectivity. Moreover, heterogeneity in some correlations and high variability in connectivity across HD patients was seen which indicates that regional interactions may vary with HD severity, although correlations of functional connectivity with clinical measures was non-significant. Additionally, other studies (Fennema-Notestine et al., 2004) have observed equal proportional loss of white and gray matter in the frontal and parietal lobes which may account for the reduced connectivity seen in HD using SEM. Clower et al. (2005) also show that the basal ganglia and posterior

parietal cortex are anatomically connected and neuronal degeneration in these regions in HD could cause the reduced fronto-parietal connectivity seen in the SEM study.

The major finding of this thesis is that regional interactions are compromised in HD. This is observed despite increased functional activation seen at these regions in the patient group. A similar observation was made in a study by Grady et al. (2002) with Alzheimer's disease patients. They examined memory performance in patients using a face recognition task and showed a functional disconnection between the prefrontal cortex and medial temporal lobe, despite showing greater activity at these regions compared with controls. The results here also demonstrate, similarly, that HD patients show significantly increased prefrontal activity but reduced regional interactivity compared to controls. Moreover, Paulsen et al. (2004) observed increased prefrontal activity in presymptomatic HD subjects. Hence, from previous and current research it appears that, during cognitive task performance, the lateral and medial prefrontal regions show significant activation but reduced interactivity. The HD patients' significantly greater levels of activation (compared to controls) bilaterally in caudal anterior cingulate, right dorsal premotor cortex, right inferior frontal gyrus, left middle frontal gyrus and left superior parietal lobule, could all be in partial compensation for the otherwise compromised interactions between cortical regions.

In summary, this thesis has demonstrated that the communication between brain regions in HD patients is significantly weakened during cognitive task performance. Increased functional connectivity is not observed from baseline to task in patients, and task-related functional connectivity is weak in HD patients compared to controls. The SEM study further confirms these findings. Collectively, these three findings suggest a loss of synchrony between brain regions, confirming the hypothesis regarding prefrontal pathology in HD.

6.3 Recommendations and Future Work

Given brain regions known to be activated during Simon task performance, this thesis has shown that functional and effective connectivity methods are a good indicator of regional interactions. They provide a way by which brain region interactivity can be compared between two or more groups of subjects using fMRI.

The functional connectivity direct method is the most straightforward way to examine fMRI connectivity. This method can be used to obtain a high level view of interactions between activated regions during the performance of a task. Once the magnitudes of the interactions are known it is possible to distinguish between two or more groups of subjects with high statistical validity. Variability within groups should be examined to determine if the correlations that arise are due to large changes within the group. The meta-analytic method provides functional connectivity estimates that are less affected by individuals or changes between sessions than the direct method. However, it is imperative that the group size be large, preferably equal to or greater than 30 individuals in each group to use this method. If the desired group size is available, then this is the preferred method for functional connectivity analysis. Homogeneity analysis is possible using Q statistics which indicates variability within group. A combination of the two methods is ideal for functional connectivity analysis in fMRI when group sizes are small (< 20 subjects)(see Chapter 3 for limitations of these methods).

The SEM method for examining effective connectivity in fMRI has been the most common method used in the last decade. While some concerns with the technique have been raised, the main aim in this thesis was to examine SEM as a partially exploratory approach for identifying regional interactions. The approach in this thesis has shown that directional interactions unique to a task can be elucidated by SEM. Given the large amount of data, i.e., greater than 2500 data points, the SEM

models for task activated regions are approximately similar. Therefore, when the functional interactions between regions known to be implicated in the performance of a task are not known fully (the prefrontal and parietal regions in the Simon task in this study), they can be identified by defining an anatomical model where connections are allowed to vary when testing with data (see Chapter 4 for limitations of SEM).

Modeling connectivity over time with SEM showed a similar network of interactions between prefrontal and parietal regions needed to perform the Simon task in HD patients. With the availability of more data, significant differences can be expected in HD patients, who should show reduced connectivity over time. Measuring differences over time and considering clinical measures can also be used to predict deterioration rate in HD. For example, an artificial neural network can be trained to predict impaired functional connectivity between prefrontal regions using C-A-G index as an input.

The DCM results did not show significant interactions between the same prefrontal and parietal regions assessed with SEM. While SEM is conducted at the group level, i.e. regions are selected based on group activation maps and time courses are concatenated across subjects in a group, DCM is conducted on each individual. The DCM study undertaken is a confirmatory study as it is more appropriate to confirm a network of regional interactions with DCM than to explore a possible set of interactions. Furthermore, significant regional activation is necessary in each individual in order to obtain a high degree of connectivity. The results with activated regions in five controls during task performance shows that this is true.

DCM is more appropriate for effective connectivity in fMRI than SEM, given that the influence of the task on connections can be measured and that DCM is a time series model. With shorter temporal resolutions becoming available for experiments (< 2 s) more information can be ascertained from DCM compared to SEM.

Experiments specifically designed with modulatory effects can also be assessed with DCM (see Chapter 5 for limitations of DCM).

The next stage to assess brain region connectivity in HD will be to select a task for which activation and possibly connectivity patterns for each individual are clearly known (i.e. common regions are activated across all subjects), making sure that the task selected activates regions affected in HD. This information can be used to construct a theoretical model of connectivity for a particular task. The model can then be tested using DCM with control data followed by HD patient data and compared. Connectivity patterns can also be explored by using tools such as Bayes factor [implemented in SPM5, The Wellcome Department of Imaging Neuroscience, London, UK (Friston, Holmes, Poline, Price and Frith, 1996; FIL, 2004)] which should reveal impaired interactions in HD patients. A larger group of HD patients will also provide more useful information when assessing connectivity at the individual level.

6.4 Summary

In this thesis, functional and effective connectivity methods were tested with previously acquired fMRI data. As expected, functional connectivity provided a high level view of interactions between selected regions of interest. SEM confirmed these findings and, additionally, provided directionality to the interactions. However, reliable effective connectivity estimates from group data could not be obtained with DCM, indicating that changes to the experiment design to cater to the DCM method would be required. These results demonstrate that functional connectivity and SEM in fMRI are a valuable indicators of anatomical connectivity in the brain.

Brain region pathology in HD results in loss of anatomical connections. In this thesis, connectivity measures in fMRI were tested and showed that physical disconnections between task activated regions (i.e., in HD patients) result in reduced functional interactions compared to connections that are known not to be affected (i.e., in controls). The results obtained here further confirm findings in other connectivity studies with neurodegenerative diseases which show functional differences between controls and patients (e.g. Parkinson's disease). In conclusion, fMRI connectivity is a valuable method for ascertaining connectivity impairments in neurodegenerative diseases.

This thesis has demonstrated with fMRI data that healthy controls and HD patients differ in their recruitment of prefrontal and fronto-parietal regional connectivity to perform the Simon task. In particular, impaired prefrontal functional connectivity and impaired prefrontal and fronto-parietal effective connectivity was seen in HD patients. While functional activation and volumetric studies have shown cortical and subcortical abnormalities or deficits in HD patients, quantitative measures of regional connectivity have not been explored. Via the use of the Simon task, this thesis has taken a step forward by showing quantitatively that abnormalities in connectivity in mild to moderate stage HD patients exist and they lack the regional coupling seen in controls needed to perform the Simon task.

Appendix A

Homogeneity Analysis

The following matrices provide an indication of variability within the control and HD patient groups during baseline and task performance. Table A.1 lists the Q statistics for regional functional connectivity in controls and Table A.2 shows Q statistics for HD patients.

Table A.1: Homogeneity analysis - controls; significant statistics with $p = 0.05$ are marked with (*); - : not considered.

	Baseline				Task			
	RAC	LAC	RPC	LPC	RAC	LAC	RPC	LPC
RAC	-				-			
LAC	14.5	-			7.85	-		
RPC	25.83	33.14 (*)	-		10.00	16.76	-	
LPC	11.89	16.30	20.13	-	9.38	5.98	17.11	-

Table A.2: Homogeneity analysis - patients; Significant statistics with $p = 0.05$ are marked with (*); - : not considered.

	Baseline				Task			
	RAC	LAC	RPC	LPC	RAC	LAC	RPC	LPC
RAC	-				-			
LAC	36.41 (*)	-			25.43	-		
RPC	48.22 (*)	27.84 (*)	-		35.57 (*)	20.57	-	
LPC	44.53 (*)	37.60 (*)	39.27 (*)	-	28.70	20.49	34.81 (*)	-

Appendix B

Correlating Functional Connectivity with Clinical and Behavioural Data

The correlation thresholds for a two tailed test are computed as follows (Zar, 1997):

$$r_{p,df} = \sqrt{\frac{t^2_{p,df}}{df - t^2_{p,df}}} \tag{B.1}$$

where t is the score for a probability level chosen (e.g. $p = 0.05$) and df is the degrees of freedom which is equal to n - 2[1]. Selecting $p = 0.05$ and dividing this threshold by 24 (number of comparisons) for controls and 30 for HD patients, corrects the threshold for multiple comparisons. The new t score obtained is used in Equation B.1 to obtain a corrected threshold.

Using the method above, the threshold for 17 controls ($p_{corr} = 0.002$, $t_{15} = \pm 3.74$) is ± 0.695. The clinical data for the full set of 20 HD patients was unavailable. The thresholds for the available data are as follows:

[1] n is the number of subjects

- $n = 17$: $p_{15} = 0.001$, $t = \pm 4.05$, threshold $= \pm 0.723$.
- $n = 19$: $p_{17} = 0.001$, $t = \pm 3.95$, threshold $= \pm 0.692$.
- $n = 20$: $p_{18} = 0.001$, $t = \pm 3.90$, threshold $= \pm 0.677$.

The following Tables (B.1,B.2, B.3, and B.4) show correlations of functional connectivity with clinical and behavioural data for controls and HD patients during task and baseline states. After correcting for multiple comparison, using a Bonferroni correction, none of the correlations are significant.

Table B.1: Correlation of connectivity with clinical and behavioural data for controls during baseline state; RT: response times; BDI: Beck Depression Inventory.

	RAC-LAC	RAC-RPC	RAC-LPC	LAC-RPC	LAC-LPC	RPC-LPC
RT	0.36	0.45	-0.30	0.30	0.05	-0.50
Errors	0.50	0.40	0.20	0.50	-0.06	-0.04
Age	-0.08	-0.08	-0.16	0.01	0.02	0.02
BDI	0.24	0.41	0.27	0.44	0.33	-0.19

Table B.2: Correlation of connectivity with clinical and behavioural data for controls during task state; RT: response times; BDI: Beck Depression Inventory.

	RAC-LAC	RAC-RPC	RAC-LPC	LAC-RPC	LAC-LPC	RPC-LPC
RT	-0.18	-0.35	-0.17	-0.34	-0.04	-0.15
Errors	0.15	-0.18	-0.23	-0.30	-0.28	-0.18
Age	-0.05	-0.02	-0.03	0.23	-0.09	0.13
BDI	0.03	-0.27	-0.12	-0.37	-0.15	-0.24

Table B.3: Correlation of connectivity with clinical and behavioural data for HD patients during baseline state; RT: response times; a = 19; b = 17; BDI: Beck Depression Inventory; CI: C-A-G index;

	RAC-LAC	RAC-RPC	RAC-LPC	LAC-RPC	LAC-LPC	RPC-LPC
RT	-0.20	-0.04	-0.51	-0.36	-0.44	-0.15
Errors	-0.06	-0.06	-0.11	0.10	0.01	0.28
Age	0.02	-0.02	0.07	-0.08	0.042	-0.25
BDI[a]	-0.08	0.22	0.05	-0.03	0.01	-0.10
CI[b]	0.37	-0.12	0.08	0.05	0.33	0.24

Table B.4: Correlation of connectivity with clinical and behavioural data for HD patients during task state; RT: response times; a = 19; b = 17; BDI: Beck Depression Inventory; CI: C-A-G index;

	RAC-LAC	RAC-RPC	RAC-LPC	LAC-RPC	LAC-LPC	RPC-LPC
RT	-0.15	-0.27	-0.45	-0.28	-0.44	-0.16
Errors	-0.18	0.16	-0.35	0.04	-0.59	-0.30
Age	0.26	0.26	-0.05	0.34	0.14	-0.05
BDI[a]	-0.028	-0.12	-0.10	-0.03	-0.11	-0.07
CI[b]	0.37	-0.13	0.08	0.05	0.33	0.24

Appendix C

SEM Goodness of Fit Results

The following goodness of fit indices are reported and their formulas are obtained from (Arbuckle, 2003) and (Tabachnick and Fidell, 2001).

1. RMR: root mean square residual

$$RMR = \left(2 \times \sum_{i=1}^{n} \sum_{j=1}^{i} \frac{(o_{ij} - \hat{\sigma}_{ij})^2}{n(n+1)} \right)^{\frac{1}{2}} \tag{C.1}$$

   where n is the number of variables, o_{ij} are the observed variances (or covariances), and $\hat{\sigma}_{ij}$ are the estimated variances (or covariances).

2. GFI: goodness of fit index

$$GFI = \frac{tr(\hat{\sigma}^T \times W \times \hat{\sigma})}{tr(o^T \times W \times o)} \tag{C.2}$$

   where tr is the trace operator, T is the transpose operator, o_{ij} are the observed variances, $\hat{\sigma}$ are the estimated variances, W is the weight matrix (for ML estimation, $W = \Sigma^{-1}$, which is the inverse of the estimated covariance matrix). The numerator is the sum of the estimated weighted variances and the denominator is the sum of the observed weighted variances.

3. RMSEA: root mean square error of approximation

$$RMSEA = \left(\frac{\hat{S}_0}{df_{esm}}\right)^{\frac{1}{2}} \tag{C.3}$$

where $\hat{S}_0$ is chosen as zero or

$$\hat{S}_0 = \frac{\chi^2_{esm} - df_{esm}}{N} \tag{C.4}$$

if $\hat{S}_0$ is non-negative. N is the number of observations, df is the degrees of freedom, and esm is the estimated model.

4. AIC: Akaike information criterion

$$AIC = \chi^2_{esm} - 2 \times df_{esm} \tag{C.5}$$

where χ^2_{esm} and df_{esm} are the estimated χ^2 and degrees of freedom of the estimated model.

5. BIC: Bayesian information criterion

$$BIC = \chi^2_{esm} - df_{esm} \times ln(N) \tag{C.6}$$

where χ^2_{esm} and df_{esm} are the estimated χ^2 and degrees of freedom of the estimated model, and N is the number of observations.

Table C.1 shows all the statistics described above for the control and HD patient models. Table C.2 shows these statistics for the HD patient models in year one and year two.

Table C.1: Goodness of fit indices for controls' and HD patients' SEM computed with AMOS 5.0; degrees of freedom equal to one in both models;

	Controls	Patients
χ^2	0.003	0.720
RMR	0.000	0.002
GFI	1.000	1.000
RMSEA	0.000	0.000
AIC	40.003	40.720
BIC	167.571	171.539

Table C.2: Goodness of fit indices for 11 HD patients' in first and second year computed with AMOS 5.0; degrees of freedom equal to one in both models;

	HD patients(1)	HD Patients (2)
χ^2	0.655	0.197
RMR	0.002	0.004
GFI	1.000	1.000
RMSEA	0.000	0.000
AIC	40.197	40.197
BIC	151.517	159.058

Appendix D

SEM: Comparisons Between Path Coefficients

The following comparisons were made using the stacked models approach suggested by McIntosh & Gonzalez-Lima (1994) and is described in the methods section of chapter 4. The connections in two models are compared with a Bonferroni correction to account for multiple comparisons. χ^2_{diff} is computed using χ^2_{const} - χ^2_{vary} with degrees of freedom equal to one. Tables D.1 and D.2 show the numerical results for the differences between controls and HD patients in year one for fronto-parietal and prefrontal connectivity, respectively. Table D.3 shows that differences in fronto-parietal connectivity in HD patients from year one to year two.

Table D.1: Significant differences in connectivity between controls and HD patients in year one; Bonferroni correction: $0.05/13 = 0.00385$; $\chi^2_{const} = 430.3$, $\mathrm{DF}_{const} = 15$;

Link	χ^2_{diff}	DF_{diff}	Probability level	Significant
RAC→LAC	29.40	1	< 0.001	yes
RPC→RPL	16.00	1	< 0.001	yes
RPC→RAC	67.70	1	< 0.001	yes
RPL→LPL	0.00	1	> 0.05	no
RPL→LPL	29.40	1	< 0.001	yes
LAC→LPC	2.20	1	> 0.05	no
LAC→LPL	94.90	1	< 0.001	yes
LPC→RPL	19.40	1	< 0.001	no

Table D.2: Significant differences in connectivity within the AC-PC network; Bonferroni correction: $0.05/5 = 0.02$; $\chi^2_{const} = 306.3$, $\mathrm{DF}_{const} = 6$;

Link	χ^2_{diff}	DF_{diff}	Probability level	Significant
RAC→LAC	35.60	1	< 0.001	yes
RPC→RAC	107.80	1	< 0.001	yes
LAC→LPC	0.10	1	> 0.05	no

Table D.3: Significant differences in connectivity between HD patients in year one and HD patients in year two; Bonferroni correction: $0.05/13 = 0.00385$; $\chi^2_{const} = 527.5$, $\mathrm{DF}_{const} = 15$;

Link	χ^2_{diff}	DF_{diff}	Probability level	Significant
RAC→LAC	110.40	1	< 0.001	yes
RPC→RPL	164.30	1	< 0.001	yes
RPC→RAC	82.80	1	< 0.001	yes
RPL→LPL	9.50	1	< 0.003	yes
LAC→LPC	1.80	1	> 0.05	no
LPC→RPL	18.30	1	< 0.001	no

Appendix E

DCM Connectivity Estimates

The following tables (E.1 and E.2) show connectivity estimates obtained with DCM for the AC-PC network in controls and HD patients.

Table E.1: AC-PC connectivity for each control subject; the subjects are labeled C101 TO C117 representing the cohort of 17 subjects; probability levels greater than 0.05 are presented in parentheses; Avg: Average; t: t score;

	LAC→LPC	LAC→RPC	RAC→LAC	LPC→RAC	RPC→RAC	RPC→LPC
C101	0	0	0	0.02	-0.03	0
C102	0	0	0	-0.02	-0.09	0
C103	0	0	0	0.05	0.02	0
C104	0	0	0	0.05	0.01	0
C105	0	0	0	-0.05	0	0
C106	0	0	0.01	-0.08	0.06	-0.02
C107	0	0	0	0.01	0	0
C108	0	0	0	0	0	0
C109	0	0	0	0	-0.07	0
C110	0	0	0	0.03	0.02	0
C111	0	0	0.02	-0.03	0.19	0
C112	0	0	0	0.04	0.04	-0.01
C113	0	0	0	0.02	0.01	-0.03
C114	0	0	-0.01	-0.01	-0.14	0
C115	0	0	0	-0.07	0.03	0
C116	0	0	0	0.02	0	0
C117	0	0	0.07	0.13	-0.06	0.02
Avg	0	0	0	0	0	0
t	-0.97	0	1.79	0.44	-0.06	-0.04

Table E.2: AC-PC connectivity for each HD patient; The subjects are labeled P101 TO P120 representing the cohort of 20 subjects; Avg: Average; t: t score.

	LAC→LPC	LAC→RPC	RAC→LAC	LPC→RAC	RPC→RAC	RPC→LPC
P101	0	0	0	0	0	0
P102	0	0	0.03	-0.04	0.17	0
P103	0	0	0	0.01	0.03	0
P104	0	0	0	0.01	0	0
P105	0	0	0.05	-0.15	-0.03	0
P106	0	0	0.01	0.05	0.05	0
P107	0	0	0.02	-0.06	0.13	0
P108	0	0	0	0	0	0
P109	0	0	0.01	0.07	-0.04	0.02
P110	0	0	0	0	0.01	0.01
P111	0	0	0	0	0	0.01
P112	0	0	0.01	0.06	0.12	-0.03
P113	0	0	-0.02	0.03	0.05	0.01
P114	0	0	0	-0.05	0	0
P115	0	0	0.01	0.01	-0.04	0
P116	0	0	0	0.04	0	0
P117	0	0	0	0.03	0.03	-0.03
P118	0	0	0	0.02	0.12	0
P119	0	0	0	-0.04	0	0
P120	0	0	0	0	0	0
Avg	0	0	0	0	0	0
t	0	0.98	2.03	0.53	2.21	-0.08

Appendix F

Activation Maps for Five Controls

The activation results for five controls chosen are presented in Figures F.1 to F.5. Peak voxel were chosen in lateral prefrontal, anterior cingulate, and parietal regions. The scale for these activation maps is presented in Figure F.6.

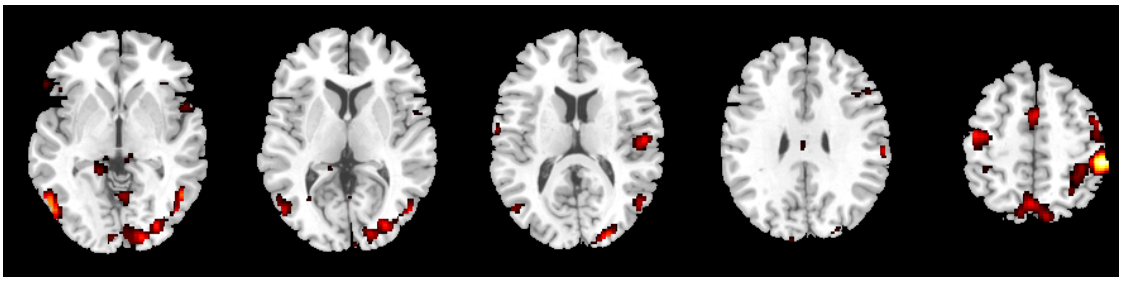

Figure F.1: Activation map for C1.

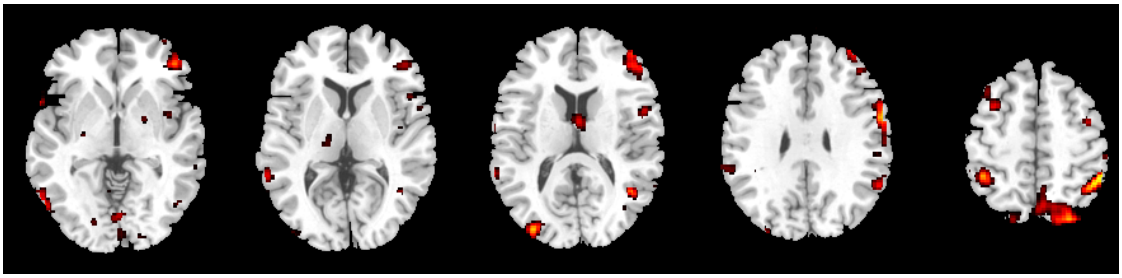

Figure F.2: Activation map for C2.

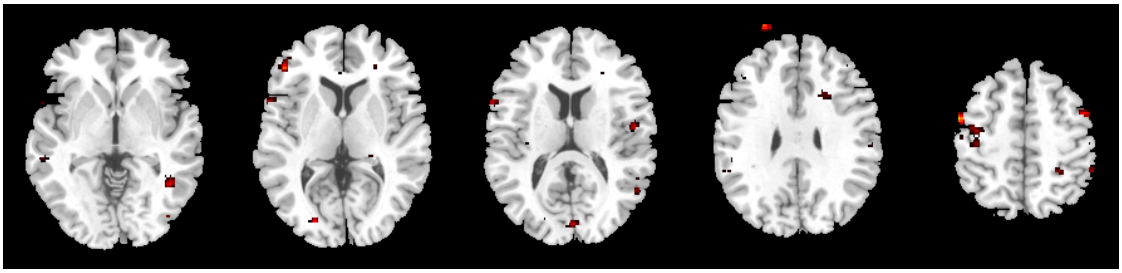

Figure F.3: Activation map for C3.

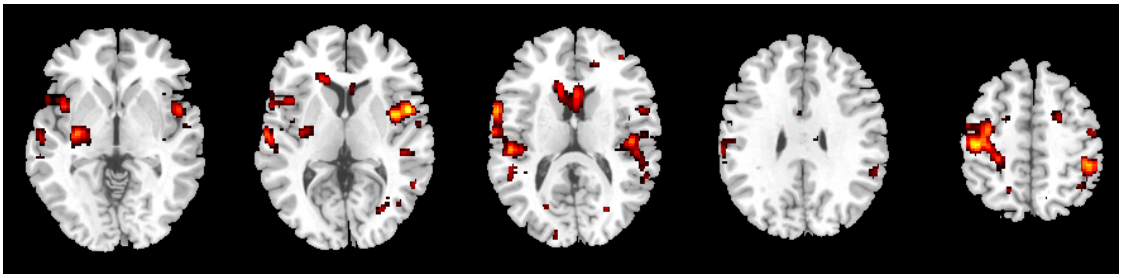

Figure F.4: Activation map for C4.

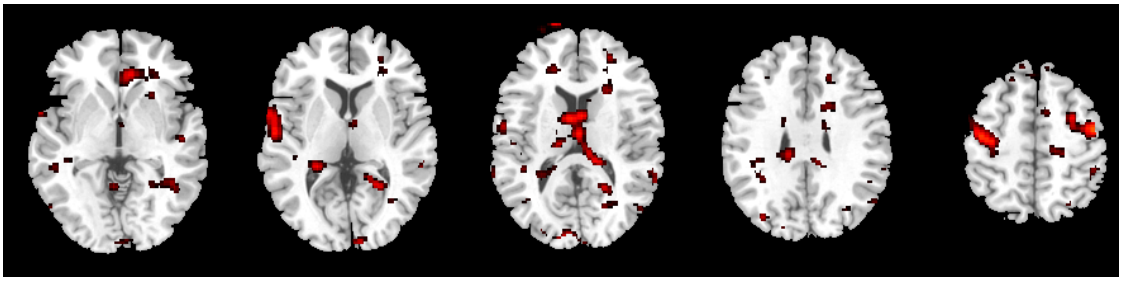

Figure F.5: Activation map for C5.

Figure F.6: The scale for the activation maps in Figures F.1 to F.5.

Appendix G

Glossary of Abbreviations

The following is a list of acronyms and abbreviations used in this thesis. They are listed according to order of appearance in the text commencing from Chapter 1.

1. HD: Huntington's Disease
2. MR: Magnetic Resonance
3. fMRI: Functional Magnetic Resonance Imaging
4. BOLD: Blood Oxygenation Level Dependent
5. ROI: Region Of Interest
6. SNR: Substantia Nigra pars Reticulata
7. GPi: Globus Pallidus internal segment
8. X-ray CT: X-ray Computed Tomography
9. PET: Positron Emission Tomography
10. MRI: Magnetic Resonance Imaging
11. RF: Radio Frequency

12. HRF: Hemodynamic Response Function

13. GLM: General Linear Model

14. SPM: Statistical Parametric Map/Statistical Parametric Mapping

15. SPECT: Single Photon Emission Computerized Tomography

16. EEG: Electroencephalograms

17. ERP: Event-Related Potential

18. TR: Temporal Resolution

19. DAG: Directed Acyclic Graph

20. SEM: Structural Equation Modeling

21. MAR: Multivariate Autoregressive Modeling

22. DCM: Dynamic Causal Modeling

23. NHMRC: National Health and Medical Research Council

24. UHDRS: Unified Huntington's Disease Rating Scale

25. BDI: Beck Depression Inventory

26. NART: National Adult Reading Test

27. MMSE: Mini Mental State Examination

28. DCT: Discrete Cosine Transform

29. INC: Incongruent

30. CON: Congruent

31. AR: Autoregressive

32. AC: Anterior Cingulate

33. PC: Prefrontal Cortex

34. PL: Parietal Lobe

35. FWHM: Full Width Half Maximum

36. LAC/RAC: Left/Right Anterior Cingulate

37. LPC/RPC: Left/Right Prefrontal Cortex

38. LPL/RPL: Left/Right Parietal Lobe

39. DF: Degrees of Freedom

40. GFIs: Goodness of Fit Indices

41. ML: Maximum Likelihood

42. RMR: Root Mean Square Residual

43. RMSEA: Root Mean Square Error of Approximation

44. GFI: Goodness of Fit Index

45. AIC: Akaike Information Criterion

46. BIC: Bayesian Information Criterion

47. rCBF: regional Cerebral Blood Flow

References

Alexander, G., Delong, M. and Strick, P. (1986). Parallel organization of functionally segregated circuits linking basal ganglia and cortex, *Annual Reviews in Neuroscience* **9**: 357–381.

Allen, J., Coan, J. and Nazarian, M. (2004). Issues and assumptions on the road from raw signals to metrics of frontal eeg asymmetry in emotion, *Biological Psychology* **67**: 183–218.

Allen, J. and Kline, J. (2004). Frontal eeg asymmetry, emotion, and psychopathology: the first, and the next 25 years, *Biological Psychology* **67**: 1–5.

Anderson, R. and Vastag, G. (2004). Causal modeling alternatives in operations research: Overview and application, *European Journal of Operational Research* **156**: 92–109.

Arbuckle, J. (2003). Amos reference guide.

Beck, A., Ward, C., Mendelson, M., Mock, J. and Erbaugh, J. (1961). An inventory for measuring depression, *Archives of General Psychiatry* **4**: 53–63.

Beiser, D., Huat, S. and Houk, J. (1997). Network models of the basal ganglia, *Current Opinion in Neurobiology* **7**: 185–190.

Bergman, H., Feingold, A., Nini, A., Raz, A., Slovin, H., Abeles, M. and Vadia, E. (1998). Physiological aspect of information processing in the basil ganglia of normal and parkinsonian primates, *Trends in Neurosciences* **21**: 32–38.

Block-Galarza, J., Chase, K., Sapp, E., Vaughn, K., Vallee, R., DiFiglia, M. and Aronin, N. (1997). Fast transport and retrograde movement of huntingtin and hap 1 in axons, *Neuroreport* **8**: 2247–2251.

Bokde, A., Tagamets, M.-A., Friedman, R. and Horwitz, B. (2001). Functional interactions of the inferior frontal cortex during the processing of words and word-like stimuli, *Neuron* **30**: 609–617.

Boksmana, K., Thebergea, J., Williamson, P., Drost, D., Malla, A., Densmore, M., Takhar, J., Pavlosky, W., Menon, R. and Neufeld, R. (2005). A 4.0-t fmri study of brain connectivity during word fluency in first-episode schizophrenia, *Schizophrenia Research* **75**: 247–263.

Bollen, K. A. (1989). *Structural equations with latent variables*, Wiley.

Borlongan, C., Koutouzis, T., Freeman, T., Cahill, D. and Sanberg, P. (1995). Behavioral pathology induced by repeated systemic injections of 3-nitropropionic acid mimics the motoric symptoms of huntington's disease, *Brain Research* **697**: 254–257.

Borlongan, C., Koutouzis, T. and Sandberg, P. (1997). 3-nitropropionic acid animal model and huntington's disease, *Neuroscience and Biobehavioral Review* **21**: 289–293.

Breckler, S. (1990). Applications of covariance structure modeling in psychology: Cause for concern?, *Psychological Bulletin* **107**: 260–273.

Buchel, C. and Friston, K. (1997). Modulation of connectivity in visual pathways by attention: Cortical interactions evaluated with structural equation modelling and fmri, *Cerebral Cortex* **7**: 768–778.

Bullmore, E., Horwitz, B., Honey, G., Brammer, M., Williams, S. and Sharma, T. (2000). How good is good enough in path analysis of fmri data?, *NeuroImage* **11**: 289–301.

Bush, G., Luu, P. and Posner, M. (2000). Cognitive and emotional influences in anterior cingulate cortex, *Trends in Cognitive Neuroscience* **4**: 215–222.

Cattaneo, E., Rigamonti, D., Goffredo, D., Zuccato, C., Squitieri, F. and Sipione, S. (2001). Loss of normal huntingtin function: new developments in huntingtons disease research, *Trends in Neurosciences* **24**: 182–188.

Cha, J.-H. (2000). Transcriptional dysregulation in huntingtons disease, *Trends in Neurosciences* **23**: 387–392.

Charniak, E. (1991). Bayesian networks without tears, *AI Magazine* **12**: 50–63.

Chen, D. (2004). A brief history of huntington's disease, Huntington's Outreach Project for Education at Stanford University. Available from: http://www.stanford.edu/group/hopes/basics/timeline/r2.html.

Clark, V., Lai, S. and Deckel, A. (2002). Altered functional mri responses in huntington's disease, *Neuroreport* **13**: 703–706.

Clower, D., Dum, R. and Strick, P. (2005). Basil ganglia cerebellar inputs to 'aip', *Cerebral Cortex* **15**: 913–920.

Coan, J. and Allen, J. (2004). Frontal eeg asymmetry as a moderator and mediator of emotion, *Biological Psychology* **67**: 7–49.

Cordes, D., Haughton, V., Arfanakis, K., Wendt, G., Turski, P., Moritz, C., Quigley, M. and Meyerand, M. (2001). Mapping functionally related regions of brain with functional connectivity mr imaging, *American Journal of Neuroradiology* **21**: 1636–1644.

Coull, J., Buchel, C., Friston, K. and Frith, C. (1999). Noradrenergically mediated plasticity in a human attentional neuronal network., *NeuroImage* **10**: 705–715.

Cummings, J. (1993). Frontal-subcortical circuits and human behavior, *Archives of Neurology* **50**: 873–880.

Deckel, A. and Cohen, D. (2000). Increased cbf velocity during word fluency in huntingtons disease patients, *Neuro-Psychopharmacology and Biological Psychiatry* **24**: 193–206.

Dragatsisa, I., Dietricha, P. and Zeitlin, S. (2000). Expression of the huntingtin-associated protein 1 gene in the developing and adult mouse, *Neuroscience Letters* **282**: 37–40.

Durston, S., Thomas, K. M., Worden, M. S., Yang, Y. and Casey, B. J. (2002). The effect of preceding context on inhibition: An event-related fmri study, *NeuroImage* **16**: 449–453.

Dursun, S., Burke, J., Andrews, H., Mlynik-Szmid, A. and Reveley, M. (2000). The effects of antipsychotic medication on saccadic eye movement abnormalities in huntington's disease, *Progress in neuro-psychopharmacology and biological psychiatry* **24**: 889–896.

Egner, T., Jamieson, G. and Gruzelier, J. (2005). Hypnosis decouples cognitive control from conflict monitoring processes of the frontal lobe, *NeuroImage* **217**: 969–978.

Ethofer, T., Anders, S., Erb, M., Herbert, C., Wiethoff, S., Kissler, J., Grodd, W. and Wildgruber, D. (2005). Cerebral pathways in processing of affective prosody: A dynamic causal modeling study, *NeuroImage* **30**: 580–587.

Fennema-Notestine, C., Archibald, S., Jacobson, M., Corey-Bloom, J., Paulsen, J., Peavy, G., Gamst, A., Hamilton, J., Salmon, D. and Jernigan, T. (2004). In vivo evidence of cerebellar atrophy and cerebral white matter loss in huntington disease, *Neurology* **63**: 989–995.

FIL (2004). Statistical parametric mapping, SPM website. Available from: http://www.fil.ion.ucl.ac.uk/spm/.

FMRIB (2004). Oxford centre for functional magnetic resonance imaging of the brain, FMRIB's website. Available from: http://www.fmrib.ox.ac.uk/.

Folstein, M., Folstein, S. and McHugh, P. (1975). 'mini-mental state'. a practical method for grading the cognitive state of patients for the clinician., *Journal of Psychiatric Research* **12**: 189–198.

Foucher, J., Vidailhet, T., Chanraud, S., Gounot, D., Grucker, D., Pins, D., Damsa, C. and Danion, J.-M. (2005). Functional integration in schizophrenia: Too little or too much? preliminary results on fmri data, *NeuroImage* **26**: 374–388.

Friman, O., Borga, M., Lundberg, P. and Knutsson, H. (2002). Exploratory fmri analysis by autocorrelation maximization, *NeuroImage* **16**: 454–464.

Friston, K. (1994a). Functional and effective connectivity in neuroimaging: A synthesis, *Human Brain Mapping* **2**: 56–78.

Friston, K. (1994b). Functional and effective connectivity in neuroimaging: A synthesis, *Human Brain Mapping* **2**: 56–78.

Friston, K. (2002). Bayesian estimation of dynamical systems: An application to fmri, *NeuroImage* **16**: 513–530.

Friston, K., Buechel, C., Fink, G., Morris, J., Rolls, E. and Dolan, R. (1997). Psychophysiological and modulatory interactions in neuroimaging, *NeuroImage* **6**: 218–229.

Friston, K., Fletcher, P., Josephs, O., Holmes, A., Rugg, M. and Turner, R. (1998). Event-related fmri: Characterizing differential responses, *NeuroImage* **7**: 30–40.

Friston, K., Harrison, L. and Penny, W. (2003). Dynamic causal modelling, *NeuroImage* **19**: 1273–1302.

Friston, K., Holmes, A., Poline, J.-B., Price, C. and Frith, C. (1996). Detecting activations in pet and fmri: Levels of inference and power, *NeuroImage* **40**: 223–235.

Friston, K., Mechelli, A., Turner, R. and Price, C. (2000). Nonlinear responses in fmri: The balloon model, volterra kernels, and other hemodynamics, *NeuroImage* **12**: 466–477.

Friston, K., Williams, S., Howard, R., Frackowiak, R. and Turner, R. (1996). Movement-related effects in fmri time-series, *Magnetic Resonance in Medicine* **35**: 346–355.

Gallinat, J. and Heinz, A. (2006). Combination of multimodal imaging and molecular genetic information to investigate complex psychiatric disorders., *Pharmacopsychiatry* **39 Supplement 1**: S76–S79.

Gaura, V., Bachoud-Levi, A.-C., Ribeiro, M.-J., Nguyen, J.-P., Frouin, V., Baudic, S., Brugieres, P., Mangin, J.-F., Boisse, M.-F., Pal, S., Cesaro, P., Samson, Y., Hantraye, P., Peschanski, M. and Remy, P. (2004). Striatal neural grafting

improves cortical metabolism in huntington's disease patients, *Brain* **127**: 65–72.

Gavrilescu, M., Stuart, G., Waites, A., Jackson, G., Svalbe, I. and Egan, G. (2004). Changes in effective connectivity models in the presence of task-correlated motion: An fmri study, *Human Brain Mapping* **21**: 49–63.

Gazzaniga, M., Ivry, R. and Mangun, G. (1998). *Cognitive Neuroscience: The Biology of the Mind*, W. W. Norton & Company.

Georgiou-Karistianis, N., Smith, E., Bradshaw, J. L., Chua, P., Lloyd, J., Churchyard, A. and Chiu, E. (2003). Future directions in research with presymptomatic individuals carrying the gene for huntingtons disease, *Neuropsychologia* **59**: 331–338.

Georgiou, N., Bradshaw, J. L., Phillips, J. G. and Chiu, E. (1995). The effect of huntington's disease and gilles de la tourette's syndrome on the ability to hold and shift attention, *Neuropsychologia* **34**: 843–851.

Gitelman, D., Parrish, T., Friston, K. and Mesulam, M.-M. (2002). Functional anatomy of visual search: Regional segregations within the frontal eye fields and effective connectivity of the superior colliculus, *NeuroImage* **15**: 970–982.

Gomez-Tortosa, E., MacDonald, M., Friend, J., Taylor, S., Weiler, L., Cupples, L., Srinidhi, J., Gusella, J., Bird, E., Vonsattel, J.-P. and Myers, R. (2001). Quantitative neuropathological changes in presymptomatic huntingtons disease, *Annals of Neurology* **49**: 29–34.

Goncalves, M., Hall, D., Johnsrude, I. and Haggard, M. (2001). Can meaningful effective connectivities be obtained between auditory cortical regions?, *NeuroImage* **14**: 1353–1360.

Grady, C., Furey, M., Pietrini, P., Horwitz, B. and Rapoport, S. (2001). Altered brain functional connectivity and impaired short-term memory in alzheimer's disease, *Brain* **124**: 739–756.

Grootoonk, S., Hutton, C., Ashburner, J., Howseman, A., Josephs, O., Rees, G., Friston, K. and Turner, R. (2000). Characterization and correction of interpolation effects in the realignment of fmri time series, *NeuroImage* **11**: 49–57.

Guidetti, P., Charles, V., Chen, E.-Y., Reddy, P., Kordower, J., Whetsell, W., Schwarcz, J. and Tagle, D. (2001). Early degenerative changes in transgenic mice expressing mutant huntingtin involve dendritic abnormalities but no impairment of mitochondrial energy production, *Experimental Neurology* **169**: 340–350.

Gusella, J., Wexler, N., Conneally, P., Naylor, S., Anderson, M., Tanzi, R., Watkins, P., Ottina, K., Wallace, M., Sakaguchi, A., Young, A., Shoulson, I., Bonilla, E. and Martin, J. (1983). A polymorphic dna marker genetically linked to huntingtons disease, *Nature* **306**: 234–238.

Hallett, M. (1993). Pathophysiology of basil ganglia disorders: an overview, *Canadian Journal of Neurological Sciences* **20**: 177–183.

Halliday, G., McRitchie, D., Macdonald, V., Double, K., Trent, R. and McCusker, E. (1998). Regional specificity of brain atrophy in huntington's disease, *Experimental Neurology* **154**: 663–672.

Hampson, M., Peterson, B., Skudlarski, P., Gatenby, J. and Gore, J. (2002). Detection of functional connectivity using temporal correlations in mr images, *Human Brain Mapping* **15**: 247–262.

Haque, N., Borghesani, P. and Isacson, O. (1997). Therapeutic strategies for huntington's disease based on a molecular understanding of the disorder, *Molecular Medicine* **3**: 175–183.

Harjes, P. and Wanker, E. (2003). The hunt for huntingtin function: interaction partners tell many different stories, *Trends in Biochemical Sciences* **28**: 425–433.

Harper, P., Houlihan, G., Jones, A., MacMillan, J., Morris, M., Quarrell, O., Scourfield, J., Shaw, D., Solden, J. and Tyler, A. (1996). *Huntington's Disease*, 2 edn, W. B. Saunders Company Ltd.

Harrison, L., Penny, W. and Friston, K. (2003). Multivariate autoregressive modeling of fmri time series, *NeuroImage* **12**: 1477–1491.

Heckerman, D. (1995). A bayesian approach to learning causal networks, *Technical report*, Microsoft Corporation.

Hedges, L. and Olkin, I. (1985). *Statistical methods for meta-analysis*, Academic press.

Hennenlotter, A., Schroeder, U., Erhard, P., Haslinger, B., Stahl, R., Weindl, A., von Einsiedel, H., Lange, K. and Ceballos-Baumann1e, A. (2004). Neural correlates associated with impaired disgust processing in pre-symptomatic huntington's disease, *Brain* **41**: 1–8.

Hertz, J., Krogh, A. and Palmer, R. (1991). *Introduction to the Theory of Neural Computation*, Addison-Wesley Publishing Company.

Hesselink, J. (2005). Basic principles of mr imaging, Hesselink MR website. http://spinwarp.ucsd.edu/NeuroWeb/Text/br-100.htm.

Ho, A., Nestor, P., Williams, G., Bradshaw, J., Sahakian, B., Robbins, T. and Barker, R. (2004). Pseudo-neglect in huntington's disease correlates with decreased angular gyrus density, *Neuroreport* **15**: 1061–1064.

Hoffner, G. and Djian, P. (2002). Protein aggregation in huntingtons disease, *Biochimie* **84**: 273–278.

Homae, F., Yahata, N. and Sakaia, K. (2003). Selective enhancement of functional connectivity in the left prefrontal cortex during sentence processing, *NeuroImage* **20**: 578–586.

Honey, G., Fu, C., Kim, J., Brammer, M., Croudace, T., Suckling, J., Pich, E., Williams, S. and Bullmore, E. (2002). Effects of verbal working memory load on corticocortical connectivity modeled by path analysis of functional magnetic resonance imaging data, *NeuroImage* **17**: 573–582.

Horwitz, B., Friston, K. and Taylor, J. (2000). Neural modeling and functional brain imaging: an overview, *Neural Networks* **13**: 829–846.

Horwitz, B., Warner, B., Fitzer, J., Tagamets, M., Husain, F. and Long, T. (2005). Investigating the neural basis for functional and effective connectivity. application to fmri, *Philosophical Transactions of the Royal Society of London B Biological Sciences* **360**: 1093–108.

Hu, L.-T. and Bentler, P. (1992). Can test statistics in covariance structure analysis be trusted?, *Psychological Bulletin* **112**: 351–362.

Huettel, S. and McCarthy, G. (2004). What is odd in the oddball task? prefrontal cortex is activated by dynamic changes in response strategy., *Neuropsychologia* **42**: 379–386.

Humbert, S. and Saudou, F. (2004). Huntingtin phosphorylation and signaling pathways that regulate toxicity in huntingtons disease, *Clinical Neuroscience Research* **3**: 149–155.

Iacoboni, M., Woods, R. and Mazziotta, J. (1998). Bimodal (auditory and visual) left frontoparietal circuitry for sensorimotor integration and sensorimotor learning., *Brain* **121**: 2135–2143.

Jakel, R. and Maragos, W. (2000). Neuronal cell death in huntingtons disease: a potential role for dopamine, *Trends in Neurosciences* **23**: 239–245.

Jernigan, T., Salmon, D., Butters, N. and Hesselink, J. (1991). Cerebral structure on mri, part ii: Specific changes in alzheimer's and huntington's diseases, *Biological Psychiatry* **29**: 68–81.

Joel, D. and Weiner, I. (1997). The connections from the primate subthalamic nucleus: indirect pathways and the open-interconnected scheme of basil ganglia-thalamocortical circuitry, *Brain Research Reviews* **23**: 62–78.

Josephs, O., Turner, R. and Friston, K. (2004). Event-related fmri, *Human Brain Mapping* **5**: 243–248.

Jupitermedia (2005). The webopedia computer dictionary, JupiterWeb Networks. Available from: http://www.webopedia.com/TERM/V/voxel.html.

Just, M., Cherkassky, V., Keller, T. and Minshew, N. (2004). Cortical activation and synchronization during sentence comprehension in high-functioning autism: evidence of underconnectivity, *Brain* **127**: 1811–1821.

Kagan, B., Hirakura, Y., Azimov, R. and Azimova, R. (2001). The channel hypothesis of huntingtons disease, *Brain Research Bulletin* **56**: 281–284.

Kahlem, P., Green, H. and Djian, P. (1997). Transglutaminase action imitates huntingtons disease: Selective polymerization of huntingtin containing expanded polyglutamine, *Molecular Cell* **1**: 595–601.

Kemmotsu, N., Villalobos, M., Gaffrey, M., Courchesne, E. and Muller, R.-A. (2005). Activity and functional connectivity of inferior frontal cortex associated with response conflict, *Cognitive Brain Research* **25**: 335–342.

Kim, J., Reading, S., Brashers-Krug, T., Calhoun, V., Ross, C. and Pearlson, G. (2004). Functional mri study of a serial reaction time task in huntington's disease, *Psychiatry Research* **131**: 23–30.

Kobbert, C., Apps, R., Bechmann, I., Lanciego, J., Mey, J. and Thanos, S. (2001). Current concepts in neuroanatomical tracing, *NeuroImage* **62**: 327–351.

Kondo, H., Osaka, N. and Osakac, M. (2004). Cooperation of the anterior cingulate cortex and dorsolateral prefrontal cortex for attention shifting, *NeuroImage* **23**: 670–679.

Koshino, H., Carpenter, P., Minshew, N., Cherkassky, V., Keller, T. and Just, M. (2005). Functional connectivity in an fmri working memory task in high-functioning autism, *NeuroImage* **24**: 810–821.

Laufs, H., Lengler, U., Hamandi, K., Kleinschmidt, A. and Krakow, K. (2006). Linking generalized spike-and-wave discharges and resting state brain activity by using eeg/fmri in a patient with absence seizures., *Epilepsia* **47**: 444–448.

Lawrence, A., Sahakian, B. and Robbins, T. (1998). Cognitive functions and corticostriatal circuits: insights from huntingtons disease, *Trends in Cognitive Sciences* **2**: 379–388.

Lee, L., Friston, K. and Horwitz, B. (2005). Large-scale neural models and dynamic causal modelling, *NeuroImage* **In Press**.

Lekeu, F., der Linden, M. V., Chicherio, C., Collette, F., Degueldre, C., Franck, G., Moonen, G. and Salmon, E. (2003). Brain correlates of performance in a free/cued recall task with semantic encoding in alzheimer disease, *Alzheimer Disease and Associated Disorders* **17**: 35–45.

Li, S.-H. and Li, X.-J. (2004). Huntingtinprotein interactions and the pathogenesis of huntingtons disease, *Trends in Genetics* **3**: 146–154.

Lin, F.-H., McIntosh, A., Agnew, J., ZeffiroO, T. and Belliveau, J. (2001). Multiple subject effective connectivity analysis of voluntary movement, *Schizophrenia Research* **13**: 168.

Liu, X., Banich, M., Jacobson, B. and Tanabe, J. (2004). Common and distinct neural substrates of attentional control in an integrated simon and spatial stroop task as assessed by event-related fmri., *NeuroImage* **22**: 1097–1106.

Lowe, M., Dzemidzic, M., Lurito, J., Mathews, V. and Phillips, M. (2000). Correlations in low-frequency bold fluctuations reflect cortico-cortical connections, *NeuroImage* **12**: 582–587.

Lowe, M., Mock, B. and Sorenson, J. (1998). Functional connectivity in single and multislice echoplanar imaging using resting-state fluctuations, *NeuroImage* **7**: 119–132.

MacCallum, R., Wegener, D., Uchino, B. and Fabriger, L. (1993). The problem of equivalent models in covariance structure analysis, *Psychological Bulletin* **114**: 185–199.

McIntosh, A. (2000). Towards a network theory of cognition, *Neural Networks* **13**: 861–870.

McIntosh, A., Grady, C., Ungerleider, L., Haxby, J., Rapoport, S. and Horwitz, B. (1994). Network analysis of cortical visual pathways mapped with pet, *Journal of Neuroscience* **14**: 655–666.

Mclntosh, A. and Gonzalez-Lima, F. (1994). Structural equation modeling and its application to network analysis in functional brain imaging, *Human Brain Mapping* **2**: 2–22.

Mechelli, A., Penny, W., Price, C., Gitelman, D. and Friston, K. (2002). Effective connectivity and intersubject variability: Using a multisubject network to test differences and commonalities, *Schizophrenia Research* **17**: 1459–1469.

Mechelli, A., Price, C. and Friston, K. (2001). Effective connectivity during reading: the effects of word type and stimulus rate, *NeuroImage* **13**: S1292.

Mechelli, A., Price, C., Noppeney, U. and Friston, K. (2003). A dynamic causal modeling study on category effects: Bottomup or topdown mediation?, *Journal of Cognitive Neuroscience* **15**: 925–934.

Middleton, F. and Strick, P. (2001). A revised neuroanatomy of frontal-subcortical circuits, *Frontal Subcortical Circuits in Psychiatric and Neurological Disorders* pp. 44–58.

Miller, L., Sun, F., Curtis, C. and DEsposito, M. (2005). Functional interactions between oculomotor regions during prosaccades and antisaccades, *Human Brain Mapping* **26**: 119–127.

Mizuhara, H., Wang, L., Kobayashi, K. and Yamaguchi, Y. (2005). Long-range eeg phase synchronization during an arithmetic task indexes a coherent cortical network simultaneously measured by fmri, *NeuroImage* **27**: 553–563.

Murphy, C., Cerf-Ducastel, B., Calhoun-Haney, R., Gilbert, P. and Ferdon, S. (2005). Erp, fmri and functional connectivity studies of brain response to odor in normal aging and alzheimer's disease, *Chemical Senses* **30**: i170–i171.

Nelson, H. (1982). National adult reading test (nart): Test manual, Windsor: Nfer-Nelson.

Nitschke, J., Heller, W., Etienne, M. and Miller, G. (2004). Prefrontal cortex activity differentiates processes affecting memory in depression, *Biological Psychology* **67**: 125–143.

Obeso, J., Rodriguez, M. and DeLong, M. (1997). Basil ganglia pathophysiology: a critical review, *Advances in neurology* **74**: 3–15.

Parent, A. and Cicchetti, F. (1998). The current model of basil ganglia organisation under scrutiny, *Movement Disorders* **13**: 199–202.

Paulsen, J., Zimbelman, J., Hinton, S., Langbehn, D., Leveroni, C., Benjamin, M., Reynolds, N. and Rao, S. (2004). fmri biomarker of early neuronal dysfunction in presymptomatic huntington's disease, *American Journal of Neuroradiology* **25**: 1715–1721.

Pavese, N., Andrews, T., Brooks, D., Ho, A., Rosser, A., Barker, R., Robbins, T., Sahakian, B., Dunnett, S. and Piccini, P. (2003). Progressive striatal and cortical dopamine receptor dysfunction in huntington's disease: a pet study, *Brain* **126**: 1127–1135.

Pearl, J. (1993). Graphical models, causality, and interventions, *Statistical Science* **8**: 266–273.

Peltier, S., LaConte, S., Niyazov, D., Liu, J., Sahgal, V., Yue, G. and Hu, X. (2005). Reductions in interhemispheric motor cortex functional connectivity after muscle fatigue, *Brain Research* **1057**: 10–16.

Penney, J., Vonsattel, J., MacDonald, M., Gusella, J. and Myers, R. (1997). Cag repeat number governs the development rate of pathology in huntington's disease., *Annals of Neurology* **41**: 689–692.

Penny, W., Stephan, K., Mechelli, A. and Friston, K. (2004). Comparing dynamic causal models, *Neural Networks* **22**: 1157 1172.

Peterson, B., Kane, M., Alexander, G., Lacadie, C., Skudlarski, P., Leung, H., May, J. and Gore, J. (2002). An event-related functional mri study comparing interference effects in the simon and stroop tasks., *Brain research. Cognitive Brain Research.* **13**: 427–440.

Petersson, K., Reis, A., Askelof, S., Castro-Caldas, A. and Ingvar, M. (2000). Language processing modulated by literacy: A network analysis of verbal repetition in literate and illiterate subjects, *Journal of Cognitive Neuroscience* **12**: 364–382.

Posner, M. and Raichle, M. (1997). *Images of Mind*, Scientific American Library.

Radiological Society of North America, I. R. (2004). Functional mr imaging of the brain (fmri). Available from: http://www.radiologyinfo.org/.

Ramnani, N., Behrens, T., Penny, W. and Matthews, P. (2004). New approaches for exploring anatomical and functional connectivity in the human brain, *Biological Psychiatry* **56**: 613–619.

Reading, S., Dziorny, A., Peroutka, L., Schreiber, M., Gourley, L., Yallapragada, V., Rosenblatt, A., Margolis, R., Pekar, J., Pearlson, G., Aylward, E., Brandt, J., Bassett, S. and Ross, C. (2004). Functional brain changes in presymptomatic huntington's disease, *Annals of Neurology* **55**: 879–883.

Rissman, J., Gazzaley, A. and D'Esposito, M. (2004). Measuring functional connectivity during distinct stages of a cognitive task, *NeuroImage* **23**: 752–763.

Rosas, H., Koroshetz, W., Chen, Y., Skeuse, C., Vangel, M., Cudkowicz, M., Caplan, K., Marek, K., Seidman, L., Makris, N., Jenkins, B. and Goldstein, J. (2003). Evidence for more widespread cerebral pathology in early hd: an mri-based morphometric analysis, *Neurology* **60**: 1615–1620.

Rosenzweig, M., Breedlove, S. and Leiman, A. (2002). *Biological Psychology*, 3 edn, Sinauer Associates, Inc.

Rowe, J., Friston, K., Frackowiak, R. and Passingham, R. (2002). Attention to action: Specific modulation of corticocortical interactions in humans, *NeuroImage* **17**: 988–998.

Rowe, J., Stephan, K., Friston, K., Frackowiak, R., lees, A. and Passingham, R. (2002). Attention to action in parkinson's disease: impaired effective connectivity among frontal cortical regions, *Brain* **125**: 276–289.

Saint-Cyr, J., Taylor, A. and Nicholson, K. (1995). Behaviour and the basil ganglia, *Advances in Neurology* **65**: 1–28.

Sathasivam, K., Amaechi, I., Mangiarini, L. and Bates, G. (1997). Identification of an hd patient with a (cag)180 repeat expansion and the propagation of highly expanded cag repeats in lambda phage, *Human Genetics* **99**: 692–695.

Schmidtke, K., Manner, H., Kaufmann, R. and Schmolck, H. (2002). Cognitive procedural learning in patients with fronto-striatal lesions, *Learning and Memory* **9**: 419–429.

Snider, B., Moss, J., Revilla, F., Lee, C.-S., Wheeler, V., Macdonald, M. and Choi, D. (2003). Neocortical neurons cultured from mice with expanded cag repeats in the huntingtin gene: Unaltered vulnerability to excitotoxins and other insults, *Neuroscience* **120**: 617–675.

Stephan, K., Penny, W., Marshall, J., Fink, G. and Friston, K. (2005). Investigating the functional role of callosal connections with dynamic causal models., *Annals of the New York Academy of Sciences* **1064**: 16–36.

Stevanin, G., Fujigasaki, H., Lebre, A.-S., Camuzat, A., Jeannequin, C., Dode, C., Takahashi, J., San, C., Bellance, R., Brice, A. and Durr, A. (2003). Huntington's disease-like phenotype due to trinucleotide repeat expansions in the tbp and jph3 genes, *Brain* **126**: 1599–1603.

Sun, F., Miller, L. and DEsposito, M. (2004). Measuring interregional functional connectivity using coherence and partial coherence analyses of fmri data, *NeuroImage* **21**: 647–658.

Tabachnick, B. and Fidell, L. (2001). *Using Multivariate Statistics*, 4 edn, Allyn & Bacon.

Templin, T. and Pieper, B. (2003). Causal modeling in woc nursing research, *J WOCN* **30**: 168–174.

Thieben, M., Duggins, A., Good, C., Gomes, L., Mahant, N., Richards, F., McCusker, E. and Frackowiak, R. (2002). The distribution of structural neuropathology in pre-clinical huntington's disease, *Brain* **125**: 1815–1828.

Tomarken, A. and Waller, N. (2003). Potential problems with 'well fitting' models, *Journal of Abnormal Psychology* **112**: 578–598.

Valet, M., Sprenger, T., Boecker, H., Willoch, F., Rummeny, E., Conrad, B., Erhard, P. and Tolle, T. (2004). Distraction modulates connectivity of the cingulo-frontal cortex and the midbrain during pain-an fmri analysis, *Pain* **109**: 399–408.

Vonsattel, J. and Difiglia, M. (1998). Huntington's disease, *Journal of Neuropathology and Experimental Neurology* **57**: 369–384.

Welchew, D., Ashwin, C., Berkouk, K., Salvador, R., Suckling, J., Baron-Cohen, S. and Bullmore, E. (2005). Functional disconnectivity of the medial temporal lobe in asperger's syndrome, *Biological Psychiatry* **57**: 991–998.

Whalley, H., Simonotto, E., Marshall, I., Owens, D., Goddard, N., Johnstone, E. and Lawrie, S. (2005). Functional disconnectivity in subjects at high genetic risk of schizophrenia, *Brain* **128**: 2097–2108.

Wikipedia (2005). Magnetic resonance imaging, Wikipedia website. http://en.wikipedia.org/wiki/.

Winograd-Gurvich, C., Georgiou-Karistianis, N., Evans, A., Millist, L., Bradshaw, J., Churchyard, A., Chiu, E. and White, O. (2003). Hypometric primary saccades and increased variability in visually-guided saccades in huntingtons disease, *Neuropsychologia* **41**: 1683–1692.

Winterer, G., Coppola, R., Egan, M., Goldberg, T. and Weinberger, D. (2003). Functional and effective frontotemporal connectivity and genetic risk for schizophrenia, *Biological Psychiatry* **54**: 1181–1192.

Xiong, J., Parsons, L., Gao, J. and Fox, P. (1999). Interregional connectivity to primary motor cortex revealed using mri resting state images, *Human Brain Mapping* **8**: 151–156.

Zar, H. (1997). *Biostatistical Analysis*, Pearson Education Inc.